

12-1-2009

Pulmonary vasoconstrictor reactivity following intermittent hypoxia

Jessica Snow

Follow this and additional works at: https://digitalrepository.unm.edu/biom_etds

Recommended Citation

Snow, Jessica. "Pulmonary vasoconstrictor reactivity following intermittent hypoxia." (2009). https://digitalrepository.unm.edu/biom_etds/3


This Dissertation is brought to you for free and open access by the Electronic Theses and Dissertations at UNM Digital Repository. It has been accepted for inclusion in Biomedical Sciences ETDs by an authorized administrator of UNM Digital Repository. For more information, please contact disc@unm.edu.

JW
Jessica Snow
Candidate

Biomedical Sciences Graduate Program: Cell Biology and Physiology
Department

This dissertation is approved, and it is acceptable in quality
and form for publication:

Approved by the Dissertation Committee:


_____, Chairperson

Mary K Walker

Mary J Kyj

By R. Wecht

**PULMONARY VASOCONSTRICTOR
REACTIVITY FOLLOWING
INTERMITTENT HYPOXIA**

BY

JESSICA SNOW

B.S., Biology, University of Illinois, 2003

DISSERTATION

Submitted in Partial Fulfillment of the
Requirements for the Degree of

**Doctor of Philosophy
Biomedical Sciences**

The University of New Mexico
Albuquerque, New Mexico

Dec, 2009

ACKNOWLEDGMENTS

I enthusiastically thank my mentor, Dr. Tom Resta, for his encouragement and guidance over the last 6 years. He has given me a strong foundation not only in research, but also in writing, presenting, and thinking like a scientist. His guidance and fundamentals will be with me throughout my career.

I would also like to thank my committee members Dr. Ben Walker, Dr. Nancy Kanagy and Dr. Mary Walker. Their backing throughout my graduate career has been of the utmost importance to my success and the completion of this dissertation.

Thanks are additionally due to the other members of our Vascular Physiology Group. The constant input and encouragement through lab meetings, journal clubs and informal time around the office are priceless. I have been so fortunate to work in such a positive collaborative environment.

Thank you to my parents for instilling in me a value for education and a desire to pursue an advanced degree. And, most importantly, thank you to my wonderful husband Craig for agreeing to undertake this graduate school endeavor with me. His patience and support during the last 6 years have been amazing.

**PULMONARY VASOCONSTRICTOR
REACTIVITY FOLLOWING
INTERMITTENT HYPOXIA**

BY

JESSICA SNOW

ABSTRACT OF DISSERTATION

Submitted in Partial Fulfillment of the
Requirements for the Degree of

**Doctor of Philosophy
Biomedical Sciences**

The University of New Mexico
Albuquerque, New Mexico

Dec, 2009

Pulmonary Vasoconstrictor Reactivity Following Intermittent Hypoxia

Jessica B. Snow

B.S., Biology, University of Illinois, 2003
Ph.D., Biomedical Sciences, University of New Mexico, 2009

ABSTRACT

Sleep apnea (SA) affects as many as 20% of the adult population in the United States. It elicits intermittent hypoxia (IH) and causes pulmonary hypertension (PH), however the mechanisms of this PH have not been well studied. IH has been shown to cause polycythemia, pulmonary vascular remodeling and increases in vasoconstrictor reactivity. CO₂ supplementation may be protective in the development of PH, therefore we assessed effects of IH with and without CO₂ supplementation on indices of PH and pulmonary vasoconstrictor reactivity. IH with CO₂ supplementation resulted in eucapnic IH (E-IH) and the lack of polycythemia or vascular remodeling. However, E-IH caused significant right ventricular hypertrophy and increased pulmonary vasoconstrictor reactivity, which was mediated by vascular smooth muscle (VSM) Ca²⁺ sensitization. We, therefore, sought to determine the mechanism of this enhanced vasoconstrictor reactivity by assessing vasoconstriction and VSM Ca²⁺ responses to the endothelium-derived vasoconstrictor peptide endothelin-1 (ET-1). Given evidence that Rho kinase (ROK), PKC and reactive oxygen species (ROS) contribute to the development of PH, we addressed their respective contributions to augmented pulmonary vasoconstrictor reactivity to ET-1 following E-IH. Interestingly, we found that ROK did not contribute to ET-1-induced pulmonary vasoconstriction. However,

PKC- and ROS- dependent signaling is augmented following E-IH and these mediators appear to signal in series, with the mitochondria providing the source of ROS. Furthermore, E-IH augments PKC α/β -dependent ROS generation. Therefore, both mitochondrial ROS and PKC α/β represent potential therapeutic targets in the development of SA-induced PH.

TABLE OF CONTENTS

LIST OF FIGURES	<i>x</i>
LIST OF TABLES	<i>xiii</i>
CHAPTER I – INTRODUCTION	<i>1</i>
<i>Sleep Apnea</i>	<i>1</i>
<i>Sleep Apnea-Induced Pulmonary Hypertension</i>	<i>2</i>
<i>Hemodynamic Components of Pulmonary Hypertension</i>	<i>5</i>
<i>Mechanisms of Pulmonary Hypertension</i>	<i>6</i>
<i>Mechanisms of VSM Cell Contraction</i>	<i>16</i>
<i>VSM Ca²⁺ Homeostasis and Myofilament Ca²⁺ Sensitivity in Pulmonary Hypertension</i>	<i>23</i>
<i>Role of Reactive Oxygen Species (ROS) in Vascular Signaling and Pathology</i>	<i>27</i>
<i>Rationale and Specific Aims</i>	<i>35</i>
CHAPTER II – METHODS	<i>44</i>
<i>General Methods</i>	<i>44</i>
<i>Experimental Groups</i>	<i>44</i>
<i>Measurement of Right Ventricular Weight</i>	<i>45</i>
<i>Isolation of Small Pulmonary Arteries for Dimensional Analysis</i>	<i>45</i>
<i>Measurement of VSM [Ca²⁺]_i</i>	<i>46</i>
<i>In Situ Calibrations of VSM [Ca²⁺]_i</i>	<i>47</i>
<i>Calculations and Statistical Analysis</i>	<i>49</i>

<i>Protocols for Specific Aim 1: Compare effects of E-IH and H-IH on indices of PH and vasoconstrictor reactivity.....</i>	<i>49</i>
<i>Protocols for Specific Aim 2: Assess the role of ROK in mediating right ventricular hypertrophy and enhanced agonist-induced pulmonary vasoconstriction following E-IH.....</i>	<i>55</i>
<i>Protocols for Specific Aim 3: Assess the contribution of PKC to increased agonist-mediated vasoconstriction following E-IH.....</i>	<i>56</i>
<i>Protocols for Specific Aim 4: Determine the contribution of ROS to right ventricular hypertrophy and enhanced agonist-induced vasoconstriction after E-IH.....</i>	<i>61</i>
CHAPTER III – RESULTS.....	67
<i>Results for Specific Aim1: Compare effects of E-IH and H-IH on indices of PH and vasoconstrictor reactivity</i>	<i>67</i>
<i>Results for Specific Aim 2: Assess the role of ROK in mediating right ventricular hypertrophy and enhanced agonist-induced pulmonary vasoconstriction following E-IH.....</i>	<i>88</i>
<i>Results for Specific Aim 3: Assess the contribution of PKC to increased agonist-mediated vasoconstriction following E-IH</i>	<i>93</i>
<i>Results for Specific Aim 4: Determine the contribution of ROS to right ventricular hypertrophy and enhanced agonist-induced vasoconstriction after E-IH.</i>	<i>108</i>
CHAPTER IV – DISCUSSION.....	130
<i>Specific Aim1: Compare effects of E-IH and H-IH on indices of PH and vasoconstrictor reactivity.....</i>	<i>131</i>
<i>Arterial Blood Gases.....</i>	<i>131</i>
<i>Right Ventricular Hypertrophy.....</i>	<i>132</i>
<i>Polycythemia.....</i>	<i>133</i>
<i>Pulmonary Arterial Remodeling.....</i>	<i>134</i>
<i>Pulmonary Vasoconstrictor Reactivity Following IH</i>	<i>135</i>
<i>Specific Aim 2: Assess the role of ROK in mediating right ventricular hypertrophy and enhanced agonist-induced pulmonary vasoconstriction following E-IH.....</i>	<i>137</i>

<i>Role of ROK in E-IH-Induced Pulmonary Hypertension</i>	137
<i>Role of ROK in Enhanced Vasoconstrictor Reactivity to ET-1 After E-IH</i>	137
<i>Specific Aim 3: Assess the contribution of PKC to increased agonist-mediated vasoconstriction following E-IH</i>	139
<i>Role of PKC in ET-1-Induced Vasoconstriction</i>	139
<i>Effect of E-IH on PKC Expression</i>	141
<i>Specific Aim 4: Determine the contribution of ROS to right ventricular hypertrophy and enhanced agonist-induced vasoconstriction after E-IH.</i>	142
<i>Role of ROS in Mediating E-IH-Induced PH</i>	142
<i>Role of ROS in Mediating an Increase in Pulmonary Artery Vasoconstrictor Reactivity After E-IH</i>	144
<i>Effect of E-IH on Basal and ET-1-Stimulated ROS Levels</i>	145
<i>Role of NOX, XO in Agonist-Induced Constriction after E-IH</i>	146
<i>Role of Mitochondrial ROS in Agonist-Induced Constriction after E-IH</i>	148
<i>Interaction Between PKC and ROS</i>	152
<i>Conclusions</i>	154
<i>Clinical Significance</i>	156
<i>Future Directions</i>	156
APPENDIX A- Abbreviations	160
REFERENCES	162

LIST OF FIGURES

Figure 1: Potential Mechanisms of IH-Induced PH.....	8
Figure 2: VSM Cell Contraction.....	17
Figure 3: Cell Diagram Illustrating NADPH Oxidase Activation.....	30
Figure 4: Image of Isolated Pressurized Small Pulmonary Artery.....	48
Figure 5: Arterial PO ₂ Measurements at the Beginning of IH Cycling.....	68
Figure 6: Arterial PCO ₂ Measurements at the Beginning of IH Cycling	69
Figure 7: Arterial pH Measurements at the Beginning of IH Cycling.....	70
Figure 8: Arterial PO ₂ Measurements Following 4 Weeks E-IH Exposure.....	72
Figure 9: Arterial PCO ₂ Measurements Following 4 Weeks E-IH Exposure.....	73
Figure 10: Arterial pH Measurements Following 4 Weeks E-IH Exposure	74
Figure 11: Right Ventricular/Total Ventricular Weight Following IH.....	75
Figure 12: Right Ventricular/Body Weight Following IH	76
Figure 13: Hematocrit Values from Sham, H-IH and E-IH Animals.....	79
Figure 14: Percent Arterial Wall Thickness of Pulmonary Arteries.....	80
Figure 15: Vasoconstrictor and VSM [Ca ²⁺] _i Responses to ET-1.....	82
Figure 16: Vasoconstrictor and VSM [Ca ²⁺] _i Responses to UTP.....	85
Figure 17: Vasoconstrictor and VSM [Ca ²⁺] _i Responses to 5-HT.....	86
Figure 18: Right Ventricular/Total Ventricular Weight and Right Ventricular/Body Weight in E-IH Rats Treated with Vehicle or Fasudil.....	89
Figure 19: Vasoconstrictor and VSM [Ca ²⁺] _i Responses to ET-1 in the presence of Fasudil.....	90
Figure 20: Vasoconstrictor Responses to PMA in the Presence and Absence of Ro 31-8220.....	94

Figure 21: Vasoconstrictor and VSM $[Ca^{2+}]_i$ Responses to ET-1 in the presence of Ro 31-8220	95
Figure 22: Vasoconstrictor Responses to PMA in the Presence and Absence myr-PKC.....	97
Figure 23: Vasoconstrictor and VSM $[Ca^{2+}]_i$ Responses to ET-1 in the Presence of myr-PKC.....	98
Figure 24: Vasoconstrictor Responses to PMA in the Presence and Absence Rottlerin	99
Figure 25: Vasoconstrictor and VSM $[Ca^{2+}]_i$ Responses to ET-1 in the Presence of Rottlerin.....	100
Figure 26: Pulmonary Arterial PKC α/β mRNA Levels	104
Figure 27: Pulmonary Arterial PKC α protein levels	106
Figure 28: Pulmonary Arterial PKC $\beta I/\beta II$ protein levels	107
Figure 29: Right Ventricle/ Total Ventricular Weight from Tempol-Treated Sham and E-IH Rats	109
Figure 30: Vasoconstrictor and VSM $[Ca^{2+}]_i$ Responses to ET-1 in the Presence of Tiron	112
Figure 31: Vasoconstrictor and VSM $[Ca^{2+}]_i$ Responses to ET-1 in the Presence of PEG-catalase	116
Figure 32: Vasoconstrictor and VSM $[Ca^{2+}]_i$ Responses to ET-1 in the Presence of Apocynin	118
Figure 33: Vasoconstrictor and VSM $[Ca^{2+}]_i$ Responses to ET-1 in the Presence of Allopurinol	119
Figure 34: Vasoconstrictor and VSM $[Ca^{2+}]_i$ Responses to ET-1 in the Presence of MITO-CP	120
Figure 35: Vasoconstrictor and VSM $[Ca^{2+}]_i$ Responses to ET-1 in the Presence of Rotenone	122
Figure 36: Pulmonary Arterial Basal and ET-1-Stimulated DHE Fluorescence in the Presence and Absence of Tiron.....	124

Figure 37: Vasoconstrictor and VSM $[Ca^{2+}]_i$ Responses to ET-1 in the Presence of Ro 31-8220/Tiron	125
Figure 38: Vasoconstrictor and VSM $[Ca^{2+}]_i$ Responses to ET-1 in the Presence of myr-PKC/Tiron	127
Figure 39: Pulmonary Arterial Basal and ET-1-Stimulated DHE Fluorescence in the Presence and Absence of myr-PKC.....	128
Figure 40: Proposed Mechanism for E-IH-Induced PH.....	155

LIST OF TABLES

Table 1: PKC Classes and Activation Mechanisms.....	22
Table 2: Body Weights and Left Ventricle + Septum Weights From Sham and IH Rats.....	77
Table 3: Basal Inner Diameter and VSM $[Ca^{2+}]_i$ in isolated arteries (Specific Aim 1).....	83
Table 4: Basal Inner Diameter and VSM $[Ca^{2+}]_i$ in isolated arteries (Specific Aim 2).....	92
Table 5: Basal Inner Diameter and VSM $[Ca^{2+}]_i$ in isolated arteries (Specific Aim 3).....	102
Table 6: In Situ Fura-2 Calibration Values (Specific Aim 3).....	103
Table 7: Body Weights and Left Ventricle + Septum Weights From Tempol-Treated Sham and E-IH Rats.....	110
Table 8: Basal Inner Diameter and VSM $[Ca^{2+}]_i$ in isolated arteries (Specific Aim 4).....	113
Table 9: In Situ Fura-2 Calibration Values (Specific Aim 4).....	115

CHAPTER I

INTRODUCTION

Sleep apnea (SA) is a disorder with increasing prevalence in the United States, affecting at least 4% of the adult population and as many as 20% of adults age 65 and older (Young *et al.*, 1993). SA causes intermittent hypoxia (IH) and arterial hypoxemia. Recently, it has been appreciated that SA patients and animals exposed to IH develop pulmonary hypertension (PH), but the mechanism by which this occurs is poorly understood. In well studied models of PH, such as chronic hypoxic (CH) PH, there is increased pulmonary vascular resistance caused by active vasoconstriction, pulmonary arterial remodeling and possibly increased blood viscosity due to polycythemia. The severity of PH may be greatly affected by the contractility of pulmonary vascular smooth muscle (VSM), particularly in the small arteries. Although previous studies indicate that IH increases pulmonary vasoconstrictor reactivity (Thomas & Wanstall, 2003), the mechanism by which this occurs has not been characterized. VSM tone is regulated by changes in VSM intracellular Ca^{2+} ($[Ca^{2+}]_i$) and sensitivity of the contractile apparatus to changes in $[Ca^{2+}]_i$. The following sections outline the conditions associated with IH, the development of PH and mechanisms of VSM cell contraction.

Sleep Apnea

Sleep apnea (SA) occurs when a person's breathing is interrupted during sleep and is classified as either obstructive, central or a mixture of both. In the case of obstructive SA, a physical collapse of the upper airway occurs because of a relaxation of

the muscles which support the soft tissues of the throat, stopping airflow for >10 seconds. Risk factors for obstructive SA include obesity, large neck circumference, and smoking (Young *et al.*, 2002). Central SA occurs because of a lack of central nervous respiratory drive during sleep, and risk factors include being male, suffering from brain tumor or stroke and congestive heart failure (Eckert *et al.*, 2007; Mayo Clinic, 2009). A patient experiences significant SA when there are more than 5 apneic or hypopneic episodes per hour of sleep as measured by the respiratory disturbance index (Mohsenin, 2001). This condition is characterized by many arousals from sleep and a fall in arterial O₂ saturation (hypoxemia). Most patients suffer from daytime sleepiness which may impair work performance and many experience associated cardiovascular diseases (Partinen & Guilleminault, 1990), such as hypertension, ischemic heart disease and stroke. More recently, it has been shown that SA is associated with an increased risk of PH, especially in patients with chronic lung disease (Alchanatis *et al.*, 2001). However, the mechanisms of SA-induced PH have not been well characterized.

Sleep Apnea- Induced Pulmonary Hypertension.

It has been known for several years that SA increases the incidence of cardiovascular complications such as heart failure, stroke and systemic hypertension (Dimsdale *et al.*, 2000; Shahar *et al.*, 2001). However, it is now appreciated that SA also elicits changes in the pulmonary vasculature and right heart (Sajkov & McEvoy, 2009). The prevalence of PH in SA has been reported to be between 17% (Chaouat *et al.*, 1996; Zielinski, 2005) and 43% (Arias *et al.*, 2006; Tilkian *et al.*, 1976). If left untreated, PH can result in right heart failure and death. Thus, understanding the mechanisms of PH

associated with SA is crucial to preventing and treating the disease and associated right heart failure in such patients.

SA causes remarkable acute changes in pulmonary artery pressure (PAP) (Bonsignore *et al.*, 1994), with PH occurring during apneic episodes (Tilkian *et al.*, 1976). Marrone *et al.* found that when measurements were corrected for intrathoracic pressure swings, transmural PAP increased progressively throughout apneic episodes (Marrone *et al.*, 1989). In agreement with this study, Schafer and colleagues determined that systolic transmural PAP increased from ~28 mmHg at the beginning of apnea to ~39 mmHg at the end of an apneic episode, indicating repetitive PH episodes occur during SA (Schafer *et al.*, 1998). These studies provided evidence for PH in SA patients during sleep, however they failed to address whether SA was sufficient to cause diurnal pulmonary hypertension.

Daytime PH has been reported to have a high occurrence in SA patients, however some studies can not rule out the contribution of underlying lung disease to PH in patients with SA (Fletcher *et al.*, 1987;Tilkian *et al.*, 1976). In such studies, the patients had a mixture of SA and chronic obstructive pulmonary diseases (COPD) such as emphysema and chronic bronchitis (Chaouat *et al.*, 1996;Fletcher, 1990) or obesity, making it difficult to assess the relative contributions of SA-induced IH and diurnal hypoxemia secondary to underlying lung disease (Sajkov & McEvoy, 2009). Bradley *et al.* studied 50 SA patients and concluded that daytime hypoxemia and/or hypercapnia were necessary for the development of right heart failure (Bradley *et al.*, 1985). Consistent with those findings, Chaouat and colleagues reported that permanent daytime PH was observed in 17% of SA patients and this occurrence was strongly linked to

hypoxemia (Chaouat *et al.*, 1996). Weitzenblum *et al.* studied 46 patients and found that 20% of them developed PH, and this was again related to the presence of sustained hypoxemia (Weitzenblum *et al.*, 1988). Furthermore, continuous positive airway pressure (CPAP) lowers PAP in patients suffering from concomitant COPD and SA (Fletcher, 1990), or so-called “overlap syndrome” (Weitzenblum *et al.*, 2008). These studies highlight the fact that SA can exacerbate PH in people who suffer from chronic lung disease.

Whether SA is sufficient to cause PH in the absence of underlying lung disease has been a subject of recent study. In order to more directly address the role of SA in the development of PH, patients suffering from SA without any other identifiable cardiopulmonary disease have been studied. Alchanatis *et al.* found that ~21 % of SA patients without any other cardiac or lung disease were pulmonary hypertensive (Alchanatis *et al.*, 2001). Consistent with these findings, Bady and colleagues found the existence of PH in 27% of patients with “pure” SA (Bady *et al.*, 2000). These studies support the idea that SA is an independent risk factor for PH, however diurnal hypoxemia may contribute to the development of PH.

Apneic episodes during sleep are simulated in rodent models of SA by exposing animals to frequent cycles of hypoxia/normoxia. These cycling models range from exposures of 15 sec- 6 min/cycle carried out 7-12 hr/day over 2-8 weeks (Bertuglia & Reiter, 2009;Bradford, 2004;Campen *et al.*, 2005;Fagan, 2001;Fletcher *et al.*, 1995;Nisbet *et al.*, 2008). In addition to developing systemic hypertension, many of these animals exposed to intermittent hypoxia (IH) show evidence of PH (Bradford, 2004;Campen *et al.*, 2005;Fagan, 2001;Fletcher *et al.*, 1987). These models have

included both IH alone (Bradford, 2004; Campen *et al.*, 2005; Fagan, 2001; Nisbet *et al.*, 2008; Snow *et al.*, 2008), as well as IH combined with supplemental CO₂ administration (Bradford, 2004; Fletcher *et al.*, 1995; Snow *et al.*, 2008), which is intended to mimic the increase in arterial CO₂ during apnea (Borges *et al.*, 2002). Both models are associated with PH, however CO₂ supplementation may blunt the effects of IH, as occurs with CH (Kantores *et al.*, 2006).

Given the strong evidence that SA can both exacerbate PH due to underlying lung disease and result in PH in the absence of concomitant lung disease, it is important to understand the mechanisms by which IH induces PH. The factors which may influence the development of IH-induced PH by increasing pulmonary vascular resistance are discussed below.

Hemodynamic Components of Pulmonary Hypertension.

The pulmonary circulation is characterized by low pressure and low resistance under normoxic conditions. However, under pathological conditions that lead to CH, vascular resistance is increased by pulmonary arterial vasoconstriction, remodeling and polycythemia. Pouseuille's equation describes the factors affecting arterial resistance:

$$\text{Resistance} = 8\eta L / \pi r^4$$

Where L is the length of the tube, η is viscosity and r is the radius of the tube. Although this equation describes resistance in a straight, rigid tube conducting a homogeneous fluid, it provides an approximation for factors that determine resistance to flow in blood vessels. Based on this relationship, an increase in blood viscosity, as occurs with polycythemia, would increase resistance. More importantly, however, a decrease in

radius of the vessel, resulting from vasoconstriction or vascular remodeling, causes a profound increase in resistance since resistance is inversely proportional to radius to the fourth power. Based on an ohmic relationship where:

$$\uparrow \text{Resistance} \times \text{Flow} = \uparrow \Delta \text{ Pressure}$$

An increase in resistance causes a proportional increase in PAP when flow is maintained constant. An increase in pressure within the pulmonary circulation places an elevated work load on the right side of the heart. To compensate for this greater workload, the right heart undergoes hypertrophy, and if untreated the end result can be right heart failure and death depending on the severity of PH.

Mechanisms of Pulmonary Hypertension

Polycythemia. Polycythemia is an increase in number of circulating red blood cells, which occurs as a result of increased erythropoiesis. Erythropoiesis normally proceeds at low basal levels in order to replace old red blood cells and can be stimulated by a decrease in number of red blood cells, hypoxia or an increase in the affinity of hemoglobin for oxygen. In response to hypoxia, the transcription factors hypoxia-inducible factor 1 and 2 (HIF-1 and HIF-2) mediate a profound increase in erythropoietin synthesis by the fetal liver and adult kidney (Semenza & Wang, 1992;Warnecke *et al.*, 2004). Erythropoietin is released from these tissues into the circulation, where it acts on erythroid progenitor cells in the bone marrow to induce erythropoiesis (Ebert & Bunn, 1999). Thus, polycythemia serves as a compensatory mechanism to facilitate greater

oxygen carrying capacity of the blood under conditions of decreased oxygen availability, but the resultant increase in viscosity may contribute to increased pulmonary vascular resistance under prolonged exposure to hypoxia (Figure 1) (Fried *et al.*, 1983).

An increase in O₂ carrying capacity of the blood is beneficial in the setting of SA, in which acute hypoxemia can occur during apneic episodes. IH has consistently been shown to elicit polycythemia in the absence of supplemental CO₂ (Bertuglia & Reiter, 2009; Bradford, 2004; Campen *et al.*, 2005; Fagan, 2001; McGuire & Bradford, 1999; Snow *et al.*, 2008). As would be predicted, SA patients have significantly greater hematocrits than normal subjects, however this is reportedly not in the range of clinical polycythemia (Choi *et al.*, 2006; Nobili *et al.*, 2000). This finding is not surprising given that apneic episodes are associated with CO₂ retention (Alford *et al.*, 1986), which may blunt the development of polycythemia as occurs in IH rats (Snow *et al.*, 2008). However, eucapnia or hypercapnia tend to blunt or prevent the IH-induced polycythemia (Snow *et al.*, 2008). In contrast, Fletcher *et al.* found that neither 35 days of eucapnic, hypocapnic nor hypercapnic IH elicited a change in hematocrit (Fletcher *et al.*, 1995). Given the discrepant findings regarding IH-induced polycythemia, this study will address changes in hematocrit in our model of SA.

Vascular Remodeling. Early studies of the pulmonary circulation of high altitude dwellers emphasized the idea that structural changes in the vascular bed were responsible for CH-induced PH. Sime *et al.* found that non-native highlanders develop PH that is

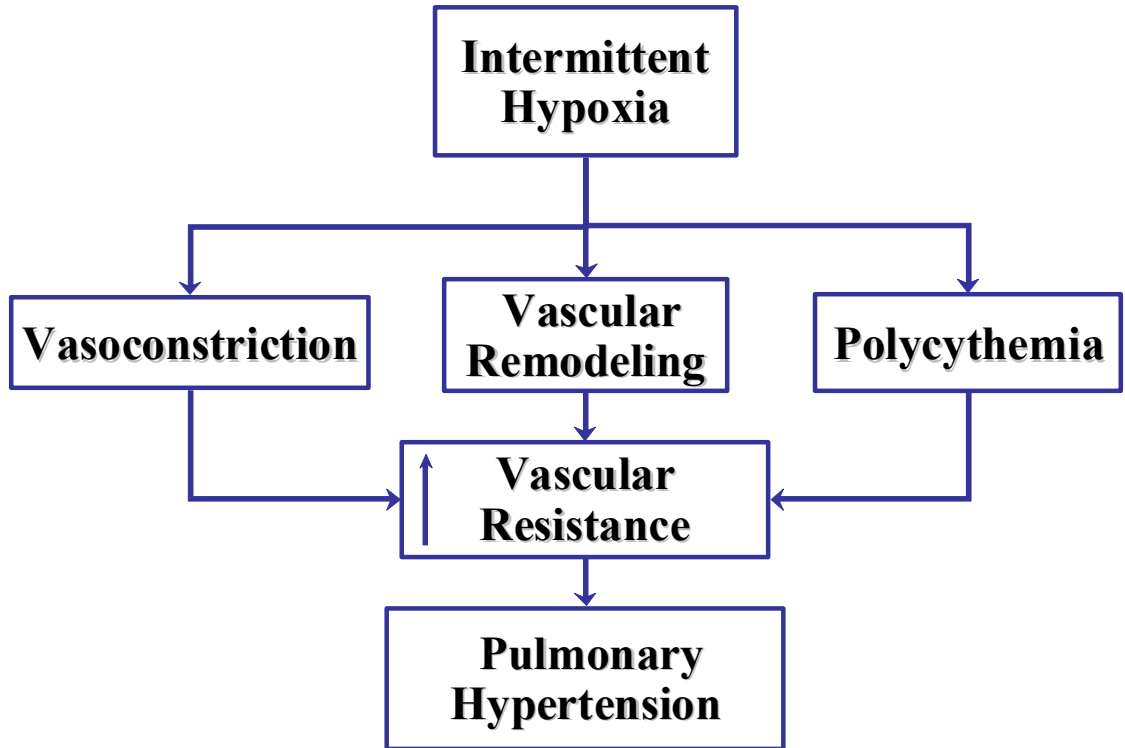


Figure 1. Intermittent hypoxia may mediate an increase in pulmonary vascular resistance via vasoconstriction, vascular remodeling or polycythemia, all of which could contribute to pulmonary hypertension.

only partially reversed by acute O₂ administration, presumably by reversing hypoxic pulmonary vasoconstriction (Sime *et al.*, 1971). The remaining elevation in PAP was thought to be related to pulmonary vascular remodeling. The occurrence of CH-induced pulmonary vascular remodeling was confirmed by studies in CH animals, showing that small pulmonary arteries became remodeled beginning after only 2 days of hypoxia (Meyrick & Reid, 1978). There are two general mechanisms by which structural alterations of the pulmonary vasculature could mediate an increase in pulmonary vascular resistance: 1) *remodeling of the walls* of pulmonary resistance arteries to mediate a decrease in luminal diameter and 2) a decrease in the total number of pulmonary arteries, a phenomenon referred to as *rarefaction* (Howell *et al.*, 2004). Arterial remodeling involves a thickening of the arterial wall, and this may encroach upon the vascular lumen, increasing pulmonary vascular resistance (Hopkins & McLoughlin, 2002). Specifically, proliferation and hypertrophy of the smooth muscle and the development of smooth muscle-like cells in previously non-muscularized vessels of the lung can reduce the luminal radius and increase vascular resistance.

Many stimuli can result in VSM proliferation, such as increases in VSM [Ca²⁺]_i (Sweeney *et al.*, 2002a) and receptor-mediated agonists such as endothelin-1 (ET-1) (Ambalavanan *et al.*, 2007; DiCarlo *et al.*, 1995; Huang *et al.*, 2009), 5-HT (Fanburg & Lee, 1997) and thromboxanes (Ko, 1997). Inhibition of Ca²⁺ influx decreases proliferation of pulmonary artery smooth muscle cells (PASMCs) from patients with idiopathic PH (Fujio *et al.*, 2006; Yu *et al.*, 2004), suggesting Ca²⁺ influx is a potent stimulus in the development of pulmonary vascular remodeling. The endothelium-

derived vasoconstrictor peptide ET-1 stimulates both ET_A and ET_B receptors on PASMC, promoting cell proliferation (Davie *et al.*, 2002) and endogenous ET-1 production by the endothelium likely contributes to the proliferative response under hypoxic conditions. Hypoxia increases 5-HT production by platelets and neuroepithelial bodies (Esteve *et al.*, 2007). The increase in 5-HT then facilitates smooth muscle cell (SMC) and fibroblast (Welsh *et al.*, 2004) mitogenesis via stimulation of 5-HT receptors (Pitt *et al.*, 1994) and 5-HT uptake (Lee *et al.*, 1994) via mechanisms that may involve ROS and stabilization of HIF-1 α (Esteve *et al.*, 2007). In addition, thromboxanes could contribute to PASMC proliferation (Ko, 1997). Thus, changes in the medial layer of the PA can be triggered by a number of stimuli, which then contribute to the development of PH. However, it is additionally possible that proliferation and hypertrophy of pulmonary VSM resulting from CH do not alter luminal diameter in small pulmonary arteries, as suggested by studies by Hyvelin and colleagues in CH rats (Hyvelin *et al.*, 2005).

This remodeling, which accompanies PH in many models of the disease, also involves changes in adventitial and intimal layers of the vessel (Stenmark *et al.*, 2006). Adventitial thickening due to increased number of fibroblasts and myofibroblasts in the vessel wall provides a substantial component of vessel wall thickening (Rose *et al.*, 2002; Short *et al.*, 2004). Endothelial cell proliferation and intimal thickening occur in models of hypoxic PH but may provide only a minimal contribution to the overall morphological changes in the vessel wall (Meyrick & Reid, 1980).

The second form of pulmonary arterial remodeling which has also been implicated in contributing to the development of PH is rarefaction. A correlation between rarefaction and PH was observed in cystic fibrosis patients who died from

complications related to PH (Ryland & Reid, 1975). In addition, Hislop and Reid found that rats exposed to 14 days of hypobaric hypoxia (380 mmHg) possessed fewer pulmonary arteries smaller than 200 μm (Hislop & Reid, 1976). This rarefaction would be expected to decrease the number of parallel pathways for blood flow, and thus increase vascular resistance (Hislop & Reid, 1976).

Although the above studies of CH-induced PH support a major role for pulmonary vascular remodeling in CH-induced increases in pulmonary vascular resistance (Sime *et al.*, 1971), more recent studies suggest that CH causes angiogenesis in the pulmonary circulation (Howell *et al.*, 2003). In lungs of rats exposed to two weeks of normobaric hypoxia, stereological studies revealed an increase in total length and volume of pulmonary vessels. In addition, endothelial surface area and number of endothelial cells is increased (Howell *et al.*, 2003). These results are consistent with the effects of hypoxia on systemic vascular beds (Lamanna *et al.*, 1992). In contrast to rarefaction, angiogenesis would provide an increase in the number of parallel pathways for blood flow, thus lowering pulmonary vascular resistance. If this is the case, a larger component of CH-induced PH must be attributed to vasoconstriction as will be discussed below.

Similar to CH, IH causes pulmonary vascular remodeling. Nisbet *et al.* found that mice exposed to 8 weeks of IH (10% O₂, 45 cycles/hour, 8 hr/day) had an increase in the number of SMCs in small pulmonary arteries, a decrease in the luminal radius and an increase arterial wall thickness (Nisbet *et al.*, 2008). In agreement with this study, we have shown that 2 week exposure to IH causes an increase in pulmonary arterial wall thickness in rats (Snow *et al.*, 2008). Furthermore, in mice lacking the gp91phox subunit of NADPH oxidase, IH-induced pulmonary vascular remodeling is eliminated (Nisbet *et*

al., 2008), suggesting that NADPH oxidase-derived superoxide mediates pulmonary vascular remodeling in IH exposed mice, as discussed in more depth in the reactive oxygen species section of this introduction.

The presence of hypercapnia under CH conditions attenuates pulmonary vascular remodeling (Ooi *et al.*, 2000). Kantores *et al.* showed that 10% CO₂ exposure, concomitant with normobaric hypoxia, attenuated right ventricular hypertrophy and the associated medial wall thickening and number of muscularized small pulmonary arteries (Kantores *et al.*, 2006). This finding is consistent with studies from our laboratory comparing hypocapnic and eucapnic IH, in which we found that the presence of supplemental CO₂ blunts the muscularization of small pulmonary arteries (Snow *et al.*, 2008). The mechanism by which CO₂ opposes pulmonary vascular remodeling is unclear but may be related to an inhibitory effect of CO₂ on ET-1 expression (Kantores *et al.*, 2006). Whole lung ET-1 as well as pulmonary arterial prepro-ET-1 protein levels are elevated in CH rats, but this is blunted by the presence of supplemental CO₂. In addition, ET_{A/B} receptor inhibition prevents the CH-induced pulmonary arterial wall thickening (Kantores *et al.*, 2006). These results indicate that CO₂ inhibits CH-induced pulmonary vascular remodeling via down regulation of ET-1 signaling in the lung. A similar effect of CO₂ may exist in the setting of IH. We therefore compared effects of CO₂ supplementation on pulmonary vasoconstrictor reactivity and indices of pulmonary hypertension.

Hypoxic pulmonary vasoconstriction. Hypoxic pulmonary vasoconstriction (HPV) is a compensatory response to low alveolar O₂ tension. In physiological or pathophysiological situations in which a fraction of alveoli are hypoxic, often due to

airway constriction or obstruction, HPV facilitates the diversion of blood from these poorly ventilated regions toward those with better ventilation.

HPV can be divided into two phases. The first phase appears to be Ca^{2+} dependent because Ca^{2+} channel inhibitors prevent this response. Phase I is also at least partially intrinsic to the VSM, given that phase I persists following disruption of the endothelium (Leach *et al.*, 1994). Isolated PASMCs contract in response to acute hypoxia (Madden *et al.*, 1992), suggesting that at least the initiation of HPV is intrinsic to the SMC. The more slowly developing phase II, however, appears to be completely endothelium-dependent and mediated by VSM Ca^{2+} sensitization (Robertson *et al.*, 2003). The endothelium-derived vasoconstrictor ET-1 may act as a priming stimulus for HPV (Liu *et al.*, 2001; Sato *et al.*, 2000), which could partially explain the contribution of the endothelium to these responses. In addition, PKC activation potentiates HPV responses in isolated lungs, suggesting that PKC contributes to hypoxia-induced constriction (Orton *et al.*, 1990).

A crucial step in the mechanism of HPV is O_2 sensing. Two opposing models for intrinsic VSM O_2 sensing have gained support over the years. Both theories support an important role for mitochondrial reactive oxygen species (ROS), however the conflict lies in whether ROS increase or decrease with hypoxia. Based on measurements of ROS in isolated, perfused lungs as well as in endothelium-denuded small pulmonary arteries exposed to hypoxia, it is suggested that the mitochondria of PASMCs produce a tonic level of ROS, which is inhibited by lower O_2 tension (Archer *et al.*, 1989; Michelakis *et al.*, 2002). The decrease in ROS is proposed to cause a more reduced cytosol which then inhibits K^+ channels, effectively depolarizing the SMC membrane potential and

activating L-type Ca^{2+} channels to mediate Ca^{2+} influx and VSM cell contraction (Weir & Archer, 1995). Conversely, a hypoxic increase in ROS in the mitochondria of PASMC (Rathore *et al.*, 2008) is suggested to trigger Ca^{2+} release from the sarcoplasmic reticulum (SR) which in turn activates store-operated Ca^{2+} entry (SOCE) (Robertson *et al.*, 2000;Waypa *et al.*, 2001), contributing to a rise in VSM $[\text{Ca}^{2+}]_i$ and cell contraction. Further studies are necessary to reconcile these opposing theories.

CH-induced PH is associated with a blunted HPV response. It was initially reported that 4-6 weeks of hypobaric hypoxia attenuates pressor responses to acute hypoxia (McMurtry *et al.*, 1978) in lungs isolated from rats. It was subsequently found that merely 40 hours of hypobaric hypoxia were sufficient to diminish pressor responses to acute hypoxia (McMurtry *et al.*, 1980;Reeve *et al.*, 2001) A similar phenomenon occurs in rabbits exposed to normobaric hypoxia (Weissmann *et al.*, 2003). This decreased responsiveness to hypoxia appears to be related to decreased K^+ channel expression and activity and may be related to changes in SMC redox status (Reeve *et al.*, 2001) and NO production (Weissmann *et al.*, 2003). These data suggest that HPV is not the mechanism which sustains PH in the setting of CH.

Although little is known about effects of IH on HPV, repeated exposure to IH in a canine lobar hypoxic model suggests that repeated exposure to acute hypoxia augments HPV responses (Benumof, 1983). This idea is consistent with the effect of IH on the carotid body. IH augments carotid body and sympathetic effector responses to acute hypoxia in addition to facilitating persistent activation of carotid body and sympathetic output (Peng *et al.*, 2003). In agreement with these findings from studies of IH-exposed animals, SA patients experience persistent sympathetic nervous system activity (Carlson

et al., 1993). However, unpublished results from our laboratory suggest that, similar to CH, IH attenuates HPV responses in isolated lungs. These discrepant findings demonstrate the need for further investigation into the effect of IH on acute hypoxic vasoreactivity.

Agonist-Induced Vasoconstriction. VSM cell contractile state is also influenced by hormones, neurotransmitters and other paracrine agonists, which bind to specific receptors on the cell membrane. Many of these factors such as ET-1, UTP and 5-HT bind to G_q-coupled receptors. Upon ligand binding, these receptors activate phospholipase C which cleaves phosphatidyl inositol bisphosphate (PIP₂) yielding diacylglycerol (DAG) and inositol trisphosphate (IP₃). IP₃ binds to and activates IP₃ receptors on the SR, causing Ca²⁺ release and an increase in [Ca²⁺]_i. This Ca²⁺ release mediates SOCE, further increasing [Ca²⁺]_i. In addition, DAG directly activates receptor-operated cation channels (ROC) and also increases PKC activity, serving as an indirect activator of ROC. Thus, ROCs provide an additional contribution to the agonist-mediated increase in [Ca²⁺]_i.

Active pulmonary vasoconstriction contributes to PH, as demonstrated by the decrease in PAP in response to acute vasodilator inhalation in PH patients (MacNee *et al.*, 1983;Moinard *et al.*, 1994) and rats (Oka *et al.*, 1993). It has been appreciated for some time that agonist-induced pulmonary vasoconstriction is augmented in experimental models of PH (McMurtry *et al.*, 1978). McMurtry *et al.* showed that isolated lungs from CH rats were hyperresponsive to agonists such as angiotensin and prostaglandin F₂α (McMurtry *et al.*, 1978). Augmented pulmonary vasoconstrictor reactivity in PH has been confirmed by studies showing increased vasoreactivity to U-46619, ET-1, 5-HT, and norepinephrine (Porcelli & Bergman, 1983;Raffestin *et al.*, 1991;Snow *et al.*,

2008; Wanstall & O'Donnell, 1990). ET receptor inhibition prevents hypoxic PH (Oparil *et al.*, 1995) and reverses established PH (DiCarlo *et al.*, 1995). ET_A and ET_B receptor expression is increased during hypoxia (Li *et al.*, 1994) and ET-1 mRNA, protein and plasma levels are increased by CH (Li *et al.*, 1994), suggesting that ET-1-induced vasoconstriction may contribute to CH-induced PH.

Similar to the setting of CH, agonist-induced vasoconstriction may contribute to IH-induced PH. Indeed, previous studies from our laboratory and others indicate that IH increases pulmonary vasoconstrictor reactivity to agonists, such as the thromboxane mimetic U-46619 (Snow *et al.*, 2008), 5-HT and ET-1 (Thomas & Wanstall, 2003). Thus, increases in agonist-induced pulmonary vasoconstriction may provide an important contribution to IH-induced PH, however the mechanism by which this occurs is not understood and is a focus of this dissertation.

Mechanisms of VSM Cell Contraction

The contractile state of VSM cells is largely regulated by changes in $[Ca^{2+}]_i$. Four Ca^{2+} ions bind to calmodulin, which can then activate myosin light chain kinase (MLCK). When activated, MLCK phosphorylates the myosin regulatory light chain (MLC), facilitating actin-myosin interaction and cell shortening (Figure 2) (Takashima, 2009). Mechanisms of increases in VSM $[Ca^{2+}]_i$ are discussed below.

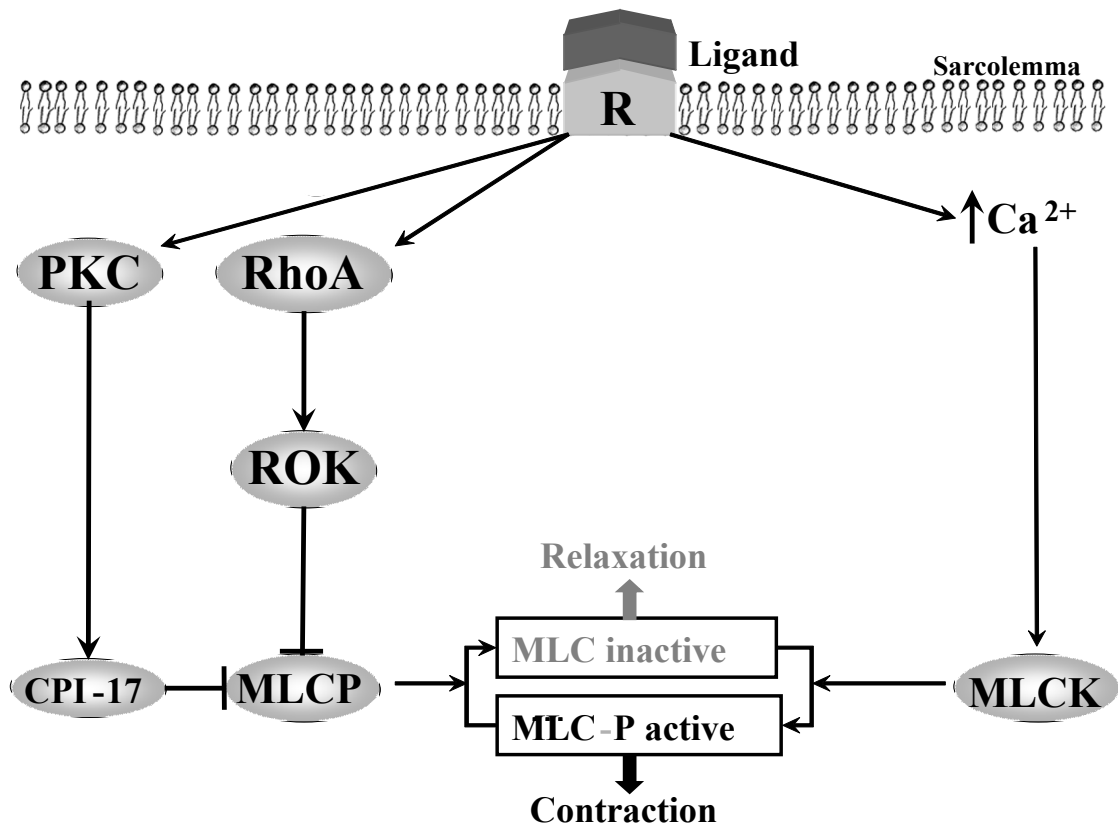


Figure 2. Vascular smooth muscle cell contraction is regulated by both increases in $[Ca^{2+}]_i$ as well as increases in Ca^{2+} sensitivity in response to receptor-mediated agonists. Rho kinase (ROK), myosin light chain (MLC), myosin light chain phosphatase (MLCP), myosin light chain kinase (MLCK).

VSM Ca²⁺ Entry Pathways

Voltage-Gated Ca²⁺ Entry. Voltage-gated Ca²⁺ channels become permeable to Ca²⁺ upon membrane depolarization. The L-type Ca²⁺ channel has been extensively characterized in VSM. These channels play a crucial role in coupling electrical signals to chemical signals. For example, ET-1 elicits depolarization of the PASMC membrane by inhibiting voltage-gated potassium channels (K_v) (Shimoda *et al.*, 2001), which are thought to be the main regulators of resting membrane potential in these cells (Shimoda *et al.*, 1998). Therefore, ET-1-induced depolarization activates L-type Ca²⁺ channels to mediate Ca²⁺ influx and increased VSM cell tone. L-type Ca²⁺ channels are also important in mediating HPV, as described above.

Store-operated Ca²⁺ entry. Store-operated Ca²⁺ entry (SOCE) is a ubiquitous Ca²⁺ entry mechanism which is activated by a fall in endoplasmic reticulum (ER) or sarcoplasmic reticulum (SR) [Ca²⁺]_i. Originally termed capacitative Ca²⁺ entry (Putney, Jr., 1986), SOCE occurs in response to receptor-mediated agonists which generate IP₃ from PIP₂. IP₃ then binds to the IP₃ receptor (IP₃R) on the SR, eliciting Ca²⁺ release. In addition to contributing to contraction in response to receptor-mediated agonists, SOCE may facilitate refilling of the intracellular Ca²⁺ stores (Jousset *et al.*, 2007; Parekh & Putney, Jr., 2005). SOCE can be elicited by pharmacologically depleting SR Ca²⁺ stores with sarcoplasmic endoplasmic reticulum Ca²⁺ ATPase (SERCA) pump inhibitors such as thapsigargin and cyclopiazonic acid. The SR Ca²⁺ sensor appears to be stromal interaction molecule 1 (STIM1) (Dziadek & Johnstone, 2007; Lu *et al.*, 2009). Until recently, the best candidates for SOC proteins were the canonical transient receptor potential (TRPC) family of non-selective ion channels, which assemble as homo- and

hetero-tetramers to form a functional channel (Sweeney *et al.*, 2002b). Studies using siRNA against TRPC1 show that it is an essential component of SOCE (Sweeney *et al.*, 2002b). However, more recently, evidence suggests an important role for TRPC5 (Ma *et al.*, 2008) and Orai1 in mediating SOCE (Potier *et al.*, 2009). Jernigan *et al.* have recently shown that acid-sensing ion channels (ASIC) additionally conduct Ca^{2+} in response to store depletion in pulmonary arteries (Jernigan *et al.*, 2009). It is likely that multiple influx pathways act in concert to mediate functional SOCE.

Receptor-operated Ca^{2+} entry. Another important Ca^{2+} entry pathway that contributes to agonist-induced increases in $[\text{Ca}^{2+}]_i$ is receptor-operated Ca^{2+} entry (ROCE). As discussed above, when an agonist binds a G_q -coupled receptor, PLC cleaves PIP_2 into IP_3 and diacylglycerol (DAG). While IP_3 has effects on IP_3 -sensitive Ca^{2+} stores, DAG activates receptor-operated non-selective cation channels (ROC) to mediate Ca^{2+} influx. Similar to SOC, TRPC proteins assemble as homo- and hetero-tetramers to form ROC. The DAG analog, OAG (1-Oleoyl-2-acetyl-*sn*-glycerol), activates ROC, which in general are comprised of TRPC 3/6/7 proteins (Hofmann *et al.*, 2000). In PSMCs, TRPC6 is thought to mediate ROCE (Lin *et al.*, 2004). The mechanism by which DAG activates ROC may be both direct (Trebak *et al.*, 2003) and indirect via activation of PKC and subsequent phosphorylation of TRPC proteins (Venkatachalam *et al.*, 2003).

The above mechanisms of increasing VSM cell $[\text{Ca}^{2+}]_i$ facilitate an increase in MLCK activity and cell contraction. In addition to mediating VSM cell contraction via changes in $[\text{Ca}^{2+}]_i$, agonists can increase contraction via changes in sensitivity to Ca^{2+} . DAG generation in response to agonist stimulation activates PKC which is a well

characterized regulator of Ca^{2+} sensitivity. A second mechanism of Ca^{2+} sensitization is involves stimulation of Rho kinase (ROK). Regulation of VSM tone via alterations in Ca^{2+} sensitivity is discussed below.

Ca²⁺ Sensitization Mechanisms

Classically, VSM cell contraction was thought to be regulated mainly by $[\text{Ca}^{2+}]_i$ levels, which are largely controlled by the mechanisms discussed above. More recently, however, it has been found that the sensitivity of the VSM to $[\text{Ca}^{2+}]_i$ is a major regulator of the contractility of the cell. As depicted in figure 2, this is accomplished by regulation of myosin light chain phosphatase (MLCP), which when active dephosphorylates the MLC, thus decreasing actin-myosin cross-bridge cycling. Two of the main signaling molecules which regulate MLCP activity are Rho kinase (ROK) and PKC. Both ROK and PKC mediate a decrease in MLCP activity, resulting in contraction that is largely independent of changes in $[\text{Ca}^{2+}]_i$. This phenomenon is termed Ca^{2+} sensitization. In addition to regulation of MLCP activity, VSM cell contraction can be regulated at the level of actin, whereby actin polymerization leads to an increase in VSM cell tone. Specifically, pressure-induced tone appears to be mediated in part by increases in filamentous actin, with inhibitors of actin polymerization attenuating myogenic constriction (Cipolla *et al.*, 2002; Flavahan *et al.*, 2005).

Rho Kinase. The serine/threonine kinase ROK is activated by the small GTPase RhoA in response to stimulation with pulmonary vasoconstrictors such as ET-1, phenylephrine and 5-HT (Figure 2) (Damron *et al.*, 2002; Guilluy *et al.*, 2009; Jernigan *et al.*, 2008). Binding of RhoA to the Rho binding domain of ROK causes a conformational

change and autophosphorylation/activation of the kinase (Somlyo & Somlyo, 2003). When activated, ROK phosphorylates MLCP at two main sites, T696 and T853 (Kawano *et al.*, 2002). Phosphorylation at T696 inhibits MLCP activity, whereas phosphorylation at T853 interferes with the binding of the MYPT1 subunit to myosin, decreasing phosphatase activity of MLCP (Feng *et al.*, 1999). In addition, ROK can mediate agonist-induced actin polymerization, which provides an additional contribution to VSM contraction (Maekawa *et al.*, 1999).

PKC. In addition to ROK-dependent Ca^{2+} sensitization, PKC mediates the other classical Ca^{2+} sensitization pathway by its phosphorylation of CPI-17 (Figure 2) (Khalil *et al.*, 1992a). PKC is a key regulatory enzyme in the pulmonary circulation, contributing to both VSM cell contractility and proliferation (Barman, 2007; Bobik *et al.*, 1990). PKC is a serine/threonine kinase which consists of at least 12 isoforms in three classes. To be active, all PKC isoforms require phosphorylation by phosphoinositide dependent kinase and at least one autophosphorylation. The autophosphorylation is facilitated by the conformational change incurred by membrane binding. The main difference between the isoforms of the three classes lies in the mechanism by which they are targeted to the membrane. Classical PKC isoforms (i.e. α/β) are regulated by both Ca^{2+} and diacylglycerol (DAG), whereas the novel PKC isoforms (i.e. δ) require DAG binding, but are regulated independently of changes in Ca^{2+} (Table 1). The atypical PKC isoforms are activated by neither increases in $[\text{Ca}^{2+}]_i$ nor DAG, but rather depend on phosphatidyl serine binding and phosphorylation (Table 1) (Violin & Newton, 2003). Several of these isoforms are expressed in VSM, with the expression profile being dependent on species,

Table 1: PKC Classes and Activation Mechanisms

PKC Class	Isoforms	Activated by
Classical	α , β I, β II, γ	Ca^{2+} and DAG
Novel	δ , ϵ , η , θ , μ	DAG
Atypical	ζ , ι , λ	Phosphatidyl serine binding and phosphorylation

as well as the type and order of vessel being studied (Haller *et al.*, 1995;Khalil *et al.*, 1992b).

PKC mediates inhibition of MLCP via phosphorylation of the 17 kDa peptide CPI-17. Phosphorylation at the single site (Thr38) of CPI-17 is sufficient to inhibit MLCP, resulting in greater Ca^{2+} sensitivity of MLC and SMC contraction (Kitazawa *et al.*, 1999). Although the MYPT1 subunit of MLCP is highly regulated by ROK and other enzymes, CPI-17 exerts its effects on smooth muscle Ca^{2+} sensitivity by inhibiting the catalytic subunit of MLCP, PP1.

VSM Ca^{2+} Homeostasis and Myofilament Ca^{2+} Sensitivity in Pulmonary Hypertension

Basal Ca^{2+} . Basal VSM cell $[Ca^{2+}]_i$ is elevated in PH (Golovina *et al.*, 2001;Yuan *et al.*, 1998). Ca^{2+} influx through L-type VGCC represents a major Ca^{2+} influx pathway in PASMC. Given that L channels are activated by membrane depolarization and PASMC E_m is more depolarized following CH (Naik *et al.*, 2005), it is possible that Ca^{2+} influx through L channels contributes to elevated basal Ca^{2+} observed following CH. In agreement with this possibility, removal of extracellular Ca^{2+} decreases basal Ca^{2+} in PASMC from CH animals but not controls (Shimoda *et al.*, 2000). Mn^{2+} quenching of fura-2 fluorescence is more rapid in PASMC from CH animals, further supporting an elevation in Ca^{2+} influx (Lin *et al.*, 2007). However, Shimoda *et al.* found that inhibition of L channels under basal conditions does not affect basal VSM Ca^{2+} in either control or CH cells (Shimoda *et al.*, 2000). Other sources of Ca^{2+} influx, such as

basal SOC and ROC activity could also mediate increased basal VSM $[Ca^{2+}]_i$. Changes in SOCE and ROCE in PH are discussed below.

Despite frequent reports of elevated basal pulmonary VSM $[Ca^{2+}]_i$ in PH, our laboratory has not observed differences in resting Ca^{2+} between PASMC from control and CH Sprague Dawley rats (Broughton *et al.*, 2008; Jernigan *et al.*, 2006; Snow *et al.*, 2009). However, this appears to be dependent on the strain of rat used, because Wistar rats do demonstrate an increase in basal PASMC $[Ca^{2+}]_i$ following exposure to CH (Snow *et al.*, 2009). Elevations in basal VSM $[Ca^{2+}]_i$ could contribute to the development of PH through increased vasoconstriction, expression of pro-growth genes and vascular remodeling.

SOCE and ROCE. Discrepant results exist regarding effects of CH on these Ca^{2+} entry pathways in pulmonary VSM. Lin and colleagues reported that CH increases pulmonary VSM SOCE and ROCE in Wistar rats which may contribute to elevated basal Ca^{2+} and spontaneous tone as well as vasoconstrictor reactivity in PH (Lin *et al.*, 2004). However, previous studies from our laboratory have revealed a decrease in SOCE and ROCE following CH in Sprague Dawley rats (Jernigan *et al.*, 2006). Based on more recent studies from our laboratory, differential effects of CH on pulmonary VSM SOCE and ROCE appear to be dependent on strain, with Wistar rats representing a response which is more similar to that found in pulmonary hypertensive mice and humans (Golovina *et al.*, 2001; Snow *et al.*, 2009; Wang *et al.*, 2006a; Yuan *et al.*, 1998; Zhang *et al.*, 2007).

In PASMC from pulmonary hypertensive animals, ROCE has been shown to be both greater (Lin *et al.*, 2004; Wang *et al.*, 2006a) and less (Jernigan *et al.*, 2006; Snow *et al.*, 2009) than control tissues. Comparison of the effects of CH on ROCE in pulmonary arteries from Sprague Dawley and Wistar rats revealed no difference in ET-1-induced ROCE (Snow *et al.*, 2009). Therefore, the contrasting results concerning ROCE in pulmonary VSM from pulmonary hypertensive patients and animals are likely a function of either tissue preparation (i.e. proximal vs. distal arteries) or protocol (i.e. DAG vs. ET-1-stimulated ROCE).

Myofilament Ca²⁺ Sensitivity. Ca²⁺ sensitization of the VSM contractile apparatus represents a significant contribution to the enhanced pulmonary vascular resistance in PH (Nagaoka *et al.*, 2004). In particular, many lines of evidence support a role for ROK-mediated pulmonary vasoconstriction in CH-induced PH (Oka *et al.*, 2008). First, acute administration of ROK inhibitors elicits vasodilation in CH hypertensive rat lungs and nearly normalizes pressures between CH and control rats (Nagaoka *et al.*, 2004). It was subsequently confirmed by Hyvelin *et al.* (Hyvelin *et al.*, 2005)) and McNamara *et al.* (McNamara *et al.*, 2008) that ROK-mediated vasoconstriction was responsible for mediating CH-induced increases in PAP in CH-exposed adult and neonatal rats. In addition, acute administration of an inhaled ROK inhibitor decreased PAP in rats with monocrotaline-induced PH and the spontaneously pulmonary hypertensive fawn-hooded rats (Nagaoka *et al.*, 2005). These studies suggest that ROK contributes to the development of PH via active vasoconstriction and not merely via vascular remodeling.

CH increases both RhoA activity and ROK expression in pulmonary arteries to mediate elevated ROK-dependent vasoconstriction in pulmonary arteries (Hyvelin *et al.*, 2005;Jernigan *et al.*, 2004b). Furthermore, effects of NO to dilate the pulmonary vasculature are mediated through inhibition ROK-dependent Ca^{2+} sensitization (Jernigan *et al.*, 2004b). Agonist-mediated constriction (Jernigan *et al.*, 2008;Weigand *et al.*, 2006) and spontaneous, myogenic tone (Broughton *et al.*, 2008) are largely dependent on ROK-dependent Ca^{2+} sensitization following CH. In addition, CH-induced PH can be prevented by chronic ROK inhibition (Hyvelin *et al.*, 2005;McMurtry *et al.*, 2003). These studies underscore the importance of ROK-dependent mechanisms in the development of PH.

Although most evidence suggests ROK is the main mediator of Ca^{2+} sensitization in hypertensive pulmonary arteries, one study points to a role for PKC-dependent Ca^{2+} sensitization, specifically in the fawn hooded rat model of idiopathic PH (Barman, 2007). ET-1-mediated constriction is elevated in the pulmonary VSM of these rats and inhibition of classical PKC isoforms potently inhibits this constriction (Barman, 2007). However, it is unclear if this is due to a relatively higher PKC expression or activity in fawn-hooded rats compared to controls. PKC-dependent constriction of systemic arteries is enhanced following IH (Allahdadi *et al.*, 2008b). The role of PKC in the pulmonary circulation following IH is unclear, but it is possible that similar to its role in the systemic circulation, PKC mediates constriction in the pulmonary circulation following IH and contributes to IH-induced PH. A focus of this study is, therefore, to determine the contribution of PKC-dependent Ca^{2+} sensitization to IH-induced increases in pulmonary vasoconstrictor reactivity.

Role of Reactive Oxygen Species (ROS) in Vascular Signaling and Pathology

Virtually all types of vascular cells produce superoxide anion (O_2^-) and hydrogen peroxide (H_2O_2) (Dikalov *et al.*, 2008; Matsubara & Ziff, 1986; Suzuki & Ford, 1999). O_2^- is generated when an electron is donated to molecular oxygen (O_2) and this is catalyzed by oxidases, such as NADPH oxidases (NOX) and xanthine oxidase (XO). O_2^- itself may modulate vascular signaling cascades, regulating contractility, cell migration and proliferation, in addition to providing a source for other ROS. Dismutation of O_2^- by superoxide dismutase (SOD) produces H_2O_2 which is a more stable form of ROS and has been shown to have direct signaling properties. While there is basal production of O_2^- , constitutive activity of SOD maintains these levels low. The main enzymes which eliminate cellular H_2O_2 are catalase, glutathione peroxidase and peroxiredoxins which convert H_2O_2 into H_2O and other metabolites (Rhee *et al.*, 1999). Under normal physiological conditions, antioxidant enzymes are sufficient to keep ROS low (Wolin, 2009). Under pathological conditions, elevated levels of ROS due to enhanced production or decreased metabolism can lead to cellular oxidative stress.

One of the best understood effects of O_2^- on vascular contractility arises from its affinity for nitric oxide (NO) which it readily scavenges and inactivates to form peroxynitrite ($ONOO^-$) (Rubanyi & Vanhoutte, 1986). Diminished NO bioavailability impairs endothelium-dependent relaxation in vessels with an intact endothelium. In addition, oxidative stress in the endothelium causes oxidation of BH_4 , an essential cofactor for endothelial nitric oxide synthase (eNOS), resulting in decreased production of NO and increased production of O_2^- , a process often referred to as eNOS uncoupling (Li *et al.*, 2006). The direct effects of O_2^- on VSM cell contractility remain less well

understood, but recent evidence suggests that O_2^- constricts intrapulmonary arteries via ROK-dependent Ca^{2+} sensitization (Jernigan *et al.*, 2008;Knock *et al.*, 2008). H_2O_2 on the other hand has been characterized as both a vasoconstrictor and a vasodilator, based upon the vascular bed and the signaling cascade in question (Ardanaz *et al.*, 2008;Burke & Wolin, 1987;Lin *et al.*, 2007). In PASMCs, exogenous H_2O_2 causes an increase in $[Ca^{2+}]_i$ via both SR Ca^{2+} release and Ca^{2+} influx to mediate cell contraction (Lin *et al.*, 2007).

ROS appear to contribute to the development of PH (DeMarco *et al.*, 2008;Elmedal *et al.*, 2004) through vascular remodeling (Jankov *et al.*, 2008) and potentially vasoconstriction. Hypoxia has been shown to elicit an increase in pulmonary artery ROS levels (Killilea *et al.*, 2000;Wang *et al.*, 2006b;Waypa *et al.*, 2001), and O_2^- generation in the vasculature is an effective stimulus for both vasoconstriction and vascular remodeling (Nagaoka *et al.*, 2004). Superoxide-dependent RhoA activation contributes to enhanced pulmonary artery vasoconstrictor reactivity following CH (Jernigan *et al.*, 2008). As discussed below, a major source of ROS in the setting of CH is NADPH oxidase (NOX) which contributes to the development of CH-induced PH. Wild type mice exposed to normobaric hypoxia have increased pulmonary artery O_2^- generation, pulmonary vascular remodeling and right ventricular hypertrophy, whereas these alterations are prevented in mice lacking the gp91phox subunit of NOX (Liu *et al.*, 2006). CH increases expression of NOX4 in pulmonary arteries (Mittal *et al.*, 2007). Similarly, NOX-derived O_2^- contributes to pulmonary vascular remodeling following IH (Nisbet *et al.*, 2008). Effects of ROS on vasoconstriction in the setting of IH are unknown and are a focus of the present study.

Enzymatic Sources of ROS

NADPH Oxidase. NOX was first characterized as a key mediator of bactericidal activity of phagocytes through its production of large quantities of O_2^- during the oxidative burst. NOX isoforms comprise a multisubunit class of enzymes which function in plasma membranes of endothelial cells, VSM cells and fibroblasts in the vascular wall (Forstermann, 2008). Two membrane spanning subunits, NOX1 (or NOX2 also known as gp91^{phox}) and p22^{phox}, three cytosolic subunits, p47^{phox}, p67^{phox} and p40^{phox} and a regulatory small G protein Rac assemble when activated to catalyze the production of O_2^- from molecular O_2 (Cave, 2009) (Figure 3). In addition, NOX4 and NOX5 are expressed in some vascular cells, where they may function independent of cytosolic subunits.

NOX is a major source of O_2^- in vascular endothelium and SMCs (Mohazzab *et al.*, 1994; Pagano *et al.*, 1993). Vascular forms of NOX (i.e. NOX1,2,4,5) are low-output enzymes, estimated to produce one third the amount of O_2^- produced by neutrophil NOX (Griendling & Ushio-Fukai, 1998). Several animal models of systemic hypertension have been shown to be dependent upon NOX (Li *et al.*, 2006; Matsuno *et al.*, 2005). In addition, NOX is implicated in contributing to PH. For example, NOX4 expression is increased in pulmonary arteries from CH mice and human patients with idiopathic PH (Mittal *et al.*, 2007). Furthermore, Rac1 and p47^{phox} expression are increased in lungs from pulmonary hypertensive lambs, and treatment with NOX inhibitors decreases ROS levels in these lungs, suggesting that NOX-dependent ROS to contribute to the development of PH (Grobe *et al.*, 2006).

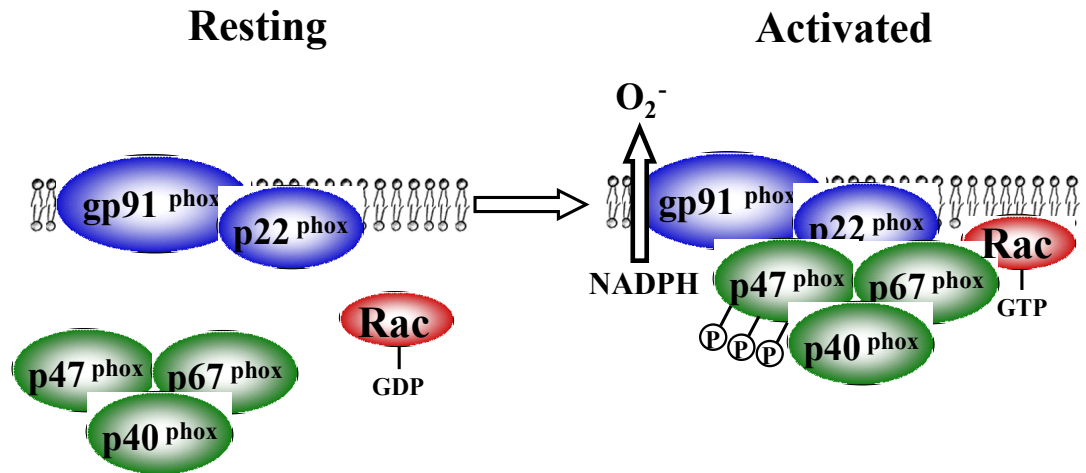


Figure 3. NADPH oxidase (NOX2-prototype NOX) is activated when three cytosolic subunits and a regulatory G protein (rac) assemble with the membrane-spanning subunits (gp91^{phox} and p22^{phox}). The active enzyme uses NADPH as a substrate and generates superoxide (O₂⁻).

CH increases O_2^- generation via NOX in intrapulmonary arteries, as shown by the lack of an increase in ROS in CH-exposed mice lacking the gp91^{phox} subunit (Liu *et al.*, 2006). Furthermore, knocking out the gp91^{phox} subunit prevents CH-induced right ventricular hypertrophy, pulmonary vascular remodeling as well as the increased vasoconstrictor reactivity (Liu *et al.*, 2006). Based on these findings that sustained hypoxia elicits PH via NOX-dependent mechanisms, it is not surprising that NOX was recently shown to contribute to IH-induced PH in mice (Nisbet *et al.*, 2009). In this study, Nisbet *et al.* found that exposure of mice to 8 weeks of IH induces PH, as evidenced by an increase in RV wall thickness and RV systolic pressure in anesthetized mice. This IH-induced PH is associated with decreased pulmonary arterial diameter, (although the vasculature was not fully dilated prior to tissue fixation), increased NOX subunit expression as well as O_2^- production in the lung (Nisbet *et al.*, 2009). Interestingly, the IH-induced PH and vascular remodeling did not occur in gp91^{phox} knockout mice. These results support a role for NOX-dependent pulmonary vascular remodeling to mediate at least a component of IH-induced PH. However, the role of NOX in pulmonary vasoconstriction following IH is unclear and is addressed in this study.

Xanthine Oxidase. XO is another major source for vascular ROS under hypoxic conditions. XO is an enzyme that catalyzes oxidative hydroxylation of purine substrates and generates O_2^- (Borges *et al.*, 2002). XO can be activated by hypoxia in cultured PSMCs (Hassoun *et al.*, 1994). In addition, Hoshikawa *et al.* found that normobaric hypoxia increases lung XO activity and that treatment of adult rats with XO inhibitor

allopurinol blunts CH-induced PH and associated pulmonary vascular remodeling (Hoshikawa *et al.*, 2001). Consistent with results in adult rats, XO inhibition in neonatal rats blunts CH-induced PH and the associated pulmonary arterial remodeling (Jankov *et al.*, 2008). Based on these findings, we further evaluated the role of XO in augmented vasoconstrictor reactivity following IH.

Mitochondrial Electron Transport Chain. Mitochondria are considered the primary cellular source of ROS formation under physiological conditions. When the mitochondrial respiratory chain is uncoupled, ROS “leak” from complexes I and III. Under normal conditions the mitochondria convert up to 5% of molecular oxygen to O_2^- (Packer L., 2002), however these mitochondrial ROS are well buffered by antioxidants in the mitochondria. The mitochondrial Mn-SOD (SOD-2) is considered the major antioxidant with regards to mitochondrial ROS generation (Faraci & Didion, 2004). This is demonstrated by the finding that mice lacking functional Mn-SOD die within weeks of birth due to cardiac abnormalities and mitochondrial damage (Packer L., 2002).

Under conditions of hypoxia/reoxygenation or IH, mitochondrial dysfunction occurs and an increase in ROS production results (Grill *et al.*, 1992). In obstructive SA patients, changes in mitochondrial cytochrome oxidase redox state during obstructive apneas contribute to elevated mitochondrial-derived ROS (McGown *et al.*, 2003). The occurrence of increased oxidative stress in systemic arteries, adrenal glands, liver and carotid bodies of rats exposed to IH (Kumar *et al.*, 2006;Kuri *et al.*, 2007;Peng *et al.*, 2006;Troncoso Brindeiro *et al.*, 2007) further supports the idea that IH increases ROS formation.

PASMC mitochondria are important in acutely sensing O_2 levels, modulating ROS production and mediating HPV responses, as discussed above (Archer *et al.*, 2008). Acute hypoxia may increase or decrease mitochondrial ROS generation to mediate increases in PASMC Ca^{2+} and vasoconstriction (Waypa *et al.*, 2006; Weir & Archer, 1995). Mitochondrial function in PASMC from patients with PH and fawn hooded rats with PH was recently reported to be disrupted, resulting in decreased ROS generation (Bonnet *et al.*, 2006). In contrast, Iqbal *et al.* reported that dysfunction of lung mitochondrial complexes I and III mediates increased ROS production in pulmonary hypertensive chickens (Iqbal *et al.*, 2001). The possibility that mitochondrial ROS production could be similarly enhanced by IH and contribute to enhanced pulmonary vasoconstrictor reactivity has not been studied. Therefore, an additional goal of the present study is to evaluate the role of mitochondrial ROS in increased pulmonary vasoconstrictor reactivity after IH.

Interactions Between ROS and Ca^{2+} Sensitization Pathways in Regulation of Vascular Tone

ROS Activate Rho Kinase. ROS may mediate their effects on pulmonary vasoconstriction via modulation of VSM Ca^{2+} sensitization pathways. In fact, O_2^- was found to cause aortic ring contraction via ROK-dependent Ca^{2+} sensitization (Jin *et al.*, 2004). In addition, our laboratory has recently shown that CH increases pulmonary VSM Ca^{2+} in response to vasoconstrictor agonists via ROS-dependent activation of RhoA/ROK signaling (Jernigan *et al.*, 2008). Consistent with these findings, Knock *et al.* recently showed that O_2^- generation with LY83583 constricts rat pulmonary arteries via ROK-

dependent Ca^{2+} sensitization (Knock *et al.*, 2008). Thus, it is plausible that IH increases vasoconstrictor reactivity via ROS-dependent activation of ROK to mediate increased pulmonary vascular resistance.

PKC Increases ROS Production. PKC can stimulate ROS generation through a variety of mechanisms, but the best characterized of those mechanisms is through activation of NOX (Inoguchi *et al.*, 2003; Rathore *et al.*, 2008; Thamilselvan *et al.*, 2009), and PKC-dependent activation of NOX is a key component of many vascular signaling pathways (Gupte *et al.*, 2009). PKC phosphorylates and activates the p47^{phox} subunit of NOX (Park & Babior, 1997), which increases ROS generation. In bovine coronary arteries, constriction in response to PKC activation is mediated largely by NOX-dependent, XO-independent ROS generation. In rat femoral veins, inhibition of $\text{PKC}\epsilon$ attenuates H_2O_2 production in response to ischemia/reperfusion (Teng *et al.*, 2008). These studies demonstrate that PKC activation occurs proximal to ROS generation in some vascular settings.

ROS Activate PKC. Although PKC-dependent generation of ROS is well established, recent studies show that ROS can also act proximal to PKC activation. Hypoxia increases mitochondrial ROS generation in PASMCs, which in turn increases $\text{PKC}\epsilon$ activity (Rathore *et al.*, 2006). This results in an increase in VSM $[\text{Ca}^{2+}]_i$. However, given the important role of PKC in Ca^{2+} sensitization, it is additionally possible that ROS mediate pulmonary artery Ca^{2+} sensitization via PKC activation in the hypertensive pulmonary circulation.

Rationale and Specific Aims

SA is an increasingly common disorder in the United States, affecting an estimated 1 in 5 adults (Young *et al.*, 2002). Those who suffer from SA have frequent nocturnal episodes of apnea, leading to nighttime IH which may be associated with hypercapnia (Bady *et al.*, 2000). In addition to causing systemic hypertension (Okabe *et al.*, 1995), SA can lead to right ventricular hypertrophy and PH (Guidry *et al.*, 2001). While some evidence suggests that IH increases pulmonary vasoconstrictor reactivity (Snow *et al.*, 2008; Thomas & Wanstall, 2003), the mechanism by which this occurs has not been well studied. Vasoconstriction has been implicated as a major component of PH in several animal models of the disease. However, it is not clear whether a similar increase in pulmonary vasoreactivity occurs with IH and what the mechanism of this potential increase is. Therefore, the objective of the current study was to determine the effect of IH on pulmonary vasoconstrictor reactivity. We hypothesized that *IH increases agonist-induced vasoconstriction via mechanisms that involve ROK, PKC and ROS*. Furthermore, considering that continuous CO₂ supplementation blunts the pulmonary hypertensive response to CH (Kantores *et al.*, 2006; Ooi *et al.*, 2000), it is possible that intermittent hypercapnia associated with SA provides a protective mechanism to limit the severity of IH-induced PH.

To test our hypothesis, we exposed rats to IH (3 min cycles of 5% O₂ air flush, 7 hr/day, 2 or 4 wk) with and without supplemental CO₂, (5% CO₂) or Sham conditions (air/air cycling for equal duration). We characterized effects of CO₂ supplementation on blood gases during IH and found that IH causes hypocapnia in the absence of

supplemental CO₂ [hypocapnic IH (H-IH)] and maintains eucapnia in the presence of CO₂ [eucapnic IH (E-IH)]. We compared effects of E-IH and H-IH on indices of PH and on vasoconstrictor reactivity in isolated small pulmonary arteries, and evaluated the contribution of ROK, PKC and ROS to enhanced vasoreactivity following IH.

Specific Aims

- 1. Compare effects of E-IH and H-IH on indices of PH and vasoconstrictor reactivity.**
- 2. Assess the role of ROK in mediating right ventricular hypertrophy and enhanced agonist-induced pulmonary vasoconstriction following E-IH**
- 3. Assess the contribution of PKC to increased agonist-mediated vasoconstriction following E-IH.**
- 4. Determine the contribution of ROS to the development of right ventricular hypertrophy and enhanced agonist-induced vasoconstriction after E-IH.**

Specific Aim 1: Compare effects of E-IH and H-IH on indices of PH and vasoconstrictor reactivity.

Hypotheses: 1) IH mediates PH and increases VSM sensitivity to receptor-mediated vasoconstrictor agonists; 2) supplemental CO₂ attenuates IH-induced polycythemia, arterial remodeling, right ventricular hypertrophy, and enhanced vasoconstrictor sensitivity.

Specific Aim 1.1 – Compare effects of E-IH and H-IH on arterial blood gases.

To characterize the degree to which breathing hypoxic/hypocapnic gas mixtures leads to arterial blood gas alterations, *we compared effects of IH with and without supplemental CO₂ on arterial O₂ and CO₂ tensions. Specifically, we measured arterial PO₂, PCO₂ and pH in rats during H-IH and E-IH cycling. In addition, we assessed arterial blood gases under noncycling conditions at the conclusion of the 4 week exposure period to determine whether E-IH produces persistent alterations in blood gas tensions reflective of renal compensation for respiratory acidosis/alkalosis.*

Specific Aim 1.2 - Assess effects of E-IH and H-IH on right ventricular hypertrophy.

Right ventricular hypertrophy closely correlates with the degree of CH-induced PH (Resta *et al.*, 1999b). *Therefore, we assessed right ventricular hypertrophy as an index of the severity of IH-induced PH and further evaluated possible inhibitory effects of supplemental CO₂ on this hypertrophic response.*

Specific Aim 1.3 – Assess the degree of polycythemia resulting from E-IH and H-IH exposure.

It is well documented that CH elicits polycythemia and this factor often correlates closely with the degree of developed PH. However, the effects of IH with and without supplemental CO₂ are less clear. *We therefore measured hematocrit in both E-IH and H-IH groups, as well as Sham-treated rats to determine the degree of polycythemia and to evaluate potential inhibitory influences of supplemental CO₂ on this response.*

Specific Aim 1.4 – Compare pulmonary arterial remodeling responses to E-IH and H-IH.

CH increases pulmonary arterial wall thickness and muscularization of arterioles, a response that may contribute to elevated pulmonary vascular resistance and resultant PH in this setting. To determine whether pulmonary arterial remodeling similarly occurs in response to IH, and to assess effects of supplemental CO₂ on this response, we measured wall thickness of small pulmonary arteries from both E-IH and H-IH rats by quantitative morphometric analyses of lung sections.

Specific Aim 1.5 - Assess effects of E-IH and H-IH on pulmonary vasoconstrictor reactivity.

Increases in vasoconstrictor reactivity may provide an important contribution to the development of CH-induced PH. CH augments vasoconstrictor reactivity of small pulmonary arteries to a number of agonists including the thromboxane mimetic U-46619 (Eichinger & Walker, 1994; Resta & Walker, 1996), ET-1 (Jernigan *et al.*, 2008), UTP (Jernigan *et al.*, 2004b) and 5-HT (Rodat *et al.*, 2007). However, effects of IH on pulmonary vasoreactivity have not been mechanistically investigated. *We, therefore, measured vasoconstrictor reactivity and VSM [Ca²⁺]_i responses to ET-1, UTP and 5-HT in isolated pulmonary arteries from Sham and IH rats.*

A portion of the work in Aim 1 has been published (Snow *et al.*, 2008).

Specific Aim 2: Assess the role of ROK in mediating right ventricular hypertrophy and enhanced agonist-induced pulmonary vasoconstriction following E-IH.

ROK represents a major agonist-dependent signaling pathway in VSM. In addition, CH increases ROK-dependent pulmonary VSM Ca^{2+} sensitization and ROK contributes to CH-mediated PH. However, whether a similar signaling mechanism mediates augmented pulmonary vasoreactivity following E-IH has not been previously addressed.

Hypothesis: E-IH augments receptor-mediated pulmonary vasoconstriction through ROK-dependent myofilament Ca^{2+} sensitization.

Specific Aim 2.1 - Evaluate the contribution of ROK to E-IH-induced RV hypertrophy.

To further strengthen this specific aim, *we designed experiments to assess the role of ROK in E-IH-dependent RV hypertrophy.* We inhibited ROK in vivo during E-IH exposure and assessed RV hypertrophy as an index of PH.

Specific Aim 2.2 - Determine the role of ROK in mediating enhanced ET-1-induced vasoconstrictor reactivity following E-IH.

Experiments in Specific Aim 1 revealed that E-IH augmented vasoconstrictor reactivity to UTP, 5-HT and ET-1, suggesting that E-IH mediates a generalized increase in reactivity to receptor-mediated agonists. Therefore, we employed ET-1 as a vasoconstrictor stimulus for all subsequent protocols to evaluate the mechanism of this enhanced vasoreactivity following E-IH. In addition, preliminary studies for Specific Aim 1 indicated that 4 weeks of E-IH exposure elicited RV hypertrophy in Wistar rats,

indicative of PH. Because E-IH more closely approximates the blood gas changes seen in patients with SA, all subsequent studies were performed in 4 week E-IH Wistar rats. Therefore, we examined effects of pharmacologic ROK inhibition on vasoconstrictor and VSM $[Ca^{2+}]_i$ responses to ET-1 in isolated, endothelium disrupted pulmonary arteries from Sham and E-IH rats.

Specific Aim 3: Assess the contribution of PKC to increased agonist-mediated vasoconstriction following E-IH.

Based on findings in Specific Aim 2 that enhanced ET-1-induced constriction after E-IH is mediated by Ca^{2+} sensitization but is independent of ROK, we sought an alternative mechanism by which E-IH increases ET-1-induced vasoconstriction. PKC represents a major Ca^{2+} sensitization mechanism, and E-IH increases PKC-dependent vasoconstriction to ET-1 in the systemic circulation (Allahdadi *et al.*, 2008b). However, effects of E-IH on PKC-dependent constriction in the pulmonary circulation are unknown.

Hypothesis: E-IH augments ET-1-induced vasoconstriction via PKC-dependent signaling.

Specific Aim 3.1 - Determine the role of PKC in enhanced ET-1-induced vasoconstriction following E-IH.

We used pharmacological approaches to examine the contribution of specific PKC isoforms to ET-1-induced vasoconstriction in pulmonary arteries from Sham and E-IH rats. These experiments employed a general PKC inhibitor (Ro 31-8220), a peptide

inhibitor of the classical PKC isoforms (myr-PKC) and a novel PKC inhibitor (rottlerin) to examine whether ET-1 mediates the elevated constriction following E-IH via a PKC-dependent signaling mechanism.

Specific Aim 3.2 - Examine the effect of E-IH on pulmonary arterial PKC expression.

Given our preliminary finding that inhibition of PKC α/β isoforms attenuated ET-1-induced constriction following E-IH, it was important to address whether E-IH mediates enhanced vasoconstriction to ET-1 via an increase in PKC α or PKC β expression. *We therefore examined PKC α/β I/ β II mRNA and protein expression in isolated pulmonary arteries from Sham and E-IH rats using real time PCR and Western blot analysis, respectively.*

Specific Aim 4: Determine the contribution of ROS to the development of right ventricular hypertrophy and enhanced agonist-induced vasoconstriction after E-IH.

Based on our findings in Specific Aim 3 that enhanced agonist-induced vasoconstriction after E-IH is mediated by PKC, and given evidence that ROS can activate PKC in pulmonary artery smooth muscle (Rathore *et al.*, 2008), we proposed the following hypothesis.

Hypothesis: E-IH augments agonist-induced pulmonary vasoconstriction via ROS-dependent PKC activation.

Specific Aim 4.1 – Determine the role of ROS in mediating E-IH-induced right ventricular hypertrophy.

We sought to determine the *in vivo* role of ROS in E-IH-induced PH. We accomplished this by chronically administering the SOD mimetic, tempol, to Sham and E-IH rats in their drinking water and *assessing right ventricular hypertrophy at the end of 4 weeks*.

Specific Aim 4.2- Assess the role of ROS in mediating augmented ET-1-induced vasoconstrictor reactivity following E-IH.

Hypoxia has been shown to increase ROS such as O_2^- and H_2O_2 in PSMCs (Killilea *et al.*, 2000; Rathore *et al.*, 2008; Waypa *et al.*, 2001) and endothelial cells (Grishko *et al.*, 2001). In addition, scavenging ROS attenuates the elevated ET-1-induced pulmonary VSM Ca^{2+} sensitization following CH (Jernigan *et al.*, 2008). However, the effects of E-IH on ET-1-induced ROS generation and vasoconstriction are unclear. We therefore conducted experiments to investigate effects of ROS scavenging on vasoconstrictor and VSM $[Ca^{2+}]_i$ responses to ET-1 in small pulmonary arteries from Sham and E-IH rats.

Specific Aim 4.3 - Evaluate the relative contributions of NOX, XO, and mitochondrial sources of ROS to increased ET-1-mediated vasoconstriction following E-IH

Major cellular sources of ROS include NOX, XO and mitochondria, and ROS have been demonstrated to occupy many significant signaling roles in VSM cells. *We designed experiments that examined whether ROS from each of these three sources*

contribute to the elevated ET-1-induced pulmonary vasoconstriction following E-IH. These experiments employed inhibitors of NOX, XO and mitochondrial ROS generation in isolated pulmonary arteries exposed to ET-1. By inhibiting each of these ROS generators, we sought to identify through which pathway ET-1 signals to mediate greater constriction following E-IH.

Specific Aim 4.4 - Determine the effect of E-IH on pulmonary arterial ROS levels under basal and stimulated conditions.

There is an increase in oxidant stress in the lungs (Kantores *et al.*, 2006) of CH pulmonary hypertensive rats as well as in patients with idiopathic PH. E-IH increases vascular ROS levels, and this contributes to systemic hypertension (Troncoso Brindeiro *et al.*, 2007). *We therefore examined whether E-IH increases pulmonary arterial ROS levels using dihydroethidium (DHE) fluorescence measurements in isolated, pressurized pulmonary arteries.* Both basal and ET-1-stimulated O₂⁻ levels were measured in vessels from Sham and E-IH rats.

Specific Aim 4.5 - Assess the role of ROS-dependent PKC activation in enhanced ET-1-dependent vasoconstriction following E-IH.

Based on evidence that ROS can activate PKC in PASMC (Rathore *et al.*, 2008), and increased reactivity to ET-1 following E-IH involves both ROS and PKC, we sought to determine whether ROS activate PKC to mediate vasoconstriction. *We therefore designed studies to investigate the relationship between ROS and PKC in mediating the augmented ET-1-induced vasoconstriction following E-IH.*

CHAPTER II

METHODS

General Methods

All protocols used in this study were reviewed and approved by the Institutional Animal Care and Use Committee of the University of New Mexico Health Sciences Center.

Experimental Groups

Male Sprague Dawley and Wistar rats (Harlan Industries) were used for all studies. H-IH, E-IH and Sham control rats were housed in Plexiglas chambers with free access to food and water and exposed to either IH or air-air sham cycling for 7 hrs/day for 2 or 4 wk as described previously (Allahdadi *et al.*, 2005; Kanagy *et al.*, 2001; Snow *et al.*, 2008). During exposure, the atmosphere was controlled by a constant flow of gas through the boxes. For H-IH and E-IH treatment, the atmosphere alternated every 90 s between room air and hypoxic (nadir $F_{IO_2} = 5\%$) or hypoxic/hypercapnic air (nadir $F_{IO_2} = 5\%$; peak $F_{ICO_2} = 5\%$), respectively. Previous studies from our group have demonstrated systemic hypertension characteristic of SA in this model of E-IH (Allahdadi *et al.*, 2005; Kanagy *et al.*, 2001). For Sham exposure, the inflow gas was always room air but the solenoid switches and inlets reproduced the noise and airflow disturbances of the IH protocol. All animals were maintained on a 12:12hr light:dark cycle.

Measurement of Right Ventricular Weight

Right ventricular hypertrophy was assessed as an index of PH, as previously described (Resta *et al.*, 1999a; Resta & Walker, 1996). Briefly, after isolation of the heart, the atria and major vessels were removed from the ventricles. The right ventricle (RV) was dissected from the left ventricle and septum (LV + S), and each was cleaned of blood and weighed. The degree of right ventricular hypertrophy is expressed as the ratio of RV to total ventricle weight (T) and as the ratio of RV to body weight (BW).

Isolation of Small Pulmonary Arteries for Dimensional Analysis

The isolated, pressurized pulmonary artery is a valuable tool for studying vasoconstrictor reactivity, because it provides assessment of VSM function independent of circulating factors, sympathetic innervation or shear stress. In addition, the endothelium can be disrupted to remove complicating influences such as endothelium-derived vasodilators or vasoconstrictors. In addition, this approach allows for simultaneous measurement of VSM $[Ca^{2+}]_i$. Due to the advantages of studying isolated, pressurized pulmonary arteries, we employed this method in order to assess vasoconstrictor reactivity, the role of Ca^{2+} signaling by measuring VSM $[Ca^{2+}]_i$ and vessel diameter.

Rats were anesthetized with pentobarbital sodium (200 mg/kg ip) and the heart and lungs were exposed by midline thoracotomy. The left lung was removed and immediately placed in ice-cold physiological saline solution [(PSS) containing (in mM) 129.8 NaCl, 5.4 KCl, 0.5 NaH_2PO_4 , 0.83 $MgSO_4$, 10 $NaHCO_3$, 1.8 $CaCl_2$, and 5.5 glucose, all from Sigma]. A 4th-5th order intrapulmonary artery [\sim 100-200 μ m inner

diameter (ID), at 12 mmHg] of ~1 mm length and without side branches was dissected free and transferred to a vessel chamber (Living Systems, CH-1) containing ice-cold PSS. The proximal end of the artery was cannulated with a tapered glass pipette, secured in place with a single strand of silk ligature, and gently flushed to remove any blood from the lumen. Before cannulation of the distal end of the artery, a strand of moose mane was passed through the lumen to disrupt the endothelium. The vessel was then stretched longitudinally to approximate its in situ length and pressurized with a servo-controlled peristaltic pump (Living Systems) to 12 mmHg. The absence of leaks was determined by turning off the servo-control function and observing maintenance of pressure. Any vessels with apparent leaks were discarded. The vessel chamber was transferred to the stage of Nikon Eclipse TS100 microscope and the preparation superfused with PSS equilibrated with a 10% O₂, 6% CO₂, and balance N₂ gas mixture. A vessel chamber cover was positioned to allow this same gas mixture to flow over the top of the chamber bath. Bright-field images of vessels were obtained with an IonOptix CCD100M camera, and dimensional analysis was performed by IonOptix Sarclen software to measure ID. The effectiveness of endothelial disruption was verified by the lack of a vasodilatory response to ACh (1 μM) in UTP (5 μM)-constricted vessels as we have previously reported (Broughton *et al.*, 2008; Jernigan *et al.*, 2004b; Jernigan *et al.*, 2004c; Jernigan *et al.*, 2006; Snow *et al.*, 2009).

Measurement of VSM [Ca²⁺]_i

Pressurized arteries (Figure 4) were loaded abluminally with the cell-permeant, ratiometric, Ca²⁺-sensitive fluorescent indicator fura-2 AM (Molecular Probes) as

described previously (Broughton *et al.*, 2008;Jernigan *et al.*, 2004b;Jernigan *et al.*, 2004c;Jernigan *et al.*, 2006;Snow *et al.*, 2009). Immediately before being loaded, fura-2 AM (1 mM in anhydrous DMSO) was mixed 2:1 with a 20% solution of pluronic acid (Invitrogen) in DMSO, and this mixture was diluted in PSS to yield a final concentration of 2 μ M fura-2 AM and 0.05% pluronic acid. Arteries were incubated in this solution for 45 min at room temperature in the dark. The diluted fura-2 AM solution was equilibrated with the 10% O₂ gas mixture during this loading period. Vessels were then rinsed for 20 min with aerated PSS (37°C) to wash out excess dye and to allow for hydrolysis of AM groups by intracellular esterases. Fura-2-loaded vessels were alternately excited at 340 and 380 nm with an IonOptix Hyperswitch dual excitation light source, and the respective 510 nm emissions were collected with a photomultiplier tube. Background-subtracted 340/380 emission ratios were calculated with IonOptix Ion Wizard software and recorded continuously throughout the experiment, with simultaneous measurement of ID from red wavelength bright-field images as described above.

In Situ Calibrations of VSM $[Ca^{2+}]_i$

In situ calibrations for Ca²⁺ were performed in pressurized arteries from Sham and E-IH rats using methods similar to those previously described (Knot & Nelson, 1998); Snow *et al.*, 2008}. Following each experiment, as described above, the VSM was

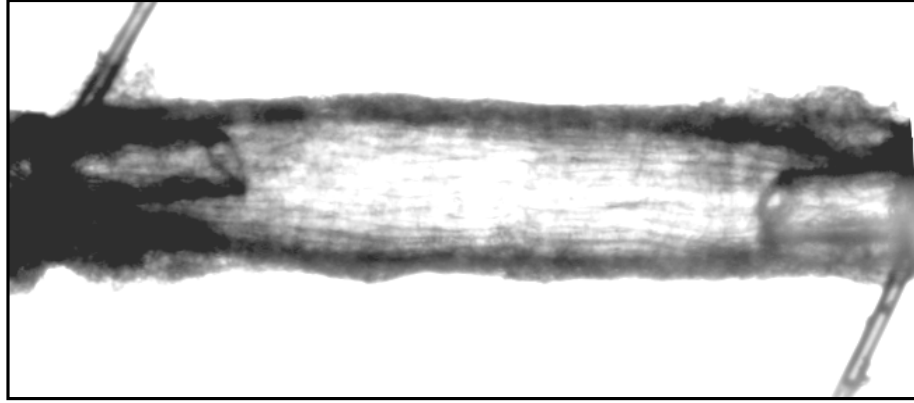


Figure 4. Isolated pressurized small pulmonary artery. Small pulmonary arteries were dissected free from adjacent lung and airway tissue. Each end was cannulated with a glass cannula and secured with strands of silk suture. Intraluminal pressure was set at 12 mmHg by a pressure servo-controller.

permeabilized to Ca^{2+} with 10 μM ionomycin, and the arteries were incubated with a bath solution containing 140 mM KCl, 5 mM NaCl, 5 mM HEPES, 1 mM MgCl_2 , 5 μM nigericin and either 5 mM EGTA (low Ca^{2+} solution) or 2 mM CaCl_2 (high Ca^{2+} solution), with a pH of 7.15 at 37°C until nadir and peak ratios were achieved. Calibrations were performed in the presence of each drug used in the study.

Calculations and Statistical Analysis

Vasoconstrictor responses were calculated as a percent of baseline ID (following pharmacological inhibitor administration) for all experiments. $\text{VSM} [\text{Ca}^{2+}]_i$ is expressed as the background-subtracted ratios of fluorescence (F) emitted following excitation at 340 and 380 nm (F_{340}/F_{380}).

All data are expressed as means \pm SEM, and values of n refer to the number of animals in each group. A t-test, one-way ANOVA or two-way ANOVA was used to make comparisons when appropriate. If differences were detected by ANOVA, individual groups were compared with the Student-Newman-Keuls test. A probability of $P < 0.05$ was accepted as significant for all comparisons.

Specific Aim 1: Compare effects of E-IH and H-IH on indices of PH and vasoconstrictor reactivity.

Preliminary studies indicated that IH alone elicits hypocapnic IH while IH with CO_2 supplementation causes eucapnic IH, thus we used the terminology H-IH and E-IH, respectively to describe our models.

Specific Aim 1.1 – Compare effects of E-IH and H-IH on arterial blood gases.

To characterize the degree of arterial hypoxemia induced by exposure to IH cycling, *in vivo* arterial blood gases were measured just prior to, during and after exposure to H-IH and E-IH. In addition, arterial PCO₂ and pH were assessed in order to determine whether exposure to supplemental CO₂ leads to hypercapnia and arterial acidosis or rather results in sustained eucapnic conditions. Blood samples were obtained quickly during cycling via femoral arterial catheters. Blood was kept in capped syringes on ice until being analyzed via ABL5 blood-gas analyzer.

To measure arterial blood gases, rats were anesthetized with isoflurane and arterial lines surgically inserted in the abdominal aorta via the femoral artery. Catheters were tunneled subcutaneously to the back of the neck where they were threaded through a plastic harness into a metal spring. The line and spring exited the cage through a small hole in the Plexiglas lid and were attached to a plastic swivel to allow the animal freedom of movement within the cage. The line was filled with saline containing heparin (10 U/ml) and flushed daily. After 7 days of recovery, three arterial blood samples were drawn to measure arterial blood gases using an ABL5 blood-gas analyzer: the first prior to the H-IH or E-IH exposure, the second during the nadir or most hypoxic portion of the cycling period ($\approx 5\%O_2$; $\approx 5\%CO_2$) and the third at the peak of the air flush ($\approx 20\%O_2$; $\approx 0\%CO_2$). These groups of rats were not carried out to 2 weeks of treatment for further study.

To determine whether 4 weeks of E-IH exposure causes any long term arterial blood gas derangements, an additional group of animals was instrumented with femoral

arterial catheters at the end of 4 weeks E-IH exposure. Blood samples were then taken before cycling began for the day, at the O₂ nadir and at the peak of recovery, similar to the above samples.

Specific Aim 1.2 - Assess effects of E-IH and H-IH on right ventricular hypertrophy.

To determine whether H-IH and E-IH elicit pulmonary hypertension, RV/T and RV/BW were assessed as an index of pulmonary hypertension, as described above. RV/T and RV/BW are measures of right ventricular hypertrophy which correlates with increases in pulmonary artery pressure (Resta *et al.*, 1999b).

Specific Aim 1.3 - Assess the degree of polycythemia resulting from E-IH and H-IH exposure.

CH, which is a potent stimulus for the development of PH and right ventricular hypertrophy, also elicits a profound increase in hematocrit. Hematocrit may be a contributing factor to IH-induced PH, thus effects of IH on hematocrit were assessed. Following lung isolation, blood samples were collected by direct cardiac puncture for measurement of hematocrit. Exposure to supplemental CO₂ has been shown to limit CH-induced polycythemia (Neckar *et al.*, 2003), so the effects of both H-IH and E-IH on hematocrit were assessed in rats exposed to 2 and 4 weeks of E-IH or Sham conditions.

Specific Aim 1.4 – Compare pulmonary arterial remodeling responses to E-IH and H-IH.

Idiopathic and CH-induced PH are associated with arterial remodeling which may encroach on the pulmonary arterial lumen, increasing vascular resistance and manifesting

a fixed component of pulmonary hypertension. To assess the degree of remodeling as a further index of the degree of PH, vascular morphometry was performed on arterial cross sections in lungs from each group of rats. Furthermore, CO₂ supplementation blunts CH-induced pulmonary vascular remodeling (Kantores *et al.*, 2006;Ooi *et al.*, 2000). Therefore, we assessed whether E-IH exposed rats had blunted pulmonary vascular remodeling as compared with H-IH rats.

Vascular Morphometry

Effects of H-IH, and E-IH on pulmonary arterial remodeling were compared by quantitative morphometric analyses of arterial cross-sections in lungs from each group of rats as we have described previously (Resta *et al.*, 1997;Resta *et al.*, 1999b;Resta *et al.*, 2001). Lungs were isolated from rats using established procedures (Resta *et al.*, 1997;Resta *et al.*, 1999a;Resta & Walker, 1996). Animals were anesthetized with sodium pentobarbital (200 mg/kg, i.p.). After cannulating the trachea with a 17-gauge needle stub, the lungs were ventilated using a Harvard positive pressure rodent ventilator (model 683) at a frequency of 55 breaths/min and a tidal volume of 2.5 mL with a warmed and humidified gas mixture (6% CO₂, 21% O₂, balance N₂). Peak inspiratory pressure was set at 9 cm H₂O and positive end-expiratory pressure was maintained at 3 cm H₂O. After a median sternotomy, heparin (100 U in 0.1 mL) was injected directly into the right ventricle, and the pulmonary artery cannulated with a 13-gauge needle stub. The preparation was immediately perfused at 0.8 mL/min by a Masterflex microprocessor pump drive (model 7524-10) with PSS containing (in mM) 129.8 NaCl, 5.4 KCl, 0.5 NaH₂PO₄, 0.83 MgSO₄, 19 NaHCO₃, 1.8 CaCl₂ and 5.5 glucose with 4% bovine serum albumin (wt/vol) added as a colloid. Papaverine (10⁻⁴ M) was also included in the PSS to

maintain the vasculature in a dilated state during subsequent fixation. The left ventricle was cannulated with a plastic tube (4 mm o.d.), and the heart and lungs were removed *en bloc* and suspended in a humidified chamber maintained at 38°C. The perfusion rate was gradually increased to 60 mL·min⁻¹·kg body wt⁻¹. Perfusate was pumped through a water-jacketed bubble trap maintained at 38°C prior to entering the pulmonary circulation. Experiments were performed with lungs in zone three conditions, achieved by elevating the perfusate reservoir until venous pressure was ~12 mmHg. Previous work from our laboratory suggests that maximal recruitment and thus maximal vascular surface area is achieved at this flow and P_v (Eichinger & Walker, 1996). Pulmonary arterial pressure and venous pressure were measured via side ports in the arterial and venous lines using Spectramed model P23 XL pressure transducers and recorded on a Gould RS 3400 chart recorder. The vasculature was initially washed with 250 mL of PSS, followed by 250 mL of fixative (0.1 M phosphate-buffered saline with 4% paraformaldehyde, 0.1% glutaraldehyde, and 10⁻⁴ M papaverine). Lungs were additionally inflated with fixative via the trachea to a pressure of 25 cm H₂O during perfusion. The trachea was ligated with 2-0 silk, the arterial and venous lines simultaneously clamped, and the lungs immersed in fixative. A transverse section (2-3 mm thick) of tissue from the left lobe was removed and rinsed in phosphate-buffered saline. Sections were dehydrated in increasing concentrations of ethanol, cleared in xylene, and mounted in paraffin.

Transverse sections of the left lung were cut (4 µm thick) and mounted onto Superfrost Plus slides (Fisher Scientific). Sections were stained for elastin (Sigma Accustain Elastic Stain kit) and arteries identified by the presence of an internal elastic lamina (Resta *et al.*, 1997; Resta *et al.*, 1999a; Resta *et al.*, 2001). Vessels were examined

with a $\times 40$ objective on a Nikon Optiphot microscope, and images generated with a digital CCD camera (Photometrics CoolSNAP_{cf}) and processed with MetaMorph software (Universal Imaging Corp.). Measurements included medial circumference, assessed from the outer margin of the external elastic lamina, and luminal diameter (Greenberg & Kishiyama, 1993), and were made using a blinded analysis.

External and luminal arterial diameters were calculated from the medial and luminal circumferences, respectively. Arterial wall thickness was assessed by subtracting luminal radius from external radius, and expressed as a percent of external diameter according to the following formula:

$$[(2 \times \text{wall thickness})/\text{external diameter}] \times 100$$

Specific Aim 1.5 – Assess effects of E-IH and H-IH on vasoconstrictor reactivity.

Vasoconstriction may provide an important contribution to the development of IH-induced PH. CH augments vasoconstrictor reactivity to agonists such as U-46619 (Eichinger & Walker, 1994; Resta & Walker, 1996), ET-1 (Jernigan *et al.*, 2008), UTP (Jernigan *et al.*, 2004b) and 5-HT (Rodat *et al.*, 2007). However, the effects of E-IH on vasoconstrictor reactivity are unknown. Based on findings in Specific Aim 1 that polycythemia and pulmonary vascular remodeling are severely blunted in E-IH rats compared to H-IH rats, in spite of considerable RV hypertrophy, we assessed vasoconstrictor and VSM Ca²⁺ responses to receptor-mediated agonists.

Following the fura-2 AM loading and 20 min equilibration, vessels from either group were exposed to increasing concentrations of ET-1 (10^{-11} - 10^{-7} M, Sigma), UTP (10^{-

$7\text{-}3\times 10^{-3}$ M, Sigma), or 5-HT (10^{-9} - 3×10^{-3} M, Sigma) generating a concentration response curve.

Specific Aim 2: Assess the role of ROK in mediating right ventricular hypertrophy and enhanced agonist-induced pulmonary vasoconstriction following E-IH.

ROK mediates a major agonist-induced signaling pathway in VSM, and CH increases ROK-dependent pulmonary VSM Ca^{2+} sensitization. Furthermore, ROK plays a role in CH-induced PH. However, it is unclear if a similar signaling mechanism contributes to augmented pulmonary vasoconstrictor reactivity following E-IH. Based on findings in Specific Aim 1 that E-IH elicited RV hypertrophy and increased pulmonary vasoconstrictor reactivity and because E-IH most closely approximates arterial blood gas changes during SA, E-IH was used for all subsequent experiments.

Specific Aim 2.1 – Evaluate the contribution of ROK to E-IH-induced RV hypertrophy.

To examine the role of ROK in the development of E-IH-induced pulmonary hypertension, *in vivo* ROK inhibition was performed with subsequent evaluation of right ventricular hypertrophy as an index of PH.

Osmotic Pump Implantation

Rats were instrumented with subcutaneous osmotic minipumps to continuously administer the ROK inhibitor fasudil for 4 weeks, during exposure to either Sham or E-IH treatment. Animals were placed in a clean Plexiglass chamber prefilled with isoflurane gas (4.5%) for induction of anesthesia. Rats were then administered

buprenorphine (0.015 mg/kg s.c.) analgesia, atropine sulfate (54 µg, s.c.) to inhibit bronchial secretions during surgery and 2-3 ml of warmed, sterile 0.9% NaCl solution (s.c.) to minimize dehydration during surgery. The rats were then ventilated with 2% isoflurane/98% oxygen, while secured to a surgical board. Osmotic pumps (Alzet model 2ML4) containing fasudil, dissolved in sterile saline, were implanted subcutaneously via midline incision between the scapulae for 4 wk administration of fasudil (30 mg/kg/day, LC Labs). This dose of fasudil has previously been shown to markedly reduce the development of PH in fawn-hooded rats which spontaneously develop pulmonary hypertension at moderate altitude (Nagaoka *et al.*, 2006). Following overnight recovery from surgery, rats were placed in either Sham or E-IH treatment.

Specific Aim 2.2 – Determine the role of ROK in mediating enhanced ET-1-induced vasoconstrictor reactivity following E-IH.

To examine the possibility that a ROK-dependent myofilament Ca²⁺ sensitization mechanism mediates the augmented vasoconstrictor reactivity following E-IH, vasoconstrictor and VSM [Ca²⁺]_i responses to ET-1 were assessed in pulmonary arteries from Sham and E-IH rats in the presence of the ROK inhibitor fasudil (10 µM, LC Labs) This concentration of fasudil inhibits ROK-dependent constriction in this preparation (Broughton *et al.*, 2008;Jernigan *et al.*, 2008)

Specific Aim 3: Assess the contribution of PKC to increased agonist-mediated vasoconstriction following E-IH.

Specific Aim 3.1 - Determine the role of specific PKC isoforms in mediating enhanced ET-1-induced vasoconstriction following E-IH.

ET-1-induced Vasoconstriction in Isolated Vessels in the Presence of a General PKC Inhibitor

To determine if the augmented ET-1-induced VSM Ca^{2+} sensitization following E-IH is mediated by PKC signaling, we measured vasoconstrictor and VSM Ca^{2+} responses to ET-1 in the presence of the general PKC inhibitor Ro 31-8220 in isolated arteries from Sham and E-IH rats. Prior to the application of increasing ET-1 concentrations, isolated, pressurized, fura-2 loaded vessels were exposed to Ro 31-8220 (5 μ M, Biomol). This concentration of Ro 31-8220 has previously been reported to inhibit contractile responses to 5-HT in isolated aortas from Wistar Kyoto and spontaneously hypertensive rats (Budzyn *et al.*, 2008). In addition, this concentration of Ro 31-8220 abolished pulmonary vasoconstrictor responses to the phorbol ester phorbol 12-myristate 13-acetate PMA (10^{-8} - 3×10^{-6} M; Sigma) (See Results Figure 20). Ro 31-8220 acts by inhibiting the catalytic site of several PKC isoforms (Salamanca & Khalil, 2005). Following 10 minutes of equilibration with Ro 31-8220 and attainment of a stable inner diameter and F_{340}/F_{380} ratio, a concentration response curve to ET-1 was performed.

ET-1-Induced Constriction in Isolated Vessels in the Presence of a PKC α/β Inhibitor

To determine if the observed increase in ET-1-induced, PKC-dependent vasoconstriction following E-IH is mediated by classical PKC isoforms, we measured

ET-1-induced vasoconstriction in the presence of PKC α/β inhibition. Arteries were pretreated with the cell permeable myristoylated PKC α/β pseudosubstrate inhibitor [20-28] (myr-PKC) (10 μ M, Biomol) and vasoconstriction to ET-1 was assessed as described above. Incubation for 45 minutes with this concentration of myr-PKC partially inhibited constrictions to PMA in pulmonary arteries (Results Figure 22) indicating that this concentration of myr-PKC inhibits PKC α/β , although isoforms other than PKC α/β contribute to PMA-induced constriction.

ET-1-induced Constriction in Isolated Vessels in the Presence of a PKC δ inhibitor

Given that ET-1-induced Ca²⁺ sensitization following E-IH is mediated by PKC δ in systemic arteries (Allahdadi *et al.*, 2008b), we sought to determine if the observed increase in ET-1-induced pulmonary vasoconstriction following E-IH is mediated by the novel PKC isoform (PKC δ). To address this question, pulmonary arterial vasoconstrictor and VSM Ca²⁺ responses to ET-1 were assessed in the presence of the PKC δ inhibitor, rottlerin (3 μ M, Biomol). Incubation with this concentration of rottlerin partially inhibited constrictions to PMA in pulmonary arteries (Results Figure 24).

Specific Aim 3.2 - Examine the effect of E-IH on pulmonary arterial PKC expression.

Effects of E-IH on PKC mRNA expression

Given our finding that enhanced ET-1-mediated vasoconstriction following E-IH is dependent on PKC α/β but not PKC δ , it is possible that there is an increase in PKC α/β but not PKC δ mRNA expression. To determine the level of PKC α/β mRNA

expression in pulmonary arteries from Sham and E-IH rats, we performed real time PCR on mRNA isolated from pulmonary arteries from both groups.

Pulmonary arteries from Sham and E-IH rats were stored in *RNAlater* (Ambion). Total RNA was isolated using the RNEasy Mini Kit (Qiagen) using the manufacturer's protocol. The High Capacity Reverse Transcription kit (Applied Biosystems) was used for reverse transcription of total RNA to cDNA. For real-time PCR detection, Taqman gene expression assay kits were used for rat PKC α and β .

Effects of E-IH on PKC Protein Expression

Expression of classical PKC isoforms was measured by western blot using antibodies specific for PKC α , PKC β I and PKC β II, using a protocol similar to previously published work (Jernigan *et al.*, 2008). To obtain sufficient tissue for analysis, intrapulmonary arteries (approximately 2nd through 5th order) were isolated from the right and left lungs of Sham and E-IH rats in *HEPES-based PSS* (in mM, 130 NaCl, 4 KCl, 1.2 MgSO₄, 4 NaHCO₃, 1.8 CaCl₂, 10 HEPES, 1.18 KH₂PO₄, 6 glucose, and 0.03 EDTA, pH adjusted to 7.4 with NaOH, all from Sigma). A HEPES-based PSS was used to maintain a pH near 7.4 during incubation since the solution was not aerated with 10% O₂, 6% CO₂, balance N₂ gas mixture as in vasoreactivity studies. Each sample was homogenized in 10 mM Tris-HCl homogenization buffer containing 255 mM sucrose, 2 mM EDTA, 12 μ M leupeptin, 1 μ M pepstatin A, 0.3 μ M aprotinin, and 1 mM phenylmethylsulfonyl fluoride (all from Sigma). Samples were centrifuged at 10,000 x g for 10 min at 4°C to remove insoluble debris. The supernatant was collected, and sample protein concentrations were determined by the Bradford method (Bio-Rad Protein Assay). Control experiments were

performed with increasing concentrations of protein to ensure linearity of the densitometry curve.

Pulmonary artery lysates (25 µg/lane) were separated by SDS-PAGE (7.5% Tris-HCl gels, Bio-Rad) and transferred to polyvinylidene difluoride membranes. Blots were blocked for 1 h at room temperature with 2.5% BSA and 2.5% milk in 0.05% Tween 20 (Bio-Rad) TBS. Blots were then incubated overnight at 4°C with monoclonal antibodies to PKC α or PKC β I, or a polyclonal antibody raised against PKC β II (1:200, Santa Cruz). For immunochemical labeling, blots were incubated 1 h at room temperature with goat anti-mouse (PKC α / β I) or goat anti-rabbit (PKC β II) IgG-horseradish peroxidase (HRP, 1:3000, Bio-Rad). After chemiluminescence labeling (ECL, Amersham), PKC α / β I/ β II bands were detected by exposing the blots to chemiluminescence-sensitive film (Kodak). Quantification of the bands was achieved by densitometric analysis of scanned images (SigmaGel software, SPSS). Bands for PKC α / β I/ β II were normalized to total protein (Coomassie staining).

Calculations and Statistics

The normalized gene expression method ($2^{-\Delta\Delta CT}$) was used for relative quantification of gene expression by real time PCR. For western blot, PKC band density was compared to total protein density (Coomassie staining) for each lane. A probability of $P < 0.05$ was accepted as statistically significant for all comparisons.

Specific Aim 4: Determine the contribution of ROS to the development of right ventricular hypertrophy and enhanced agonist-induced vasoconstriction after E-IH.

Specific Aim 4.1 - Assess the role of ROS in mediating E-IH-induced right ventricular hypertrophy.

To assess whether elevated ROS levels following E-IH mediate the development of PH, we treated Sham and E-IH rats with the superoxide dismutase mimetic tempol (4-hydroxy-2,2,6,6-tetramethyl-piperidine-1-oxyl, Fluka) (1 mM in their drinking water) for 4 weeks. Right ventricular hypertrophy was then assessed as an index of pulmonary hypertension. This method for administering tempol has previously been shown to attenuate E-IH-induced increases in systemic vascular ROS levels and to prevent the development of systemic hypertension (Troncoso Brindeiro *et al.*, 2007).

Specific Aim 4.2 - Assess the role of O_2^- and H_2O_2 in mediating augmented ET-1-induced vasoconstrictor reactivity following E-IH.

The role of ROS in mediating augmented ET-1-induced vasoconstrictor reactivity following E-IH was examined by scavenging ROS with the membrane permeable spin trap agent, tiron (10 mM, Sigma), and performing concentration response curves to ET-1 as above. Tiron was present during the fura-2 loading period and throughout the rinse period and remainder of the experiment. We have previously used this concentration of tiron to scavenge ROS in isolated lungs (Jernigan *et al.*, 2004a) and isolated arteries (Jernigan *et al.*, 2004c). In addition, we have shown that this concentration of tiron attenuates xanthine/xanthine oxidase-induced increases in DCF fluorescence in isolated

pulmonary arteries (Jernigan *et al.*, 2004a). Vasoconstrictor reactivity was expressed as percentage constriction from baseline (as above) and VSM Ca^{2+} responses were expressed as a change in the F_{340}/F_{380} ratio.

In addition, the role of H_2O_2 in mediating augmented vasoconstrictor reactivity to ET-1 after E-IH was assessed by decreasing H_2O_2 levels with cell permeable PEG-catalase (250 U/ml, Sigma). This concentration of PEG-catalase has been used to scavenge H_2O_2 in isolated pulmonary arteries (Fike *et al.*, 2008).

Specific Aim 4.3 - Evaluate the relative contributions of NOX, XO, and mitochondrial sources of ROS to increased ET-1-mediate vasoconstriction following E-IH.

Effects of Inhibition of NOX on ET-1-Induced Vasoconstrictor Reactivity

Examination of the role of NOX in mediating elevated ET-1-induced vasoconstriction after E-IH was accomplished by inhibiting NOX1/2 with apocynin (30 μ M, Sigma). Unpublished studies from our laboratory indicate that this concentration of apocynin selectively attenuates pulmonary vasoconstrictor reactivity in arteries from CH rats. Apocynin was added to the vessel superfusate following the fura-2 loading and maintained in the solution for the remainder of the experiment. Although concerns have been raised about the selectivity of apocynin for inhibition of NOX (Heumuller *et al.*, 2008), a recent study found that apocynin inhibits the acute hypoxia-induced increase in NOX activity and DCF fluorescence in PSMCs to a similar degree as genetic knockout of the $p47^{phox}$ subunit (Rathore *et al.*, 2008). ET-1-induced vasoconstrictor and VSM Ca^{2+} responses were assessed as described above.

Effects of Inhibition of Xanthine Oxidase on ET-1-Induced Vasoconstriction

The role of XO in mediating augmented ET-1-induced vasoconstrictor reactivity following E-IH was examined by inhibiting XO with allopurinol (100 μM , Sigma) (Massey *et al.*, 1970). Following fura-2 loading and rinsing, allopurinol was added to the bath solution and kept for the remainder of the experiment. Vasoconstrictor and VSM $[\text{Ca}^{2+}]_i$ responses to ET-1 were assessed as above.

Effects of Inhibition of Mitochondrial ROS Generation on ET-1-Induced Vasoconstriction

Responses to ET-1 were assessed in the presence of the specific mitochondrial ROS scavenger mito-carboxy proxyl (MITO-CP, kindly provided by Navdeep Chandel, Northwestern University). This mitochondrial-targeted nitroxyl facilitates dismutation of superoxide as well as mitigating H_2O_2 -induced cell apoptosis (Dhanasekaran *et al.*, 2005). MITO-CP (0.5 μM) was added to the artery superfusate following fura-2 loading and equilibration. A recirculating system was used and the drug was maintained in the solution during the addition of increasing concentrations of ET-1 (as described above). Confirmatory experiments using the mitochondrial complex I inhibitor rotenone (10 μM , Sigma) were also conducted. This concentration of rotenone has been used to inhibit hypoxia-induced O_2^- generation in PASMC (Wang *et al.*, 2007). Rotenone was administered during fura-2 loading, the subsequent rinse and during ET-1 exposure, because rotenone is a reversible inhibitor of complex I. Vasoconstrictor and VSM Ca^{2+} responses were assessed in response to ET-1 as above.

Specific Aim 4.4 - Determine the effect of E-IH on arterial ROS levels under basal and stimulated conditions.

Dihydroethidium (DHE, Molecular Probes) was used to evaluate effects of E-IH on basal and ET-1-induced ROS production in isolated, pressurized pulmonary arteries. DHE is cell permeant and in the presence of O_2^- , it is converted to the fluorescent products ethidium and 2-hydroxyethidium (Dikalov *et al.*, 2007; Jernigan *et al.*, 2008; Zhao *et al.*, 2005). Pulmonary arteries were isolated, cannulated and endothelium-disrupted as described above, with the exception of the makeup of the buffer. HEPES-based PSS (in mM, 130 NaCl, 4 KCl, 1.2 $MgSO_4$, 4 $NaHCO_3$, 1.8 $CaCl_2$, 10 HEPES, 1.18 KH_2PO_4 , 6 glucose, and 0.03 EDTA, pH adjusted to 7.4 with NaOH). A HEPES-based PSS was used to maintain physiological pH during dissection since the solution was not aerated with the 10% O_2 , 6% CO_2 , balance N_2 gas mixture used for vasoreactivity protocols. Following 30-min equilibration, the pressurized pulmonary arteries were loaded with DHE (10 μM DHE and 0.02% pluronic acid). Vessels were incubated in this solution for 30 min at room temperature in the dark and then rinsed for 5 min with PSS to wash out excess dye. We obtained fluorescent images using a standard tetramethylrhodamine isothiocyanate (TRITC) filter (excitation ~ 550 nm and emission ~ 600 nm). Basal fluorescence was measured at 1 frame/ min for ~ 5 min. ET-1 (10^{-8} M) was added to the superfusate and DHE fluorescence was monitored for 10 min. Images were generated with a CCD camera (Hamamatsu Orca R2) and processed with Andor IQ 1.9 software. Normalized fluorescence intensity is defined as background-subtracted mean intensity of grey-scale values for defined regions of interest, which were constant between all vessels. In separate experiments, vessels were pretreated with tiron (10 mM)

before (30 min) and during DHE loading and throughout the experiment. In addition, a group of vessels was treated with myr-PKC (10 μ M) before (30 min) and during DHE loading.

Specific Aim 4.5 - Assess the role of ROS-dependent PKC activation in enhanced ET-1-dependent vasoconstriction following E-IH.

Effect of Combined ROS Scavenging and PKC Inhibition on Vasoconstrictor Reactivity to ET-1

To address whether ROS and PKC contribute to enhanced ET-1-induced vasoconstriction after E-IH through a common signaling pathway, vasoconstrictor and VSM Ca^{2+} responses to ET-1 were assessed during combined O_2^- scavenging and PKC inhibition using a tiron/Ro 31-8220 cocktail.

Effect of Combined PKC α/β Inhibition on Basal and ET-1-Stimulated ROS Production

To determine whether PKC α/β mediate ET-1 induced O_2^- generation following E-IH, basal and ET-1-stimulated DHE fluorescence were measured in the presence of a PKC α/β inhibitor. Vessels were incubated with myr-PKC (10 μ M) 30 min prior to DHE loading and during DHE loading. Because the cell permeant myristoylate group of myr-PKC is cleaved once myr-PKC is internalized into the cell, rinsing the inhibitor should not decrease its concentration in the cell.

Calculations and Statistics

All data were expressed as means \pm SE and values of n refer to the number of animals in each group. Two-way ANOVA was used to compare vasoconstriction and VSM Ca^{2+} data between groups. Two-way repeated measures ANOVA was used to compare basal vs. ET-1-stimulated DHE fluorescence values. If differences were detected by ANOVA, individual groups were compared with the Student-Newman-Keuls test. A probability of $P < 0.05$ was accepted as significant for all comparisons.

CHAPTER III

RESULTS

Specific Aim 1: Compare effects of E-IH and H-IH on indices of PH and vasoconstrictor reactivity.

Specific Aim 1.1 - Compare effects of E-IH and H-IH on arterial blood gases.

To characterize the cyclical changes in arterial PO_2 , PCO_2 and pH that occur during H-IH and E-IH exposure, we measured arterial blood gases on the first day of cycling in both groups of rats. Prior to the first hypoxic stimulus, PO_2 values were not different between H-IH and E-IH groups (Figure 5, Pre). Both H-IH and E-IH rats showed the anticipated decrease in PO_2 during hypoxic exposure (Figure 5, Nadir) and both groups recovered to pre stimulus PO_2 values during the air flush (Figure 5, Post). In addition, PCO_2 values were not different between groups before exposure to hypoxia and CO_2 (Figure 6, Pre), however, H-IH animals were hypocapnic while E-IH animals remained eucapnic during nadir O_2 and peak CO_2 exposures (Figure 6, Post). During the air flush, H-IH animals remained slightly hypocapnic (Figure 6, Post). As expected, pH measurements were inversely related to P_{CO_2} (Figure 7). Based on these data, we designated our treatments H- IH and E- IH.

At the end of four weeks of E-IH exposure, arterial blood samples were taken from Wistar rats as above to determine whether chronic IH results in any long term

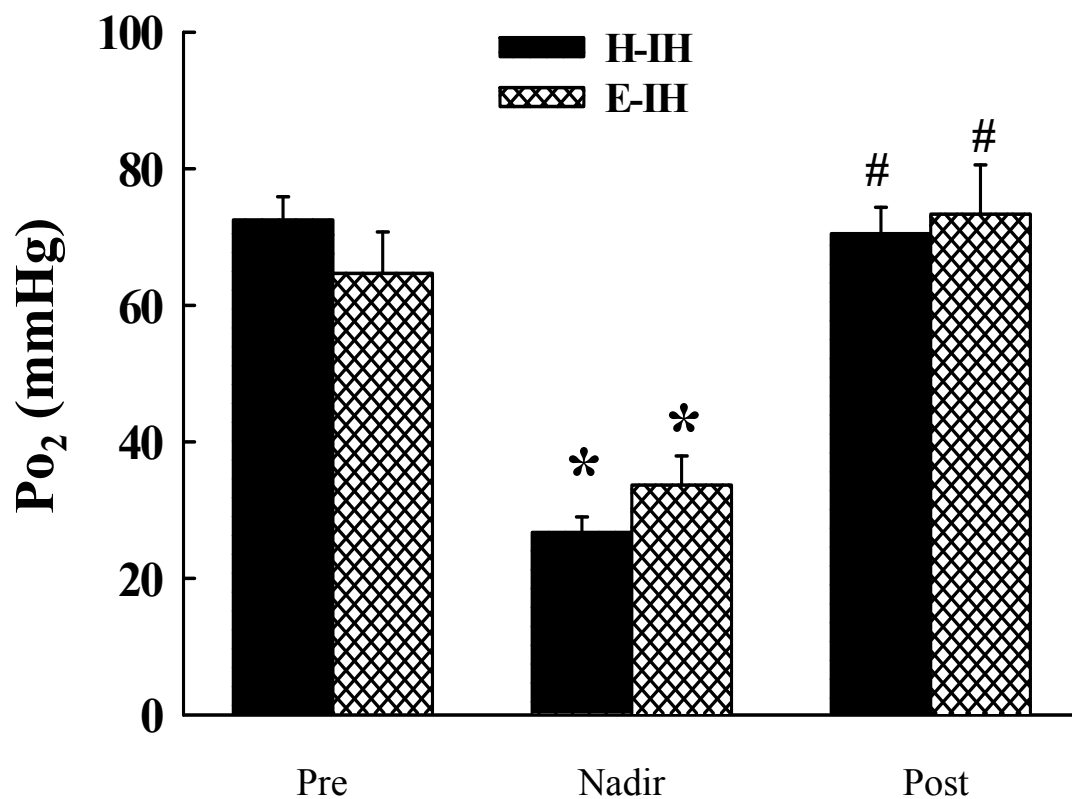


Figure 5. Arterial PO₂ measurements from Sprague Dawley rats before (Pre) during (Nadir) and after (Post) acute H-IH or E-IH exposure. Values are means ± SE of n= 4-5 rats/treatment. * P < 0.05 vs. respective pre- exposure value. # P < 0.05 vs. nadir value.

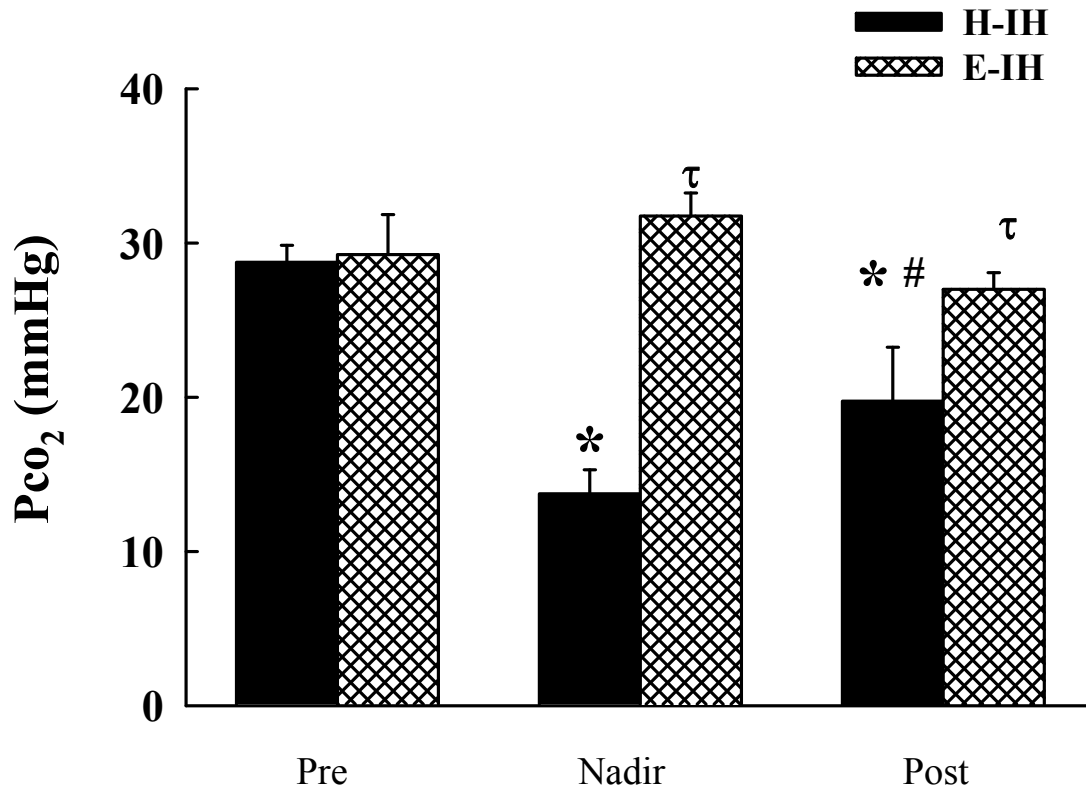


Figure 6. Arterial PCO₂ measurements from Sprague Dawlery rats before (Pre) during (Nadir) and after (Post) acute H-IH or E-IH exposure. Values are means ± SE of n= 4-5 rats/treatment. * P < 0.05 vs. respective pre exposure value. # P < 0.05 vs. nadir value. τ P < 0.05 vs. H-IH.

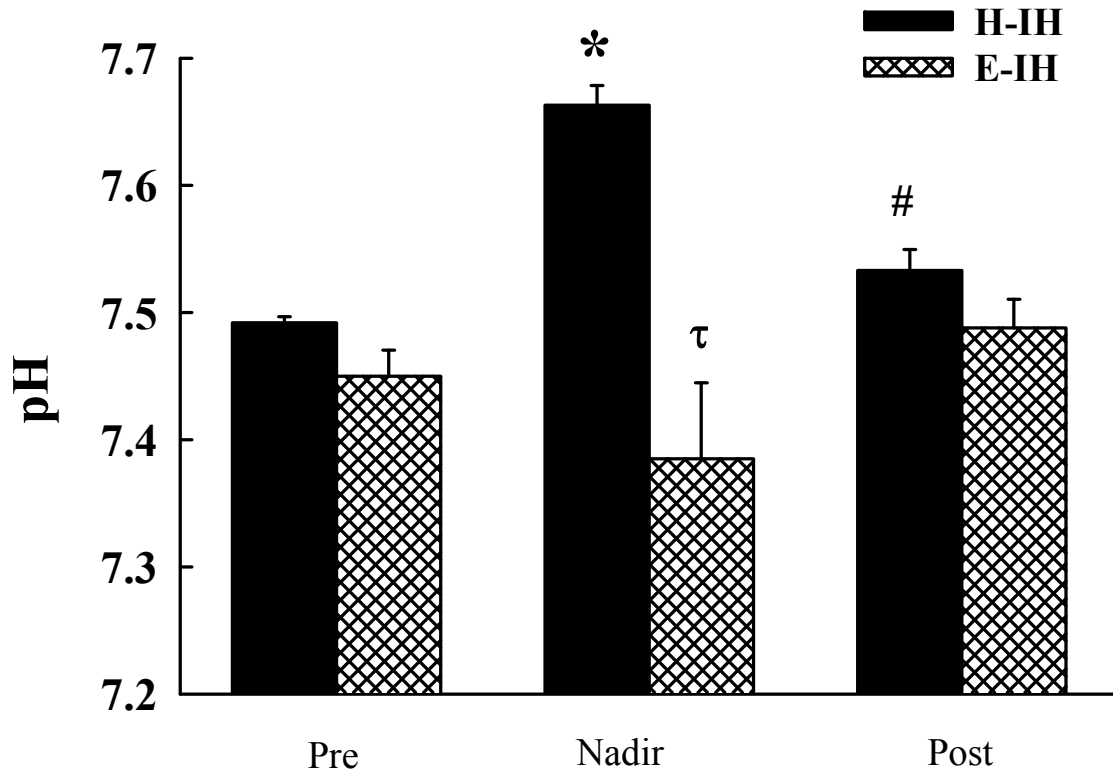


Figure 7. Arterial pH measurements from Sprague Dawley rats before (Pre) during (Nadir) and after (Post) acute H-IH or E-IH exposure. Values are means \pm SE of n=4-5 rats/treatment. * P < 0.05 vs. respective pre exposure value. # P < 0.05 vs. nadir value. τ P < 0.05 vs. H-IH.

adaptative changes in arterial blood gases. We found that PO₂ (Figure 8), PCO₂ (Figure 9), and pH (Figure 10) measurements reflected values before chronic E-IH exposure. At the nadir of O₂, PO₂ was less than under resting conditions and this value recovered to pre-exposure values during the air flush. PCO₂ did not change during exposure to IH in these 4 week E-IH rats. Similarly, arterial pH remained constant during cycling.

Specific Aim 1.2 - Assess effects of E-IH and H-IH on right ventricular hypertrophy.

Right Ventricular Hypertrophy in 2 Week IH Sprague Dawley Rats

Consistent with our hypothesis, right ventricle to total ventricle weight ratios were significantly greater following 2 weeks of H-IH compared to Sham controls, and this difference was not present following E-IH (Figure 11A). Similarly, only H-IH increased the RV/BW ratio (Figure 12A). There were no differences between groups in left ventricle plus septal weight normalized to body weight.

Right Ventricular Hypertrophy in 4 Week IH Wistar Rats

In Wistar rats exposed to 4 weeks of IH, right ventricular hypertrophy developed regardless of CO₂ supplementation. Figure 11B shows elevated RV/T in both H-IH and E-IH rats. Consistent with these findings, RV/BW ratio was greater in both H-IH and E-IH rats than Sham rats (Figure 12B). Both H-IH and E-IH exposure attenuated weight gain compared to Sham animals (Table 2). Because E-IH elicited RV hypertrophy in Wistar rats and because E-IH more closely approximates the blood gas changes in patients with SA, 4 week E-IH Wistar rats were studied for all experiments in Specific Aims 2-4.

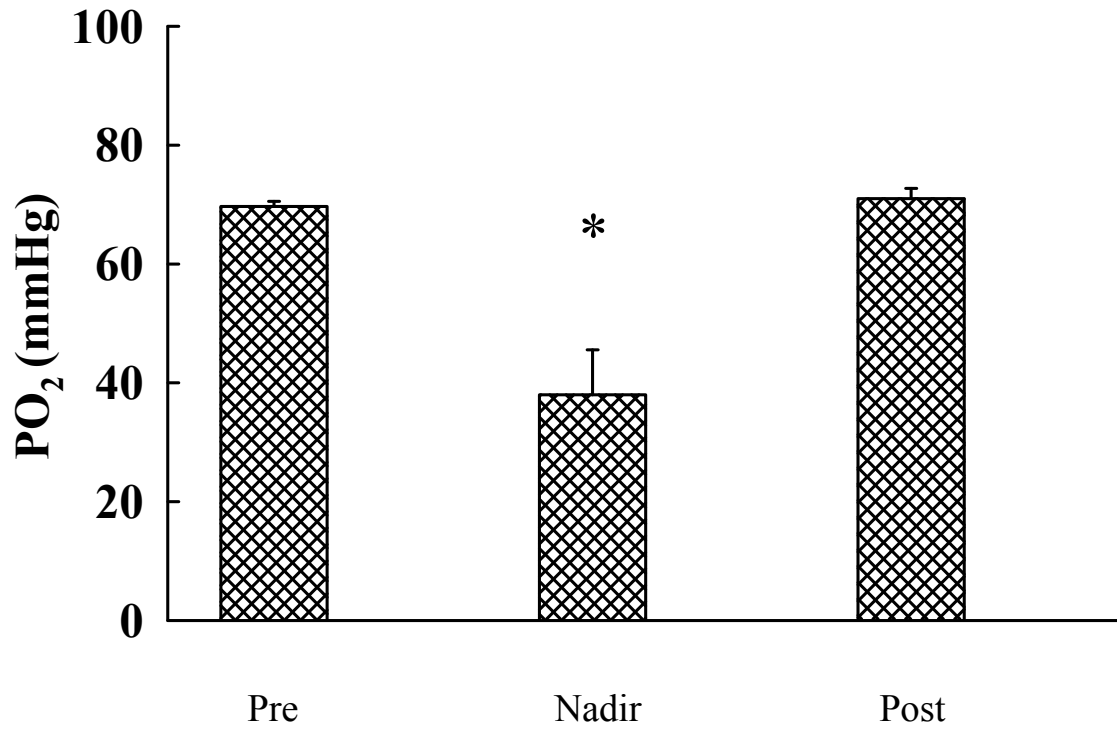


Figure 8. Arterial PO₂ following 4 week E-IH exposure in Wistar rats before (Pre), during (Nadir) and after (Post) one E-IH cycle. Values are means \pm SE of n= 4 rats. * P < 0.05 vs. respective pre- cycling value.

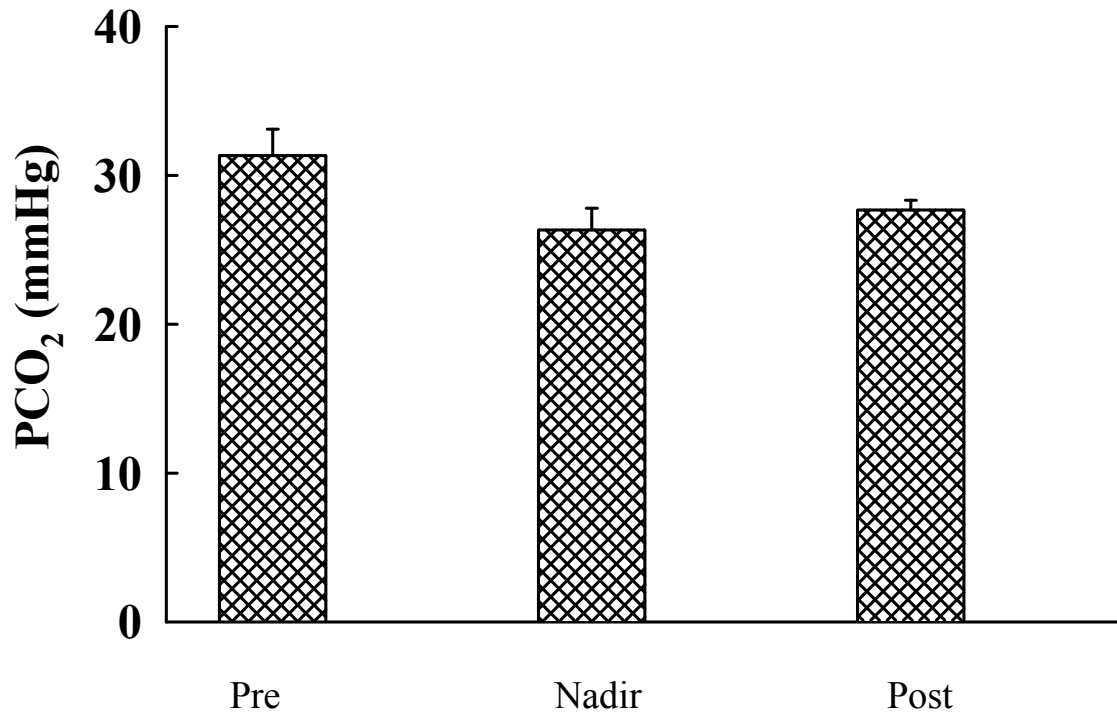


Figure 9. Arterial PCO₂ following 4 week E-IH exposure in Wistar rats before (Pre), during (Nadir) and after (Post) one E-IH cycle. Values are means \pm SE of n= 3 rats. There are no differences.

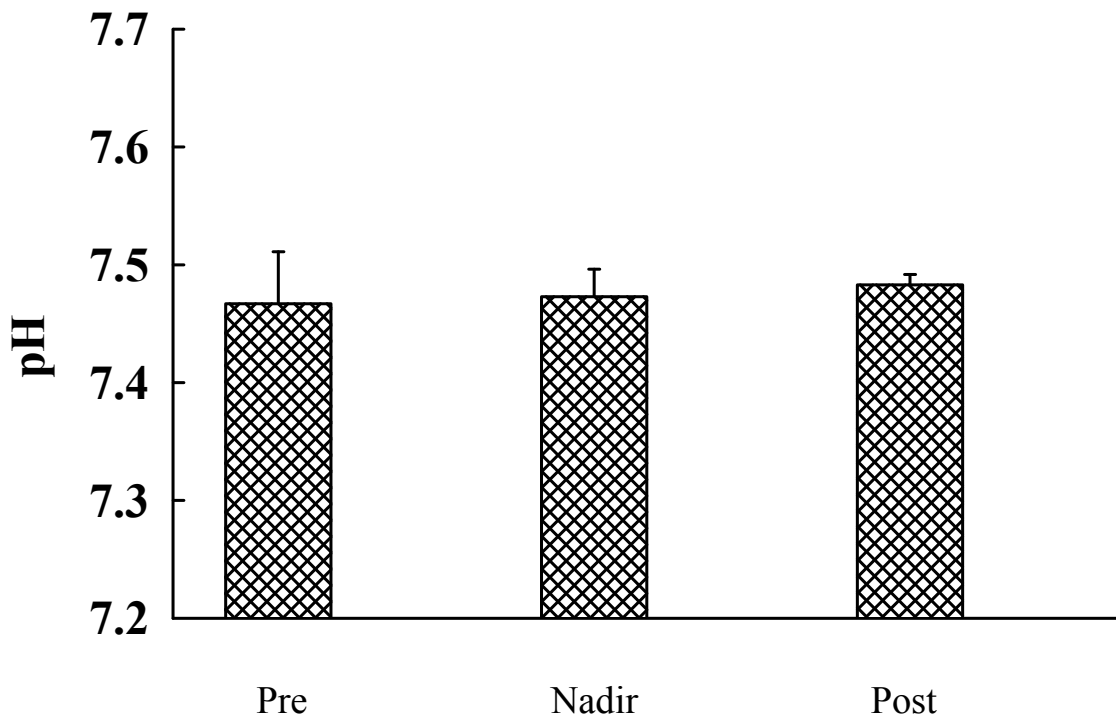


Figure 10. Arterial blood gas pH following 4 week E-IH exposure in Wistar rats before (Pre), during (Nadir) and after (Post) one E-IH cycle. Values are means \pm SE of n= 3 rats. There are no differences.

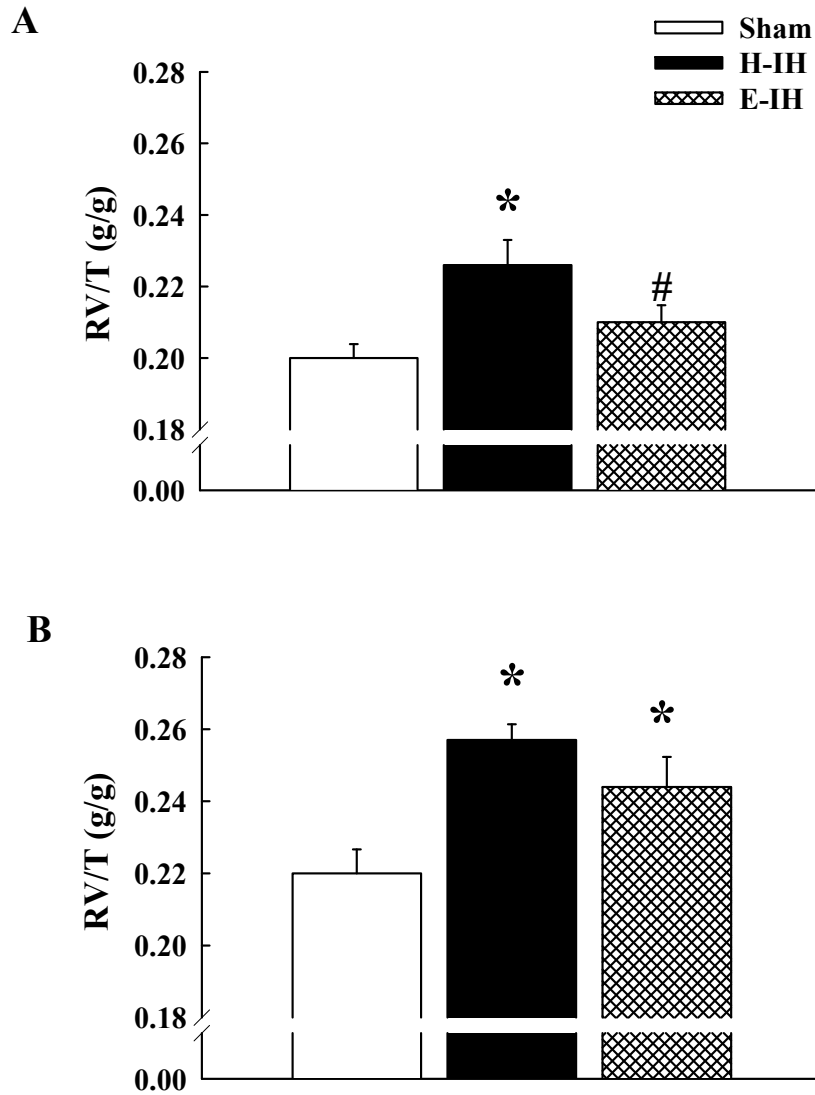


Figure 11. Ratios of right ventricle (RV) to total ventricle (T) weight in (A) 2 week Sprague Dawley and (B) 4 week Wistar Sham-treated, H-IH and E-IH rats. Values are means \pm SE of $n = 7-23$ rats/group. * $P < 0.05$ vs. Sham. # $P < 0.05$ vs. H-IH.

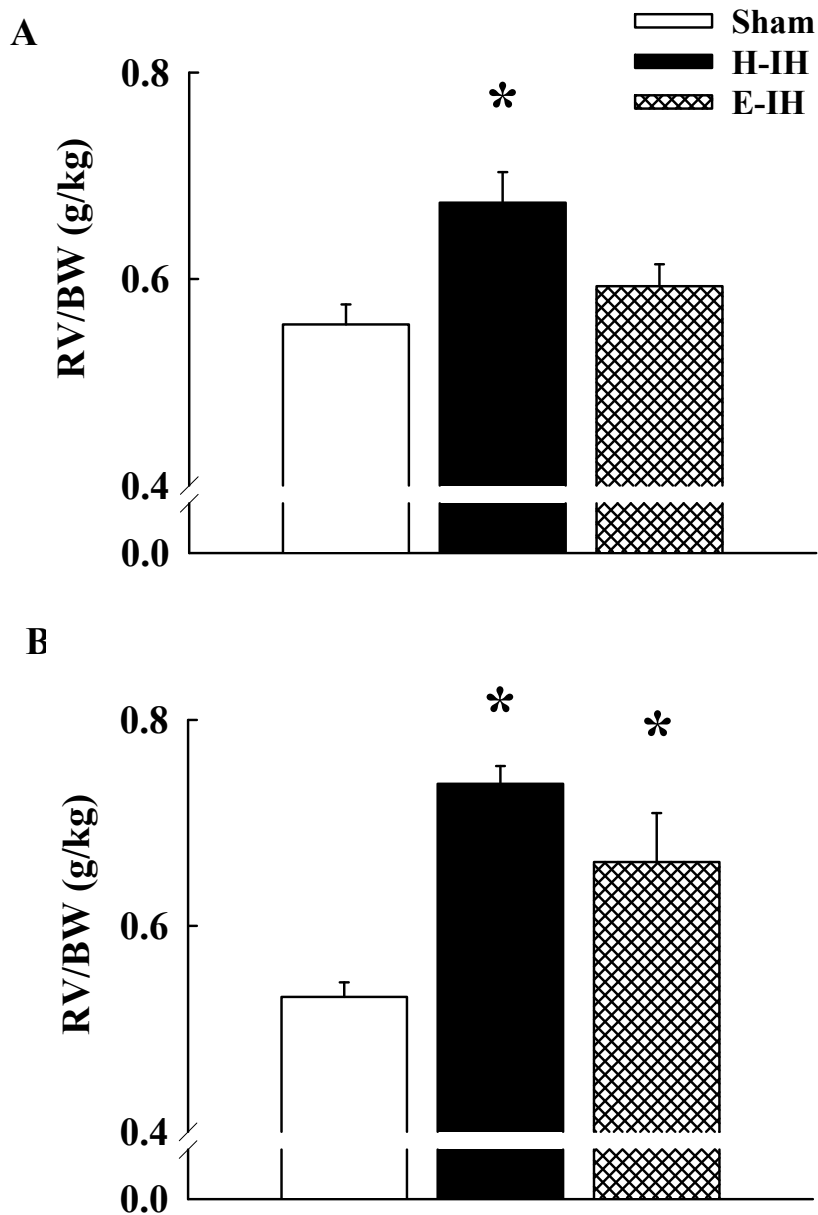


Figure 12. Ratios of right ventricle (RV) to body weight (BW) in (A) 2 week Sprague Dawley and (B) 4 week Wistar Sham-treated, H-IH and E-IH rats. Values are means \pm SE of $n = 7-23$ rats/group. * $P < 0.05$ vs. Sham.

Table 2. *Left ventricle + septum heart weight and pre and post exposure body weights in sham-treated, hypocapnic intermittently hypoxic (H-IH) and eucapnic intermittently hypoxic (E-IH) Wistar rats.*

Group	BW (Pre)	BW (Post)	LV+S/BW	n
Sham	253 ± 11	392 ± 10*	1.91 ± 0.04	7
H-IH	246 ± 12	309 ± 14*#	2.14 ± 0.05	7
E-IH	244 ± 12	324 ± 12*#	2.03 ± 0.07	8

BW (Pre and Post) denote values before and after, respectively, exposure to Sham or IH. Values are means ± SE. n, number of rats. *P<0.05 vs. pre-exposure value. #P<0.05 vs. Sham post-exposure BW.

Specific Aim 1.3 - Assess the degree of polycythemia resulting from E-IH and H-IH exposure.

Two weeks of H-IH resulted in elevated hematocrit compared to Sham-treated animals (Figure 13A). Two weeks E-IH elicited a modest increase in hematocrit that was significantly lower than the H-IH group (Figure 13A). Four weeks exposure to H-IH caused profound polycythemia in Wistar rats. However, this response was absent in 4 week E-IH Wistar rats (Figure 13B).

Specific Aim 1.4 – Compare pulmonary arterial remodeling responses to E-IH and H-IH.

Figure 14 illustrates percent wall thickness for pulmonary arteries with external diameters of $< 50 \mu\text{m}$ (Figure 14A) and $50\text{-}100 \mu\text{m}$ (Figure 14B) from Sprague Dawley rats exposed to 2 weeks of Sham or IH treatment. H-IH exposure increased wall thickness compared to control groups in each range of vessel diameters. Prevention of hypocapnia with supplemental CO_2 prevented IH-induced arterial remodeling (Fig. 14). These findings are consistent with effects of H-IH and E-IH on RV hypertrophy (Figures 11-12).

Specific Aim 1.5 - Assess effects of E-IH and H-IH on vasoconstrictor reactivity.

Vasoconstriction represents an important contribution to the development of PH. CH augments vasoconstrictor reactivity to agonists such as U-46619 (Eichinger & Walker, 1994; Resta & Walker, 1996), ET-1 (Jernigan *et al.*, 2008), UTP (Jernigan *et al.*, 2004b; Rodat *et al.*, 2007) and 5-HT (Rodat *et al.*, 2007). However, effects of IH on

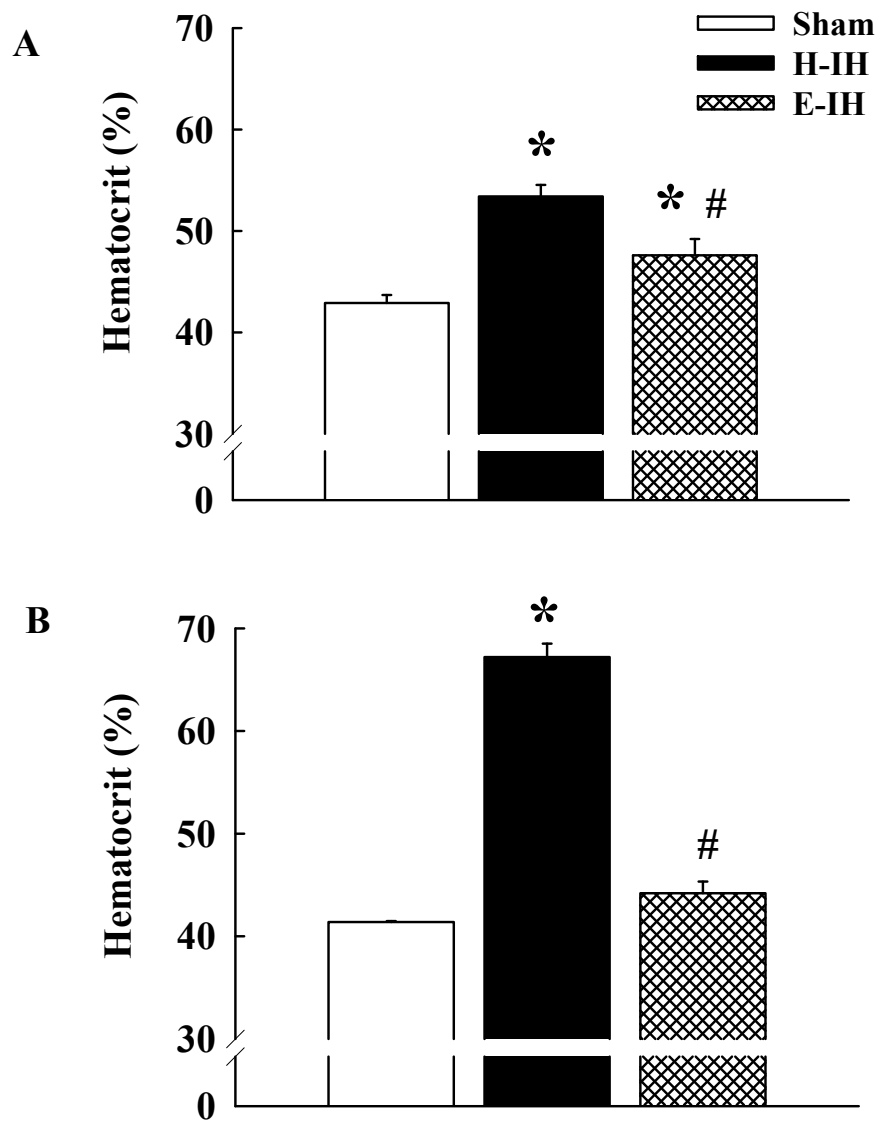


Figure 13. Percent hematocrit in **A)** 2 week Sprague Dawley and **B)** 4 week Wistar Sham-treated, H-IH and E-IH rats. Values are means \pm SE of $n = 7-10$ rats/group. * $P < 0.05$ vs. Sham. # $P < 0.05$ vs. H-IH.

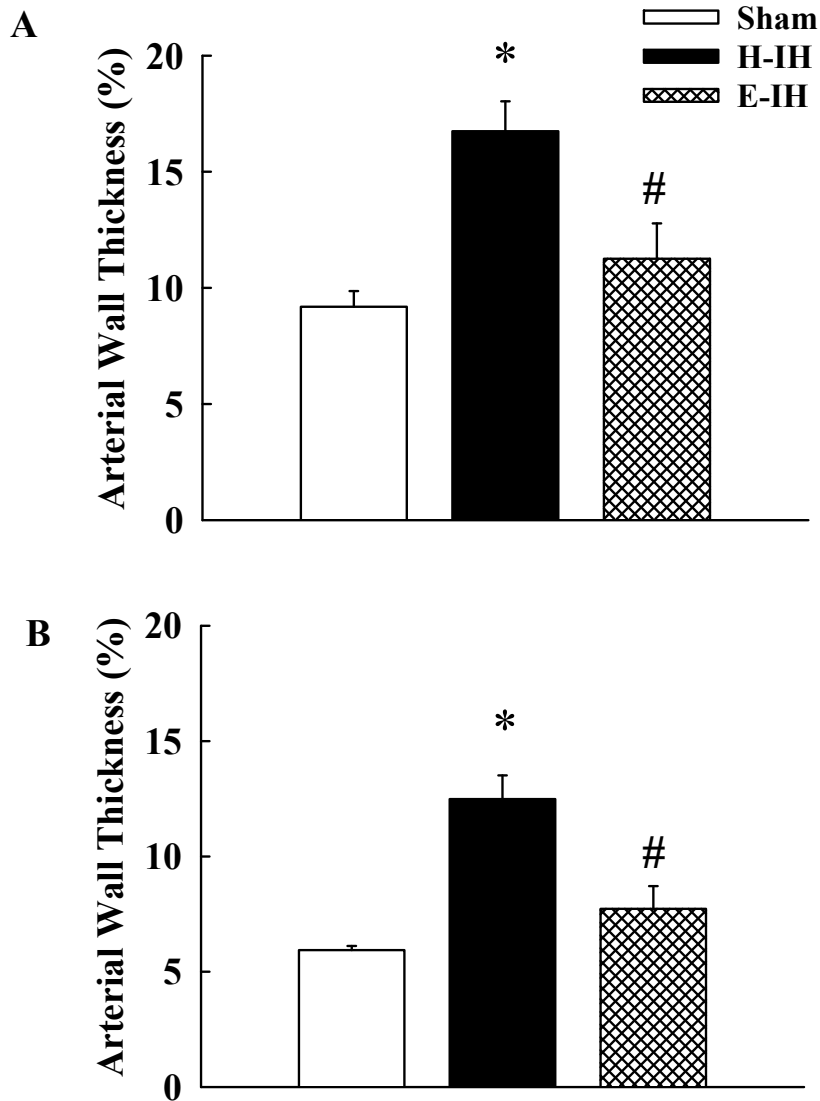


Figure 14. Percent arterial wall thickness of pulmonary arteries with external diameters of $< 50 \mu\text{m}$ (A) and $50\text{-}100 \mu\text{m}$ (B) from Sham-treated, H-IH and E-IH rats. Values are means \pm SE of $n = 4$ rats/group. * $P < 0.05$ vs. Sham. # $P < 0.05$ vs. H-IH.

vasoconstrictor reactivity have not been well studied. Given the markedly blunted polycythemia and remodeling in E-IH rats compared to H-IH, despite RV hypertrophy, we measured vasoconstrictor reactivity to various-receptor mediated agonists following 4 weeks IH exposure in Wistar rats.

Vasoconstrictor Reactivity to ET-1 Following IH in Isolated Pulmonary Arteries

To determine whether vasoconstrictor reactivity to ET-1 is augmented in pulmonary arteries from E-IH animals and whether supplemental CO₂ attenuates that increase in reactivity, vasoconstrictor and VSM [Ca²⁺]_i responses to ET-1 were assessed in isolated, pressurized, arteries from Wistar rats exposed to 4 weeks of Sham, H-IH and E-IH treatment. In order to assess effects of H-IH and E-IH on PA smooth muscle function, all arteries were endothelium-disrupted. Vasoconstrictor responses were greater in arteries from both H-IH and E-IH rats compared to Sham (Figure 15). However, vasoconstriction to ET-1 was slightly blunted in arteries from E-IH compared to H-IH rats (ET-1 10^{-9.5} and 10⁻⁹ M). Ca²⁺ responses were similar between all three groups. No differences in basal inner diameter or F₃₄₀/F₃₈₀ were detected (Table 3). These data suggest that both H-IH and E-IH increase ET-1-induced vasoconstriction via Ca²⁺ sensitization. All subsequent vasoconstrictor studies were performed only in arteries from Sham and E-IH rats because E-IH more closely mimics blood gas conditions of SA and is associated with increased agonist-induced vasoconstriction.

,

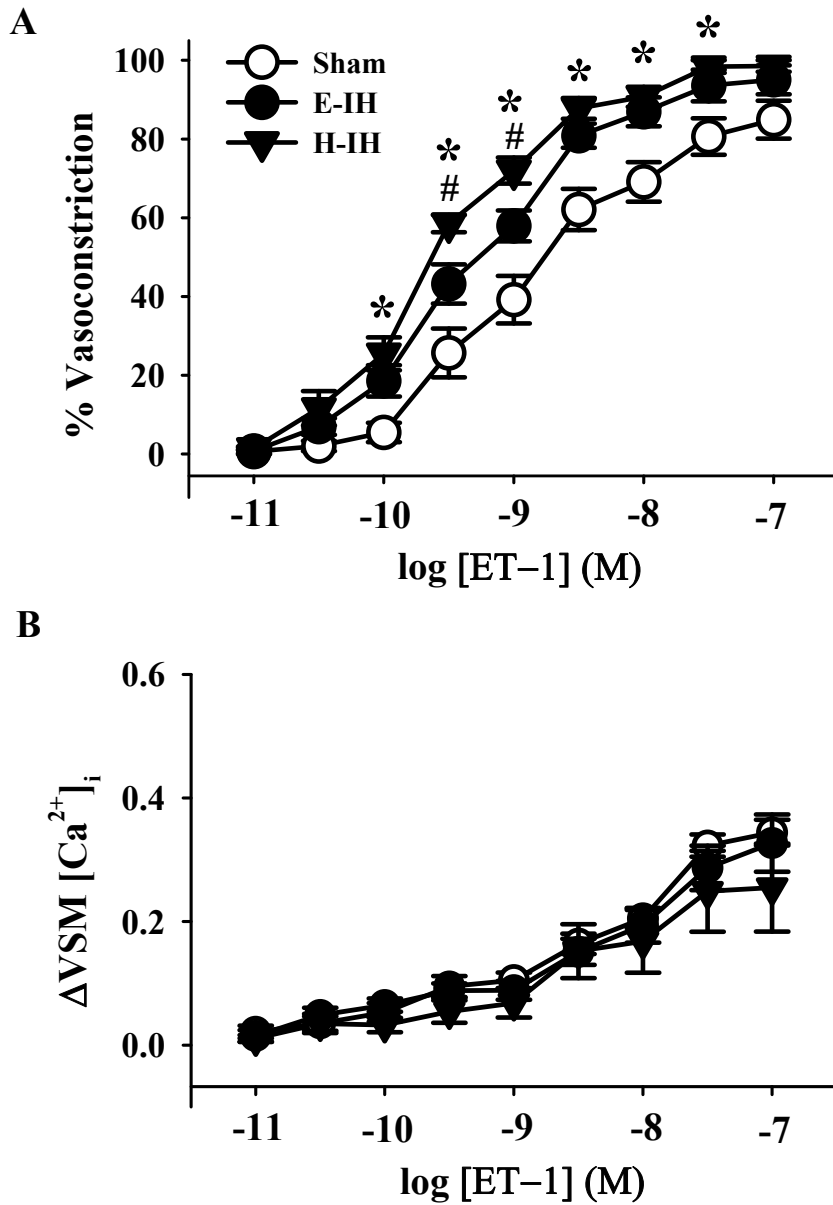


Figure 15. A) Vasoconstrictor and **B)** VSM $[Ca^{2+}]_i$ responses to ET-1 in vessels from Sham, H-IH and E-IH rats. Values are means \pm SE of $n = 6-9$ rats/group. * $P < 0.05$ H-IH and E-IH vs. Sham. # $P < 0.05$ H-IH vs. E-IH.

Table 3. Basal inner diameter and VSM $[Ca^{2+}]_i$ (F_{340}/F_{380}) in isolated, pressurized pulmonary arteries from Sham, H-IH and E-IH rats.

Group	Inner Diameter (μm)	F_{340}/F_{380}	n
Sham	156 \pm 14	0.77 \pm 0.05	9
H-IH	155 \pm 10	0.74 \pm 0.07	6
E-IH	173 \pm 8	0.75 \pm 0.09	9

Values are means \pm SE. n , number of rats. There are no significant differences.

Vasoconstrictor Reactivity to UTP in Isolated Pulmonary Arteries

To address whether the increase in ET-1-induced vasoconstrictor reactivity following E-IH reflects a generalized increase in agonist-induced vasoconstriction, vasoconstrictor reactivity to UTP was assessed in Sham and E-IH vessels. Responses to UTP were greater in pulmonary arteries E-IH rats compared to Sham controls (Figure 16). However, Ca^{2+} responses were again similar between groups.

Vasoconstrictor Reactivity to 5-HT in Isolated Pulmonary Arteries

Similar to effects of E-IH on responses to ET-1 and UTP, vasoconstrictor reactivity to 5-HT was elevated in pulmonary arteries from Wistar rats exposed to E-IH compared to those of Sham animals (Figure 17). VSM Ca^{2+} responses were modest and were not different between Sham and E-IH vessels. Together, these data suggest that E-IH causes a generalized increase in agonist-mediated vasoconstriction through increased VSM Ca^{2+} sensitivity.

Summary of Results for Specific Aim 1

- Exposure of rats to IH results in hypoxemia. IH without CO₂ supplementation causes hypocapnia and alkalosis. However, CO₂ supplementation results in hypoxemia and maintained eucapnia.
- Two weeks of H-IH but not E-IH causes right ventricular hypertrophy in Sprague Dawley rats. In contrast, both H-IH and E-IH (4 weeks) elicit right ventricular hypertrophy in Wistar rats.

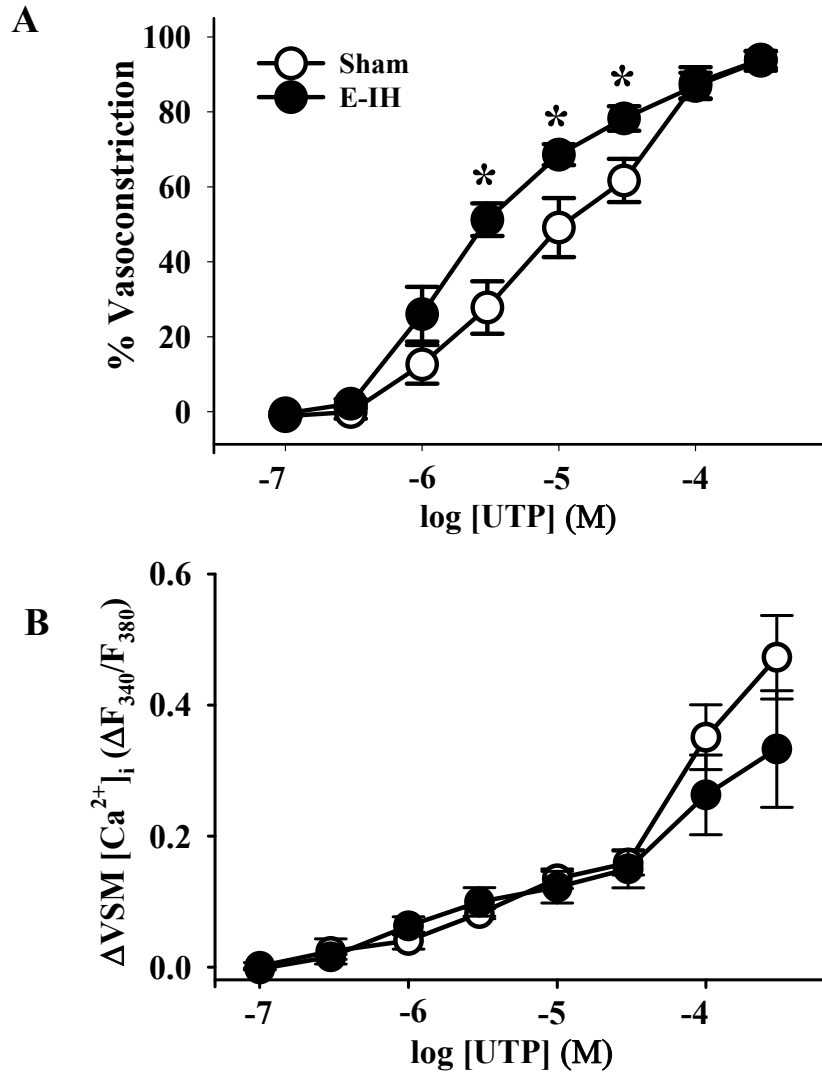


Figure 16. A) Vasoconstrictor and **B)** VSM $[Ca^{2+}]_i$ responses to UTP in vessels from Sham and E-IH Wistar rats. Values are means \pm SE of $n = 6-7$ rats/group. * $P < 0.05$ vs. Sham.

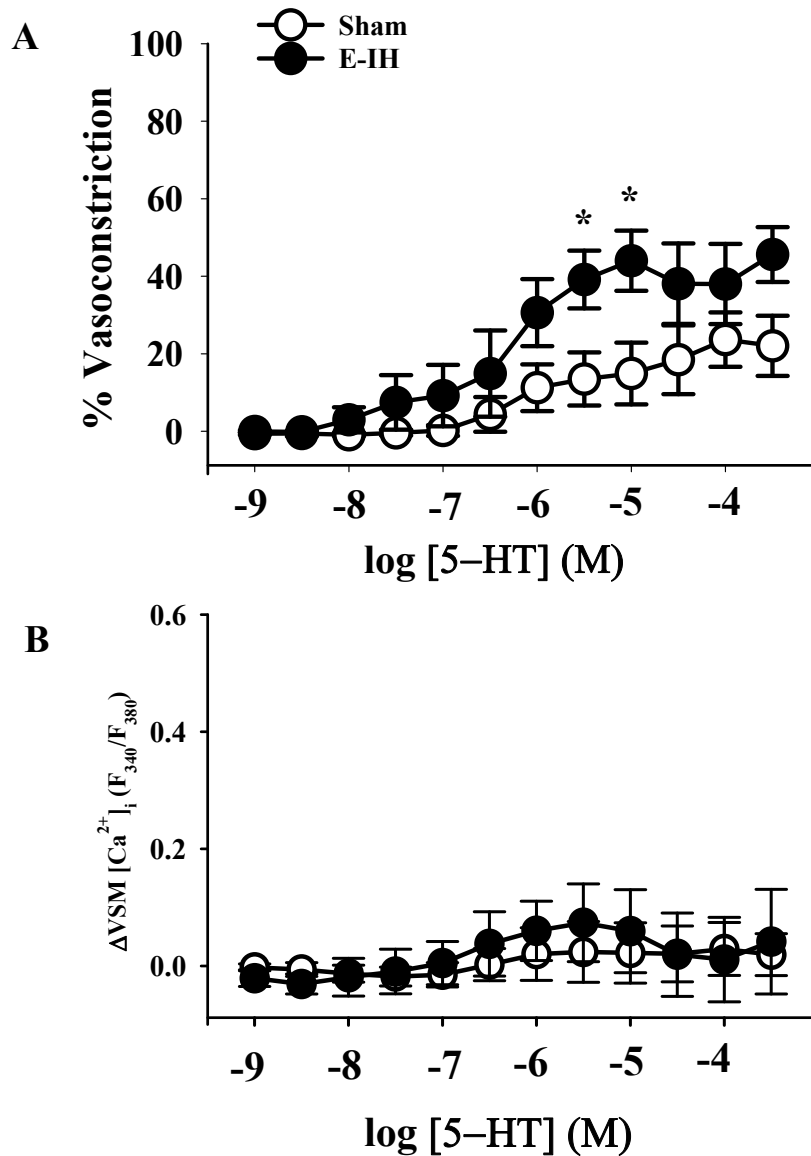


Figure 17. A) Vasoconstrictor and **B)** VSM $[Ca^{2+}]_i$ responses to 5-HT in vessels from Sham and E-IH rats. Values are means \pm SE of $n = 4$ rats/group. * $P < 0.05$ vs. Sham.

- H-IH increases hematocrit in both Sprague Dawley rats (2 wk exposure) and Wistar rats (4 week exposure). In contrast, rats exposed to E-IH do not develop polycythemia.
- H-IH causes a greater degree of pulmonary arterial remodeling than E-IH in both sizes of pulmonary arteries examined (<50 μm and 50-100 μm).
- E-IH increases vasoconstrictor reactivity to ET-1, UTP and 5-HT in pulmonary arteries without increasing associated Ca^{2+} responses.

Conclusion

E-IH most closely mimics arterial blood gases of SA patients and elicits RV hypertrophy in Wistar rats. In addition, E-IH increases pulmonary artery vasoconstrictor reactivity, likely through a Ca^{2+} sensitization mechanism.

Specific Aim 2: Assess the role of ROK in mediating right ventricular hypertrophy and enhanced agonist-induced pulmonary vasoconstriction following E-IH.

ROK mediates a major agonist-induced signaling pathway in pulmonary VSM. Also, CH increases ROK-dependent pulmonary VSM Ca^{2+} sensitization, and ROK plays a role in CH-induced PH. However, whether ROK is involved in the development of E-IH-induced PH, and whether a similar ROK signaling mechanism mediates augmented pulmonary vasoconstrictor reactivity in E-IH vessels has not been determined.

Specific Aim 2.1 - Evaluate the contribution of ROK to E-IH-induced RV hypertrophy.

Effect of Chronic ROK Inhibition on the Right Ventricular Hypertrophic Response to E-IH.

Although RV/T and RV/BW tended to be lower in E-IH rats treated with fasudil (30 mg/kg/day for 4 weeks) compared to vehicle-treated animals, this did not achieve statistical significance (Fig 18). These results suggest that ROK does not contribute substantially to E-IH-induced RV hypertrophy and associated PH.

Specific Aim 2.2 – Determine the role of ROK in mediating enhanced ET-1-induced vasoconstrictor reactivity following E-IH.

Effect of ROK Inhibition on ET-1-Induced Pulmonary Vasoconstriction and Ca^{2+} Responses in Isolated Pulmonary Arteries

Inhibition of ROK with fasudil (10 μ M) did not inhibit vasoconstrictor reactivity to ET-1 in vessels from either Sham or E-IH rats (Figure 19). In addition, there was no

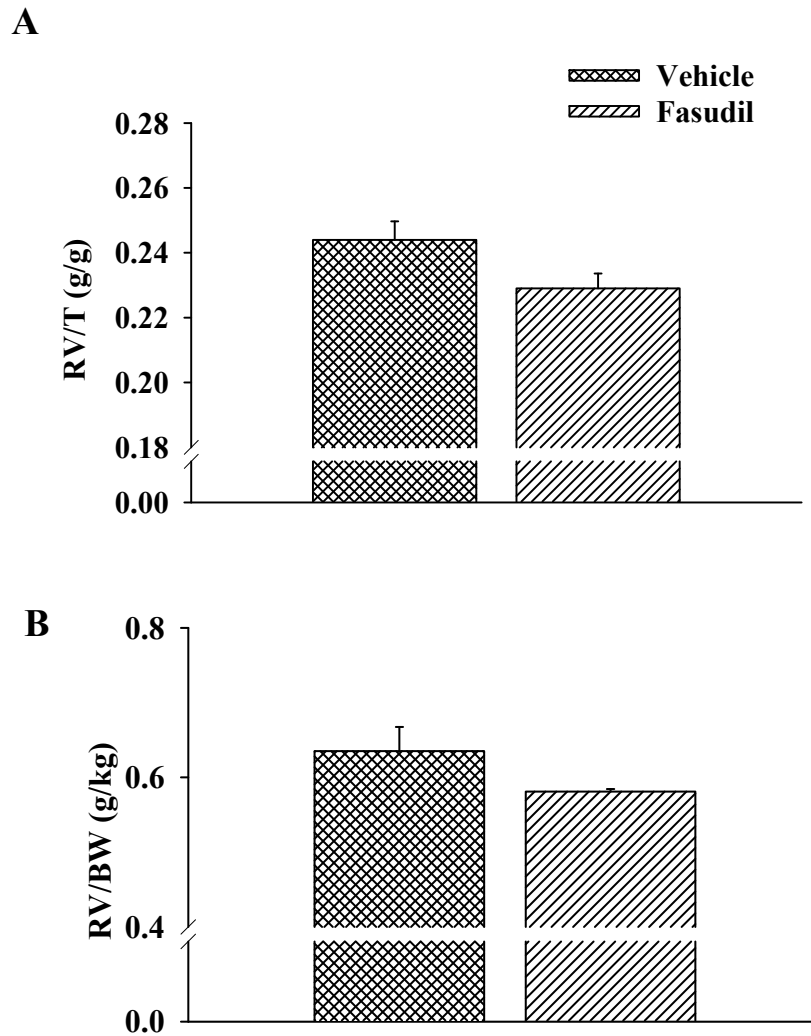


Figure 18. A) RV/T and B) RV/BW from E-IH animals treated with vehicle or fasudil (30 mg/kg/day) for 4 weeks. Data are means \pm SE of n= 4-5/group. There are no significant differences.

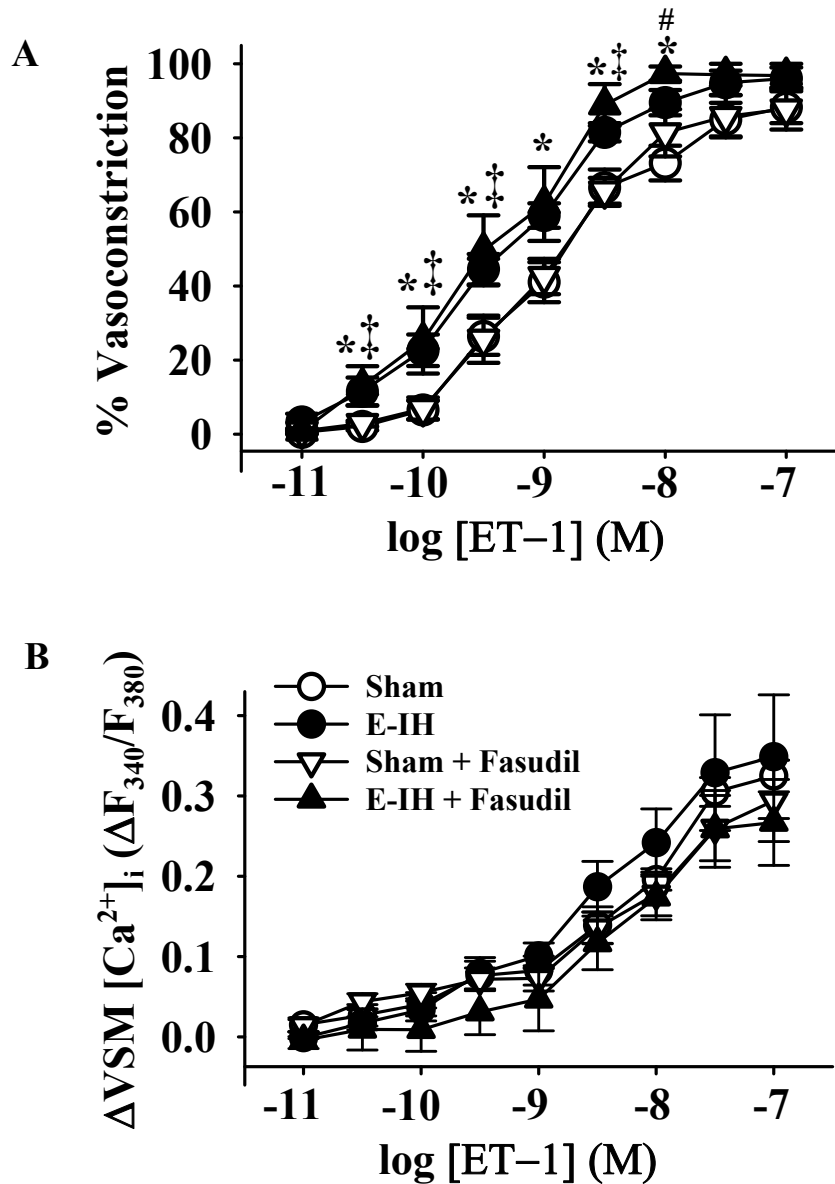


Figure 19. A) Vasoconstrictor and B) VSM $[Ca^{2+}]_i$ responses to ET-1 in the presence and absence of the ROK inhibitor fasudil (10 μ M). (* $P < 0.05$ E-IH vs. Sham; ‡ $P < 0.05$ Sham + fasudil vs. E-IH + fasudil; # $P < 0.05$ E-IH vs. E-IH + fasudil) Data are means \pm SE of $n = 6-9$ /group.

effect of ROK inhibition on VSM Ca^{2+} responses to ET-1, suggesting that ROK does not mediate the ET-1-induced response in vessels from either Sham or E-IH rats. Fasudil did not alter basal VSM $[Ca^{2+}]_i$ or inner diameter (Table 4).

Summary of Results for Aim 2

- RV/T and RV/BW were not different between vehicle-treated and fasudil-treated E-IH rats.
- Fasudil did not attenuate enhanced ET-1-induced vasoconstriction following E-IH.

Conclusion

E-IH-induced right ventricular hypertrophy and enhanced vasoconstrictor reactivity to ET-1 are independent of ROK.

Table 4. Basal inner diameters and VSM $[Ca^{2+}]_i$ (F_{340}/F_{380}) in vehicle or fasudil-pretreated arteries from Sham and E-IH rats

Group/Treatment	Inner Diameter	(F_{340}/F_{380})	<i>n</i>
Sham Vehicle	156 ± 14	0.77 ± 0.05	9
E-IH Vehicle	173 ± 8	0.75 ± 0.09	9
Sham Fasudil	122 ± 15	0.69 ± 0.04	6
E-IH Fasudil	166 ± 19	0.68 ± 0.07	6

Values are means ± SE. *n*, number of rats. There are no significant differences.

Specific Aim 3: Assess the contribution of PKC to increased agonist-mediated vasoconstriction following E-IH.

Specific Aim 3.1 - Determine the role of specific PKC isoforms in mediating enhanced ET-1-induced vasoconstriction following E-IH.

Based on findings in Specific Aim 2 that increased ET-1-dependent constriction after E-IH is mediated by Ca^{2+} sensitization, but not via ROK-dependent signaling, we sought another mechanism by which E-IH might increase ET-1-induced vasoconstriction. PKC is an alternative mediator of VSM Ca^{2+} sensitization and E-IH increases PKC-dependent constriction in the systemic circulation (Allahdadi *et al.*, 2008b). However, effects of E-IH on PKC-dependent pulmonary vasoconstriction are unknown.

Effect of Generalized PKC Inhibition on ET-1-Induced Vasoconstriction

To validate the concentration of the general PKC inhibitor Ro 31-8220 used in the present study, we assessed constrictions in pulmonary arteries to the PKC activator PMA in the presence of vehicle and Ro 31-8220 (5 μ M). PMA-induced vasoconstriction was nearly abolished by this concentration of Ro 31-8220 (Figure 20). Ro 31-8220 attenuated vasoconstrictor responses to ET-1 in both Sham and E-IH groups and normalized responses between groups (Figure 21A). In addition, Ro 31-8220 blunted the Ca^{2+} responses to ET-1 in both Sham and E-IH arteries (Figure 21B). These findings suggest that PKC is involved in ET-1-induced vasoconstriction and VSM Ca^{2+}

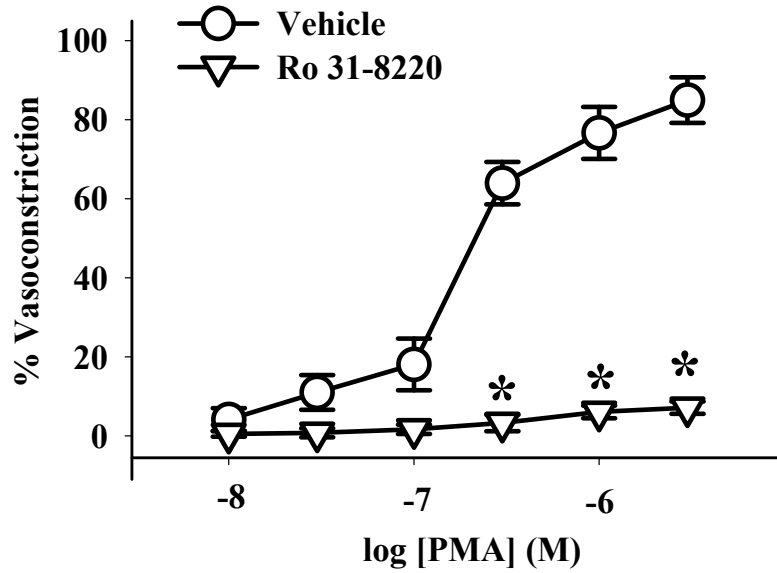


Figure 20. Vasoconstrictor responses to the PKC activator PMA in the presence of vehicle or the PKC inhibitor Ro 31-8220 (5 μ M) in endothelium-disrupted pulmonary arteries from control rats. Values are means \pm SE of $n = 3-4$ rats/group. * $P < 0.05$ vs. vehicle.

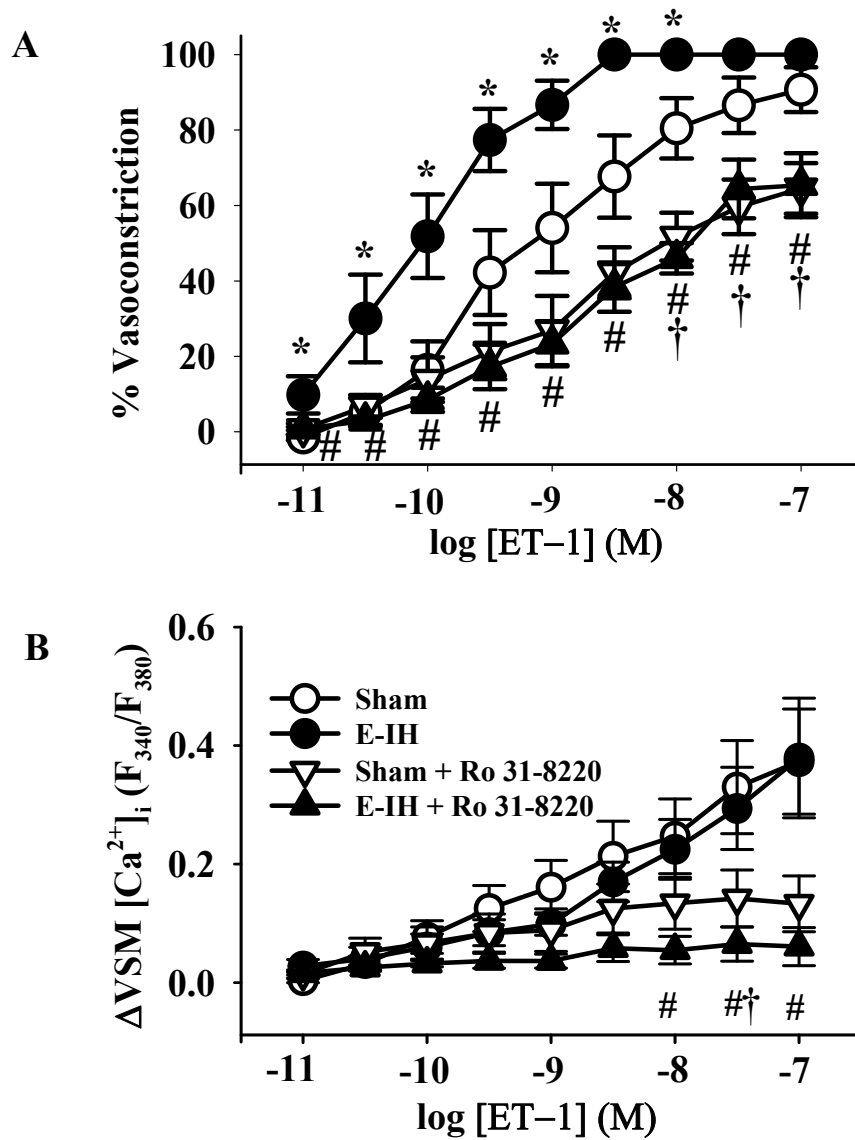


Figure 21. A) Vasoconstrictor and B) VSM $[Ca^{2+}]_i$ responses to ET-1 in the presence and absence of the PKC inhibitor Ro 31-8220 (5 μ M). (* $P < 0.05$ E-IH vs. Sham; # $P < 0.05$ E-IH vs. E-IH + Ro; † $P < 0.05$ Sham vs. Sham + Ro) Data are means \pm SE of $n = 4-9$ /group.

mobilization in both Sham and E-IH groups and that PKC mediates the elevated vasoconstrictor reactivity following E-IH.

Effect of Selective PKC α/β Inhibition on ET-1-Induced Vasoconstriction

To validate the concentration of the selective PKC α/β inhibitor myr-PKC used in the present study, we assessed constrictions in pulmonary arteries to the PKC activator PMA in the presence of vehicle and myr-PKC (10 μ M). PMA-induced vasoconstriction was significantly attenuated by this concentration of myr-PKC (Figure 22). PKC α/β inhibition decreased ET-1-induced vasoconstriction in vessels from E-IH rats, but was without effect on responses in arteries from Sham rats (Figure 23A). In addition, PKC α/β inhibition normalized constrictions between Sham and E-IH groups. Furthermore, Ca²⁺ responses to ET-1 were unaltered by myr-PKC in either group (Figure 23B), suggesting that PKC α/β contribute to elevated ET-1-induced Ca²⁺ sensitization after E-IH.

ET-1-Induced Vasoconstriction in the Presence of a PKC δ Inhibitor

The PKC δ inhibitor rottlerin (3 μ M) attenuated PMA-induced constriction in control arteries (Figure 24). Therefore, this concentration of rottlerin was used to inhibit PKC δ in Sham and E-IH arteries but did not decrease vasoconstrictor reactivity to ET-1 following E-IH (Figure 25A). In fact, constriction was significantly greater in E-IH vessels in the presence of rottlerin (at 10^{-10.5} - 10⁻¹⁰ M ET-1), and this was associated with an increased Ca²⁺ response in the presence of rottlerin at lower concentrations of ET-1 (Figure 25B).

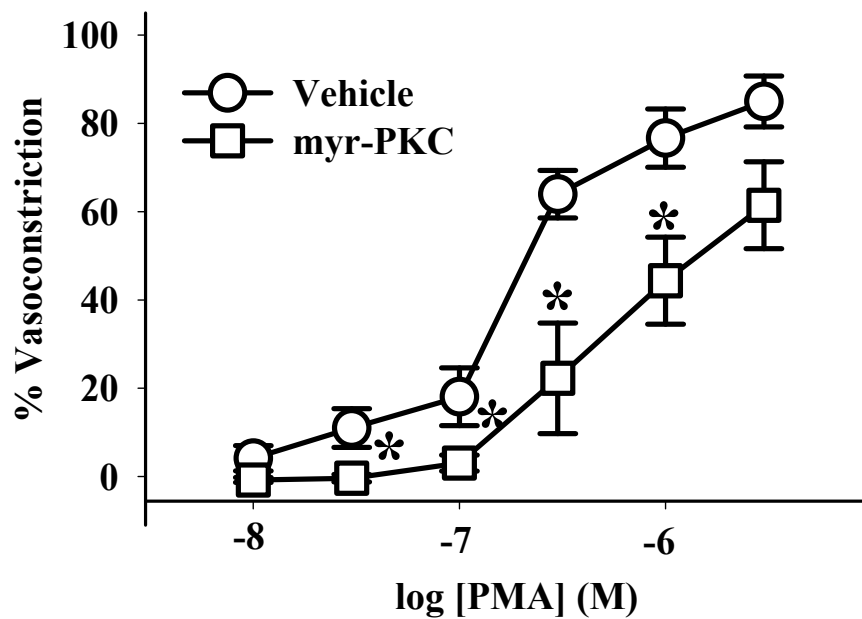


Figure 22. Vasoconstrictor responses to the PKC activator PMA in the presence of vehicle or the PKC α/β inhibitor myr-PKC (10 μ M) in endothelium-disrupted pulmonary arteries from control rats. Values are means \pm SE of $n=4-5$ rats/group * $P<0.05$ vs. vehicle.

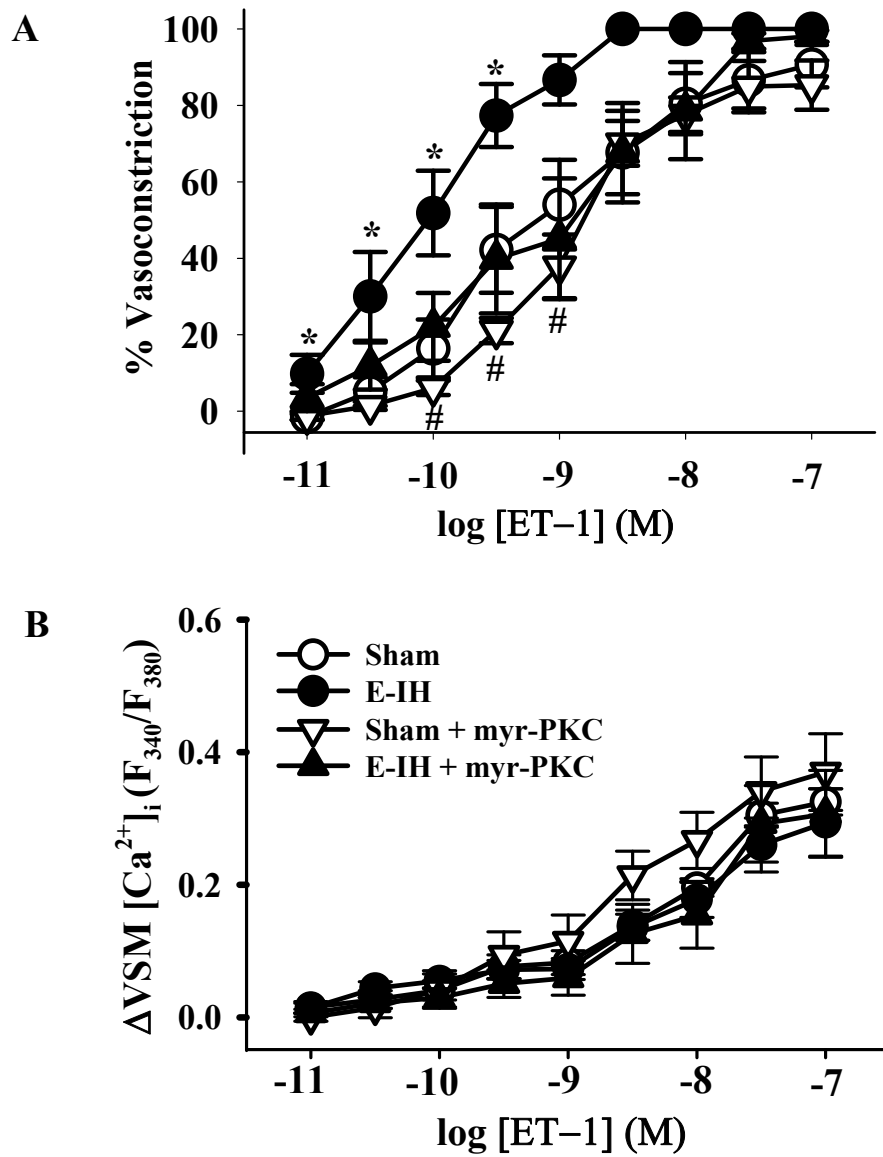


Figure 23. A) Vasoconstrictor and B) VSM $[Ca^{2+}]_i$ responses to ET-1 in the presence and absence of the PKC α/β inhibitor myr-PKC (10 μ M). (* $P < 0.05$ E-IH vs. Sham; # $P < 0.05$ IH vs. E-IH + myr-PKC) Data are means \pm SE of $n = 5-6$ /group.

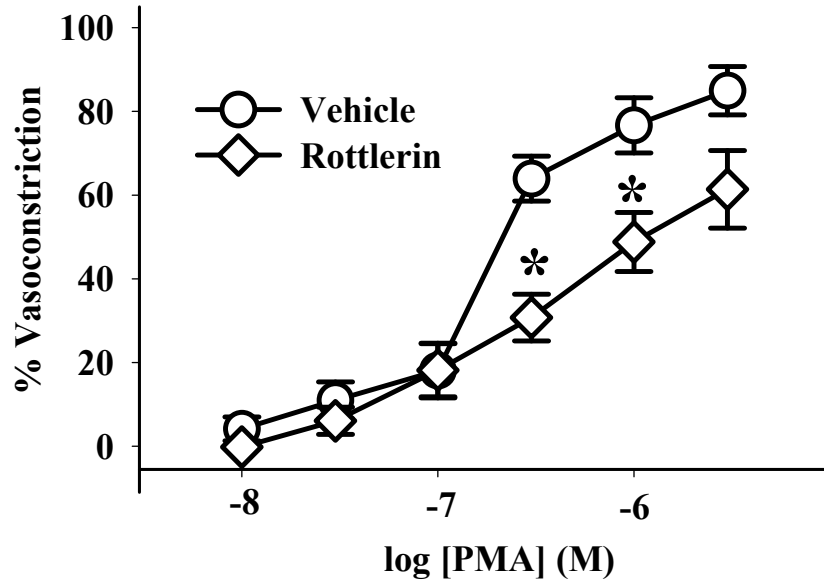


Figure 24. Vasoconstrictor responses to the PKC activator PMA in the presence of vehicle or the PKC δ inhibitor Rottlerin (3 μ M) in endothelium-disrupted pulmonary arteries from control rats. Values are means \pm SE of $n = 4$ rats/group. * $P < 0.05$ vs. vehicle.

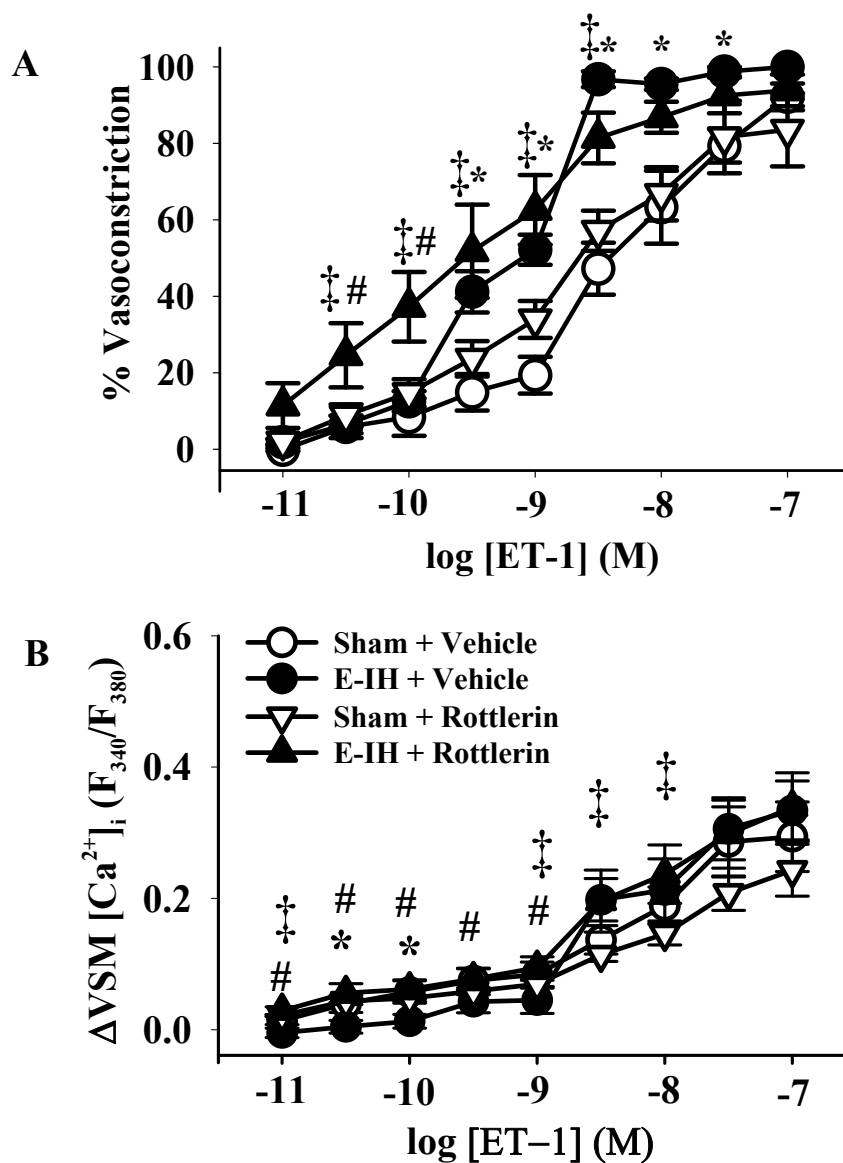


Figure 25. A) Vasoconstrictor and B) VSM [Ca²⁺]_i responses to ET-1 in pulmonary arteries from Sham and E-IH rats in the presence and absence of the PKC δ inhibitor rottlerin (3 μ M). (* P <0.05 E-IH vs. Sham; ‡ P <0.05 Sham + rottlerin vs. E-IH + rottlerin; # P <0.05 E-IH vs. E-IH + rottlerin) Data are means \pm SE of $n=5$ /group.

In the presence of the vehicle for rottlerin (ethanol) there was a slightly attenuated Ca^{2+} response in vessels from E-IH animals compared to Sham, but this was associated with the same degree of constriction in response to ET-1 in both groups. The effect of rottlerin to increase ET-1-dependent increases in Ca^{2+} in the E-IH group indicates a possible role for PKC δ to antagonize agonist-induced VSM Ca^{2+} mobilization after E-IH. Overall, these results suggest that PKC δ does not mediate enhanced ET-1-induced vasoconstriction

There were no differences in basal arterial inner diameter between groups. Basal VSM $[Ca^{2+}]_i$ (F_{340}/F_{380}) was similar between Sham and E-IH for all drugs and vehicles, except in the presence of the vehicle for rottlerin (ethanol), Sham arteries showed a larger basal VSM $[Ca^{2+}]_i$ (Table 5). In situ fura-2 calibrations were performed to evaluate potential autofluorescence of drugs or effects of drugs on the affinity of fura-2 for Ca^{2+} . Ro 31-8220, myr-PKC and rottlerin did not alter low or high in situ calibrations (Table 6).

Specific Aim 3.2 - Examine the effect of E-IH on pulmonary arterial PKC expression.

Effects of E-IH on PKC mRNA Expression

Based on findings in Specific Aim 3.1 that E-IH increases PKC-dependent vasoconstrictor reactivity, we sought to determine whether E-IH increases PKC expression to mediate enhanced PKC-dependent signaling. PKC α and β mRNA levels in intrapulmonary arteries were measured by real time PCR. E-IH did not significantly alter either PKC α or PKC β mRNA levels (Figure 26).

Table 5. Basal inner diameters and VSM $[Ca^{2+}]_i$ (F_{340}/F_{380}) in vehicle or Ro 31-8220, myr-PKC- or Rottlerin- pretreated arteries from Sham and E-IH rats

Group/Treatment	Inner Diameter (μm)	F_{340}/F_{380}	<i>n</i>
Sham + Vehicle for Ro and myr-PKC	125 ± 15	0.72 ± 0.06	6
E-IH + Vehicle for Ro and myr-PKC	150 ± 14	0.78 ± 0.10	4
Sham + Ro	139 ± 8	0.84 ± 0.06	8
E-IH + Ro	151 ± 15	0.83 ± 0.07	9
Sham + myr-PKC	140 ± 24	0.76 ± 0.04	5
E-IH + myr-PKC	161 ± 23	0.65 ± 0.04	6
Sham + Vehicle for Rottlerin	122 ± 17	0.89 ± 0.06	5
E-IH + Vehicle for Rottlerin	145 ± 23	0.75 ± 0.03*	5
Sham + Rottlerin	141 ± 14	0.77 ± 0.04	5
E-IH + Rottlerin	147 ± 16	0.72 ± 0.02	5

Values are means ± SE. *n*=number of rats. **P*<0.05 vs. Sham + Vehicle for Rottlerin. Ro, Ro 31-8220.

Table 6. *In situ fura-2 calibration values in vehicle or Ro 31-8220, myr-PKC- or Rottlerin- pretreated arteries from Sham and E-IH rats*

Group/Treatment	Low Cal (F ₃₄₀ /F ₃₈₀)	High Cal (F ₃₄₀ /F ₃₈₀)	n
Sham + Vehicle for Ro 31-8220 and myr-PKC	0.58 ± 0.02	1.61 ± 0.10	6
E-IH + Vehicle for Ro 31-8220 and myr-PKC	0.55 ± 0.02	1.60 ± 0.12	4
Sham + Ro 31-8220	0.60 ± 0.03	1.25 ± 0.04	6
E-IH + Ro 31-8220	0.57 ± 0.02	1.30 ± 0.09	7
Sham + myr-PKC	0.55 ± 0.02	1.54 ± 0.22	4
E-IH + myr-PKC	0.51 ± 0.01	1.33 ± 0.10	7
Sham + Vehicle for Rottlerin	0.56 ± 0.01	1.88 ± 0.22	4
E-IH + Vehicle for Rottlerin	0.59 ± 0.05	1.77 ± 0.03	3
Sham + Rottlerin	0.62 ± 0.03	1.62 ± 0.12	5
E-IH + Rottlerin	0.56 ± 0.02	1.60 ± 0.08	6

Values are means ± SE. n= number of rats. There are no significant differences.

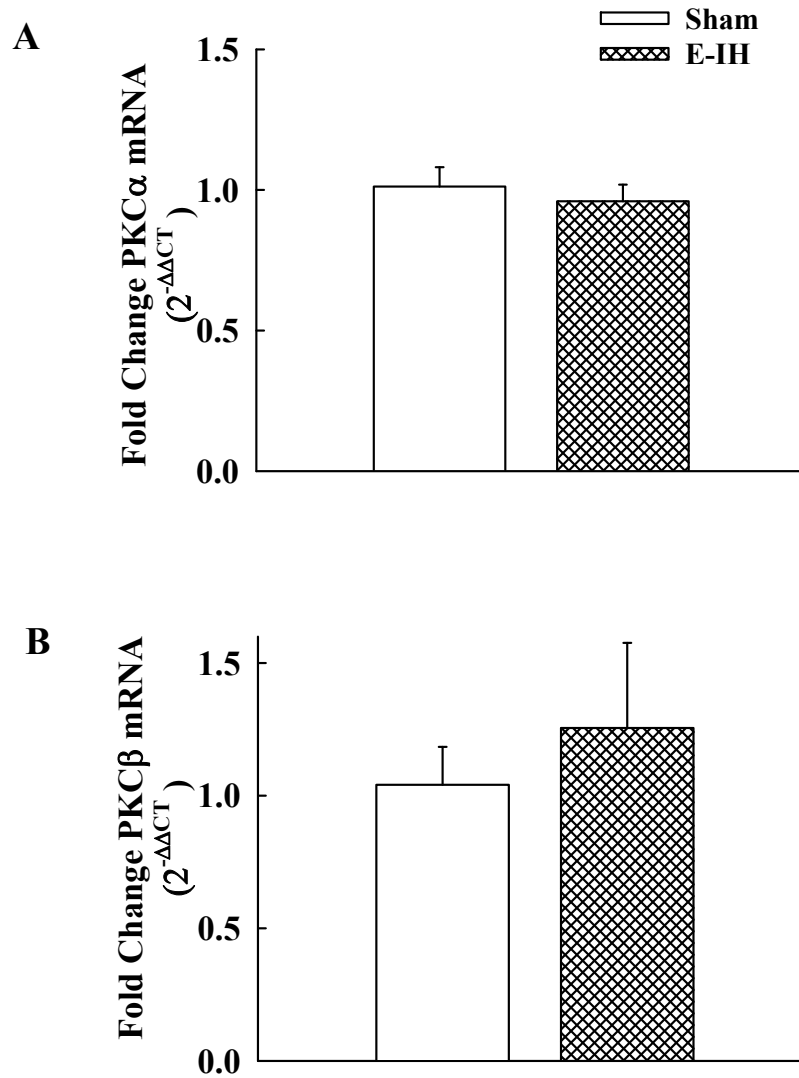


Figure 26. Pulmonary arterial A) PKC α and B)PKC β mRNA levels determined by real time PCR for in from Sham and E-IH rats. Data are means \pm SE of n= 6/group. There are no significant differences.

Effects of E-IH on PKC Protein Expression

Consistent with mRNA results, E-IH did not alter pulmonary arterial PKC α (Figure 27), PKC β I or PKC β II (Figure 28) protein levels, as determined by western blot analysis.

Summary of Results for Specific Aim 3

- General PKC inhibition and PKC α/β inhibition prevent the enhanced ET-1-dependent constriction following E-IH.
- Pulmonary arterial PKC α/β mRNA and protein expression are not different between Sham and E-IH.

Conclusion

Enhanced vasoconstrictor reactivity to ET-1 is dependent on PKC α/β , but this is not due to an increase in protein expression.

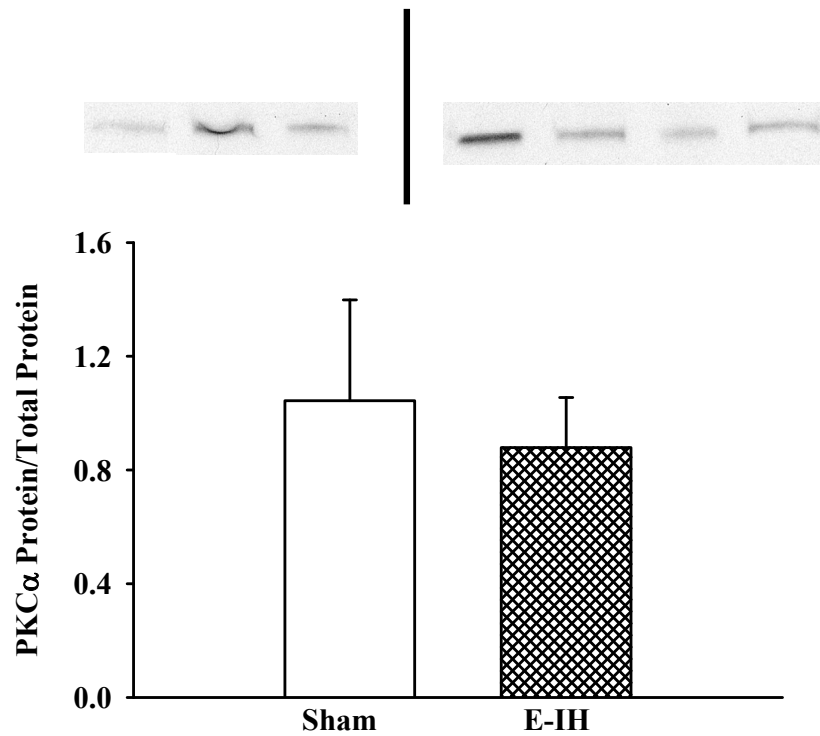


Figure 27. Western blotting data for PKC α in pulmonary arteries from Sham and IH rats. Data are means \pm SE of n= 3-4/group. There are no significant differences.

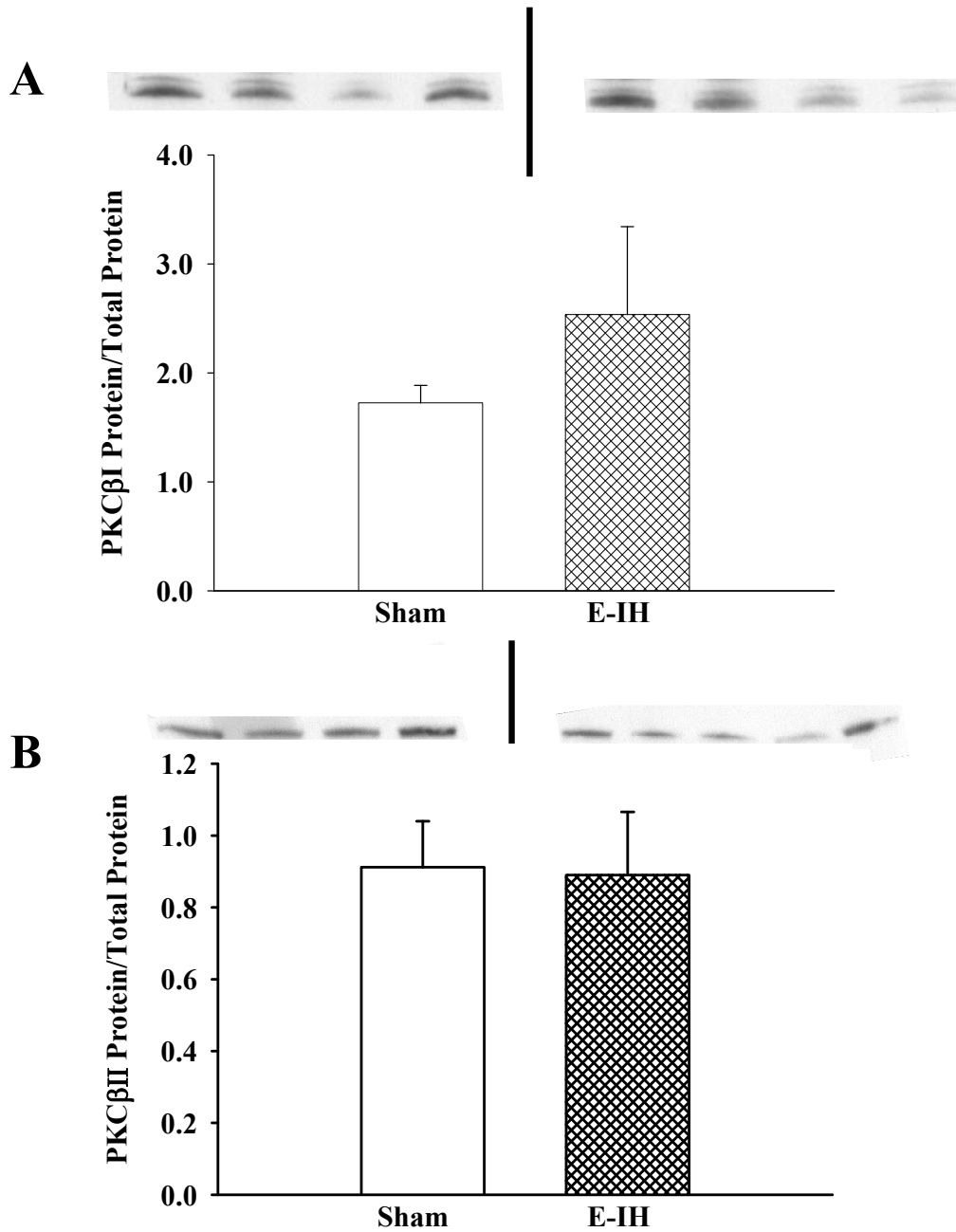


Figure 28. Western blot data for A) PKCβI and B)PKCβII in pulmonary arteries from Sham and IH rats. Data are means ± SE of n= 4-8/group. There are no significant differences.

Specific Aim 4: Determine the contribution of ROS to the development of right ventricular hypertrophy and enhanced agonist-induced vasoconstriction after E-IH.

Based on our findings in Specific Aim 3 that elevated agonist-induced vasoconstriction after E-IH is mediated by PKC, and given the evidence that ROS can activate PKC in PASMC (Rathore *et al.*, 2008), we sought to address the role of ROS in contributing to RV hypertrophy, PKC activation and enhanced agonist-induced vasoconstriction.

Specific Aim 4.1 - Assess the role of ROS in mediating E-IH-induced right ventricular hypertrophy.

To examine whether E-IH-induced RV hypertrophy is dependent on ROS generation, we administered the SOD mimetic tempol (1 mM) *in vivo* to rats treated with Sham or E-IH for 4 weeks. Following exposure to Sham or E-IH, right ventricles, left ventricle + septum, and body weight were measured. Right ventricle/total ventricular weight or body weight were calculated as indices of the degree of PH. Tempol treatment prevented E-IH-induced right ventricular hypertrophy as assessed by RV/T (Figure 29) and RV/BW (Table 7). Both Sham and E-IH tempol-treated rats gained weight over the 4 week treatment, however Sham rats gained more weight than E-IH rats. This is consistent with results from untreated rats (Table 2). There were no differences between left ventricle + septum/ body weight between Sham and E-IH rats.

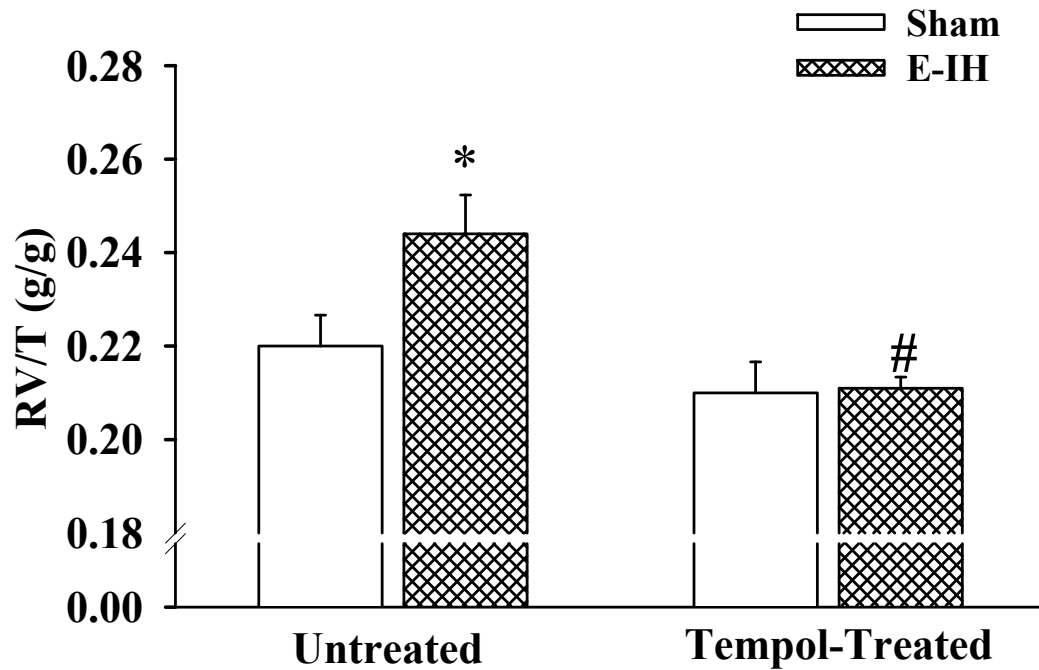


Figure 29. Ratios of right ventricle (RV) to total ventricle (T) weight in 4 week Wistar Sham and E-IH untreated or tempol-treated (1mM in the drinking water) rats. Values are means \pm SE of $n = 4$ - rats/group. * $P < 0.05$ vs. Sham. # $P < 0.05$ vs. untreated E-IH.

Table 7. *Pre and post exposure body weights, right ventricle/body weight and left ventricle + septum/body weight in tempol-treated Sham and E-IH rats.*

Group/ Treatment	Pre BW (g)	Post BW (g)	RV/BW (g/kg)	LV+S/BW (g/kg)	<i>n</i>
Sham + Tempol	185 ± 5	368 ± 11*	0.55 ± .02	2.06 ± .03	4
E-IH + Tempol	184 ± 8	304 ± 10*#	0.56 ± .02	2.11 ± .04	4

Pre BW denotes body weight before Sham or E-IH treatment. Post BW denotes body weight following 4 weeks of Sham or E-IH treatment. Values are means ± SE. *n*, number of rats. *P<0.05 vs. pre-exposure value. #P<0.05 vs. Sham post-exposure BW.

Specific Aim 4.2 - Assess the role of O_2^- and H_2O_2 in mediating augmented ET-1-induced vasoconstrictor reactivity following E-IH.

To determine whether augmented ET-1-induced vasoconstriction is mediated by ROS, responses to ET-1 were assessed in the presence of the O_2^- scavenger tiron (10 mM). As shown in Figure 30A, tiron prevented the increased vasoconstriction in response to ET-1 in arteries from E-IH rats while having little effect on the Ca^{2+} response to ET-1 (Figure 30B). In addition, tiron normalized vasoconstrictor responses between Sham and E-IH groups. Tiron did not alter basal arterial inner diameter, VSM $[Ca^{2+}]_i$ (Table 8), or in situ calibration values (Table 9).

To evaluate the potential contribution of H_2O_2 to augmented ET-1-induced vasoconstriction after E-IH, vasoconstrictor and VSM Ca^{2+} responses to ET-1 were assessed in the presence of the membrane permeable H_2O_2 scavenger, PEG-catalase. PEG-catalase did not alter vasoconstrictor responses to ET-1 in either group (Figure 31A) except for a slight augmentation at one concentration of ET-1 (10^{-11} M) in E-IH arteries. Ca^{2+} responses were similarly unaltered by PEG-catalase (Figure 31B). Basal inner diameter and F_{340}/F_{380} (Table 8) and in situ fura-2 calibration values (Table 9) were unaltered by PEG-catalase, although basal F_{340}/F_{380} was lower in E-IH arteries in the presence of PEG-catalase compared to Sham arteries + PEG-catalase (Table 8). These data suggest that H_2O_2 does not mediate the elevated ET-1-induced vasoconstriction after E-IH.

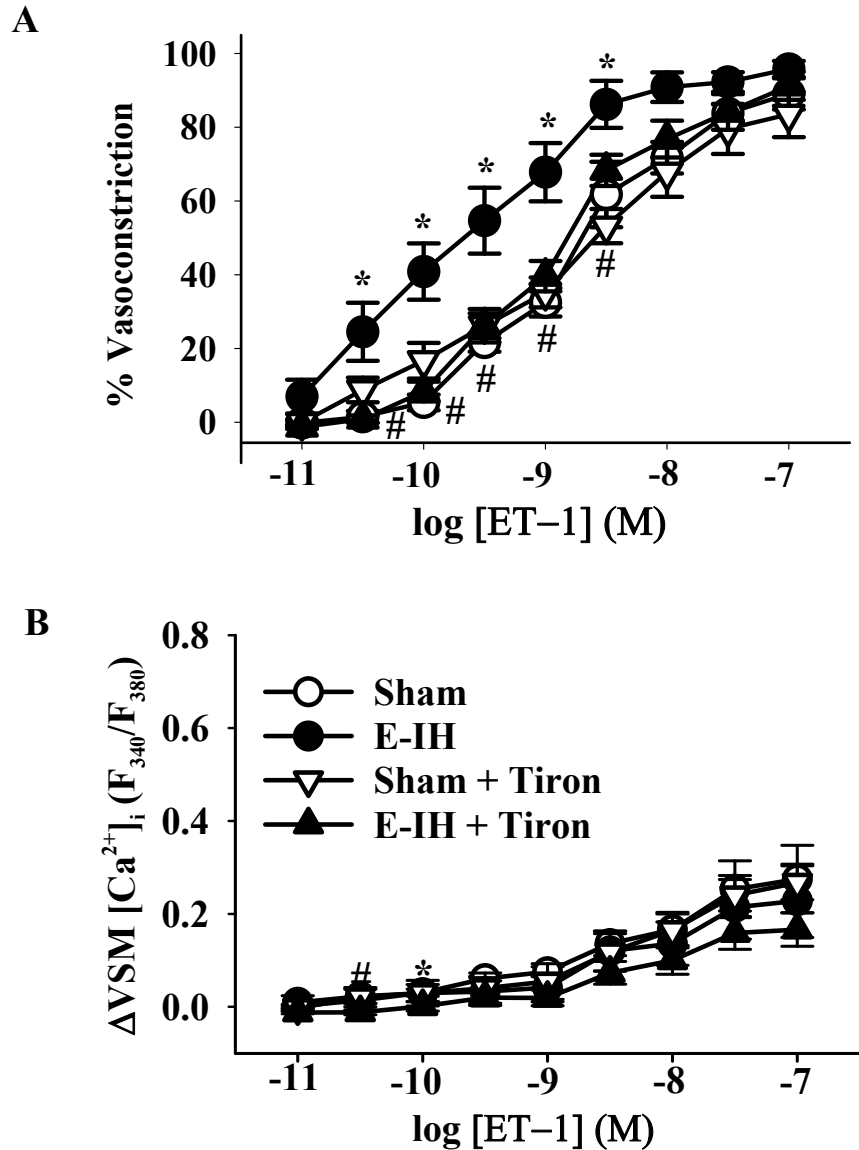


Figure 30. A) Vasoconstrictor and B) VSM $[Ca^{2+}]_i$ responses in the presence and absence of the ROS scavenger tiron (10 mM). (* $P < 0.05$ E-IH vs. Sham; # $P < 0.05$ E-IH vs. E-IH + tiron) Data are means \pm SE of $n = 5-9$ /group.

Table 8. Basal inner diameter and VSM $[Ca^{2+}]_i$ (F_{340}/F_{380}) in all vehicle- and drug-treated arteries in Specific Aim 4 from Sham and E-IH rats.

Group/Treatment	Inner Diameter (μm)	F_{340}/F_{380}	<i>n</i>
Sham + Vehicle for Tiron	134 \pm 25	0.71 \pm 0.06	6
E-IH + Vehicle for Tiron	158 \pm 20	0.85 \pm 0.10	5
Sham + Tiron	128 \pm 12	0.84 \pm 0.06	8
E-IH + Tiron	143 \pm 11	0.94 \pm 0.05	9
Sham + Vehicle for MITO-CP	116 \pm 14	0.74 \pm 0.06	5
E-IH + Vehicle for MITO-CP	144 \pm 10*	0.71 \pm 0.04	5
Sham + MITO-CP	114 \pm 8	0.92 \pm 0.07	4
E-IH + MITO-CP	118 \pm 12	0.80 \pm 0.06	5
Sham + Vehicle for PEG-catalase and Allopurinol	98 \pm 3	0.90 \pm 0.11	4
E-IH + Vehicle for PEG-catalase and Allopurinol	181 \pm 12†	0.85 \pm 0.06	5
Sham + PEG-catalase	139 \pm 14	0.94 \pm 0.06	5
E-IH + PEG-catalase	124 \pm 14	0.81 \pm 0.08**	5
Sham + Allopurinol	93 \pm 10	0.86 \pm 0.05	3
E-IH + Allopurinol	148 \pm 18#	0.77 \pm 0.19	5
Sham + Vehicle for Apocynin and Rotenone	120 \pm 22	0.88 \pm 0.07	4
E-IH + Vehicle for Apocynin and Rotenone	145 \pm 28	0.88 \pm 0.06	4
Sham + Apocynin	125 \pm 4	0.71 \pm 0.04	5
E-IH + Apocynin	156 \pm 5	0.94 \pm 0.10	5
Sham + Rotenone	147 \pm 20	0.72 \pm 0.07	4
E-IH + Rotenone	158 \pm 18	0.78 \pm 0.05	4

Sham + Vehicle for Ro + Tiron/ myr-PKC + Tiron	125 ± 15	0.72 ± 0.06	6
E-IH + Vehicle for Ro + Tiron/ myr-PKC + Tiron	150 ± 14	0.78 ± 0.10	4
Sham + Ro + Tiron	181 ± 8‡	0.85 ± 0.07	5
E-IH + Ro + Tiron	170 ± 10	0.88 ± 0.06	5
Sham + myr-PKC + Tiron	175 ± 12‡	0.74 ± 0.05	4
E-IH + myr-PKC + Tiron	152 ± 17	0.71 ± 0.04	5

Values are means ± SE. *n*, number of rats. *P<0.05 vs. Sham + Vehicle for MITO-CP. †P<0.05 vs. Sham + Vehicle PEG-catalase and Allopurinol. # P<0.05 vs. Sham + Allopurinol. **P<0.05 vs. Sham + PEG-catalase. ‡P<0.05 vs. Sham + Vehicle for Ro + Tiron/ myr-PKC + Tiron.

Table 9. *In situ fura-2 calibration values*

	Low Cal (F ₃₄₀ /F ₃₈₀)	High Cal (F ₃₄₀ /F ₃₈₀)	<i>n</i>
Sham + Vehicle for Tiron	0.56 ± 0.03	1.51 ± 0.12	5
E-IH + Vehicle for Tiron	0.54 ± 0.02	1.48 ± 0.07	5
Sham + Tiron	0.55 ± 0.03	1.52 ± 0.11	7
E-IH + Tiron	0.54 ± 0.02	1.48 ± 0.07	8
Sham + Vehicle for PEG-catalase and Allopurinol	0.63 ± 0.08	1.83 ± 0.25	4
E-IH + Vehicle for PEG-catalase and Allopurinol	0.64 ± 0.05	1.64 ± 0.16	5
Sham + PEG-catalase	0.63 ± 0.02	1.78 ± 0.19	5
E-IH + PEG-catalase	0.63 ± 0.03	1.56 ± 0.14	5
Sham + Allopurinol	0.75 ± 0.03	1.73 ± 0.12	3
E-IH + Allopurinol	0.63 ± 0.02	1.65 ± 0.11	5
Sham + Vehicle for Apocynin and Rotenone	0.63 ± 0.05	1.73 ± 0.19	4
E-IH + Vehicle for Apocynin and Rotenone	0.62 ± 0.03	1.94 ± 0.05	4
Sham + Apocynin	0.59 ± 0.08	1.88 ± 0.19	5
E-IH + Apocynin	0.59 ± 0.04	1.85 ± 0.25	4
Sham + Rotenone	0.76 ± 0.04	2.23 ± 0.23	4
E-IH + Rotenone	0.79 ± 0.06	2.47 ± 0.12	3
Sham + Vehicle for MITO-CP	0.57 ± 0.02	1.58 ± 0.14	4
E-IH + Vehicle for MITO-CP	0.63 ± 0.02#	1.56 ± 0.09	5
Sham + MITO-CP	0.63 ± 0.02*	2.12 ± 0.01*	4
E-IH + MITO-CP	0.59 ± 0.01	1.60 ± 0.08 **	4

Values are means ± SE. *n*, number of rats. *P<0.05 vs. corresponding vehicle. #P<0.05 vs. Sham + vehicle for MITO-CP. **P<0.05 vs. Sham + MITO-CP.

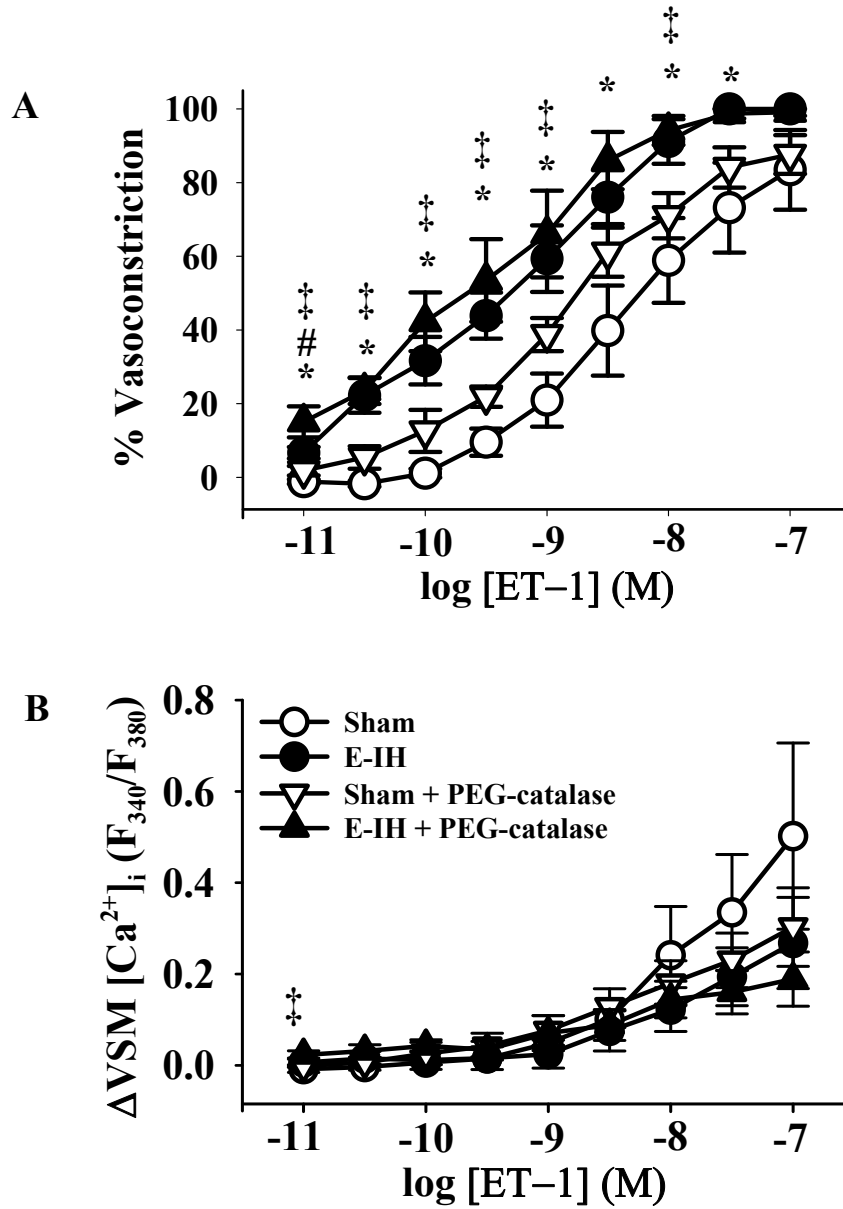


Figure 31. A) Vasoconstrictor and B) VSM $[Ca^{2+}]_i$ responses in the presence and absence of PEG-catalase (250 U/ml). (* $P < 0.05$ E-IH vs. Sham; # $P < 0.05$ E-IH vs. E-IH + PEG-catalase; ‡ $P < 0.05$ Sham + PEG-catalase vs. E-IH + PEG-catalase) Data are means \pm SE of $n = 4-5$ /group.

Specific Aim 4.3 - Evaluate the relative contributions of NOX, XO, and mitochondrial sources of ROS to increased ET-1-mediated vasoconstriction following E-IH.

Effects of Inhibition of NOX on ET-1-Induced Vasoconstriction

In the presence of apocynin, which inhibits NOX1/2 isoforms, the elevated vasoconstriction to ET-1 in E-IH vessels persists (Figure 32A). Furthermore, apocynin had no significant effect on ET-1-induced Ca^{2+} responses (Figure 32B), except for a slight decrease in the Ca^{2+} response in E-IH vessels at one concentration of ET-1 (10^{-10} M). These data suggest that E-IH-induced increases in vasoreactivity to ET-1 are NOX-independent. Basal inner diameter and F_{340}/F_{380} (Table 8) and *in situ* calibrations (Table 9) were not different between groups.

Effects Xanthine Oxidase Inhibition on ET-1-Induced Vasoconstriction

XO inhibition did not decrease either ET-1-induced constriction (Figure 33A) or Ca^{2+} responses (Figure 33B) in E-IH vessels, indicating that ET-1-induced vasoconstriction following E-IH is independent of XO-derived O_2^- . Furthermore, there was no effect of allopurinol on either vasoconstrictor or VSM $[Ca^{2+}]_i$ responses in Sham vessels. Allopurinol did not alter basal inner diameter, F_{340}/F_{380} (Table 8) or *in situ* calibrations (Table 9).

Effects of Mitochondrial ROS Scavenging on ET-1-Induced Vasoconstriction

MITO-CP substantially inhibited vasoconstriction in arteries from E-IH rats, while having minimal effects in the Sham group. Furthermore, mitochondrial ROS scavenging resulted in normalization of reactivity between groups (Figure 34A). This

attenuated

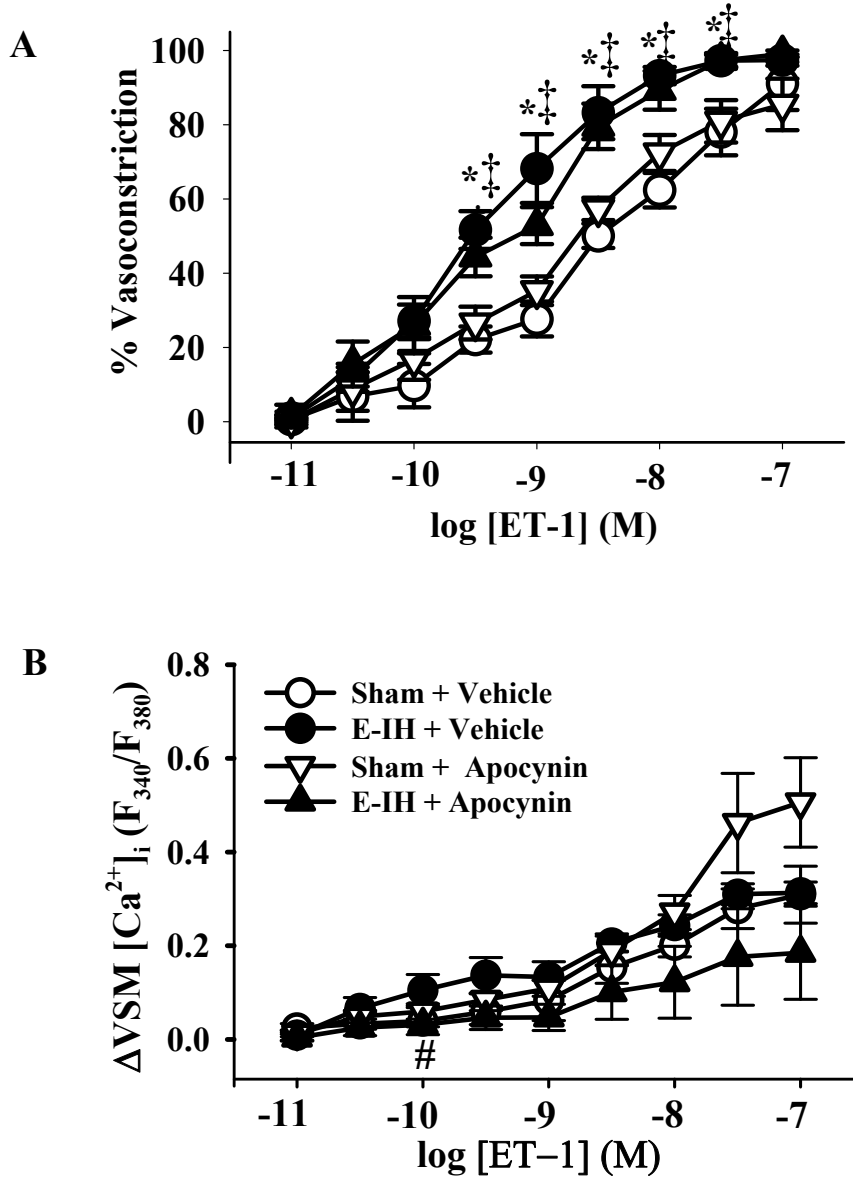


Figure 32. A) Vasoconstrictor and B) VSM $[Ca^{2+}]_i$ responses in the presence and absence of the NADPH oxidase inhibitor apocynin ($30 \mu M$). (* $P < 0.05$ E-IH vs. Sham; # $P < 0.05$ E-IH vs. E-IH + apocynin; ‡ $P < 0.05$ E-IH + apocynin vs. Sham + apocynin) Data are means \pm SE of $n = 4-5$ /group.

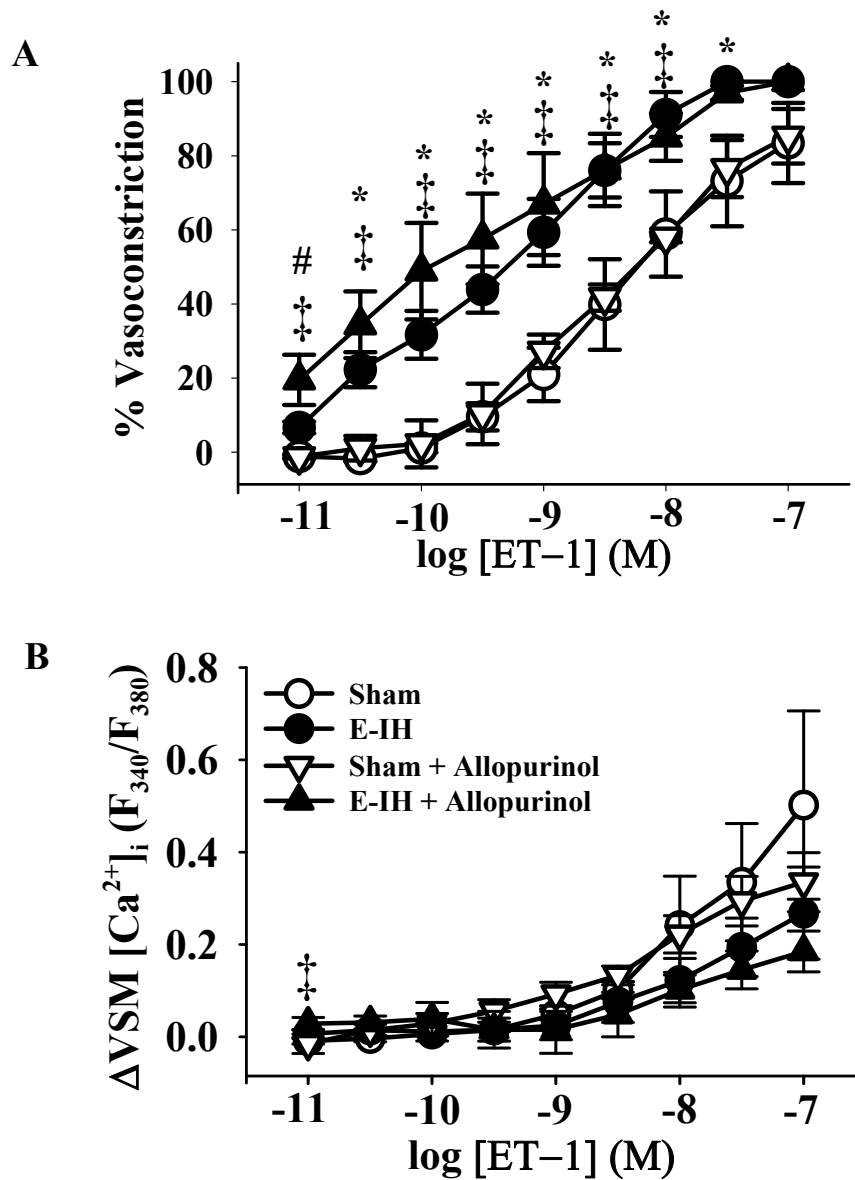


Figure 33. A) Vasoconstrictor and B) VSM $[Ca^{2+}]_i$ responses in the presence and absence of the xanthine oxidase inhibitor allopurinol (100 μ M). (* $P < 0.05$ E-IH vs. Sham; # $P < 0.05$ E-IH vs. E-IH + allopurinol; ‡ $P < 0.05$ Sham + allopurinol vs. E-IH + allopurinol) Data are means \pm SE of $n = 3-5$ /group.

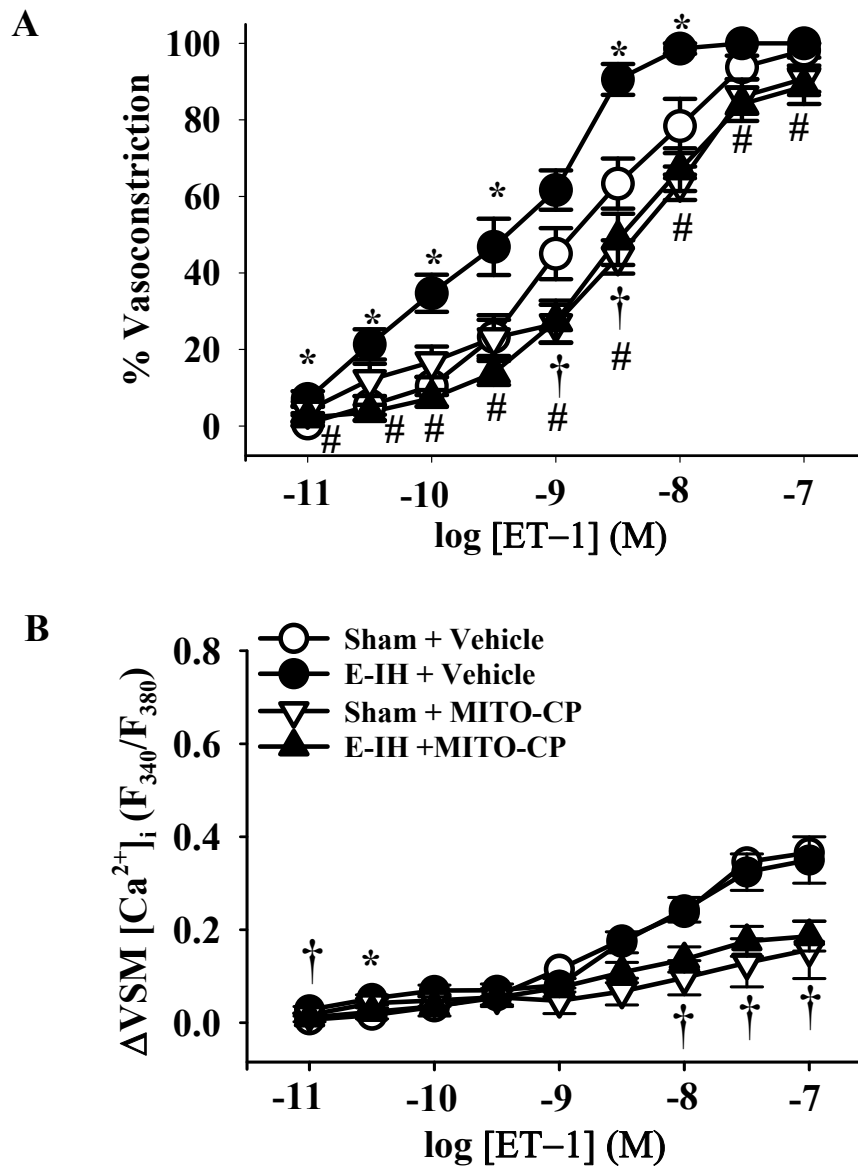


Figure 34. A) Vasoconstrictor and B) VSM $[Ca^{2+}]_i$ responses in the presence and absence of the mitochondrial ROS scavenger MITO-CP (0.5 μ M). (* $P < 0.05$ E-IH vs. Sham; # $P < 0.05$ E-IH vs. E-IH + MITO-CP; † $P < 0.05$ Sham vs. Sham + MITO-CP) Data are means \pm SE of $n = 4-5$ /group.

vasoconstriction by MITO-CP in E-IH arteries was associated with a tendency for a lesser Ca^{2+} response to ET-1, which did not achieve statistical significance (Figure 34B). MITO-CP significantly attenuated ET-1-dependent increases in VSM $[Ca^{2+}]_i$ in Sham arteries at the highest concentrations of ET-1 (10^{-8} - 10^{-7} M). In the presence of the vehicle for MITO-CP (DMSO) basal inner diameter was greater in the E-IH group (Table 8). Basal F_{340}/F_{380} was not different between Sham and E-IH and was not altered by MITO-CP. The low in situ calibration was greater in E-IH vehicle versus Sham vehicle group, whereas in the presence of MITO-CP, the low calibration value was less in the E-IH group. The high in situ calibration value was increased by MITO-CP in the Sham group and was greater in Sham vessels in the presence of MITO-CP versus E-IH vessels treated with MITO-CP (Table 9).

To confirm the effect of MITO-CP on vasoconstrictor responses to ET-1, mitochondrial ROS generation was also inhibited with the mitochondrial complex I inhibitor rotenone. Rotenone profoundly attenuated vasoconstrictor reactivity to ET-1 in E-IH vessels while decreasing vasoconstriction to ET-1 only at one concentration ($10^{-9.5}$ M) in Sham arteries. In addition, rotenone normalized responses between groups (Figure 35A). Surprisingly, rotenone increased Ca^{2+} responses to ET-1 in both groups (Figure 35B). Basal inner diameter and F_{340}/F_{380} were not different in arteries treated with rotenone or its vehicle (Table 8). Rotenone had no effect on in situ fura-2 calibrations (Table 9).

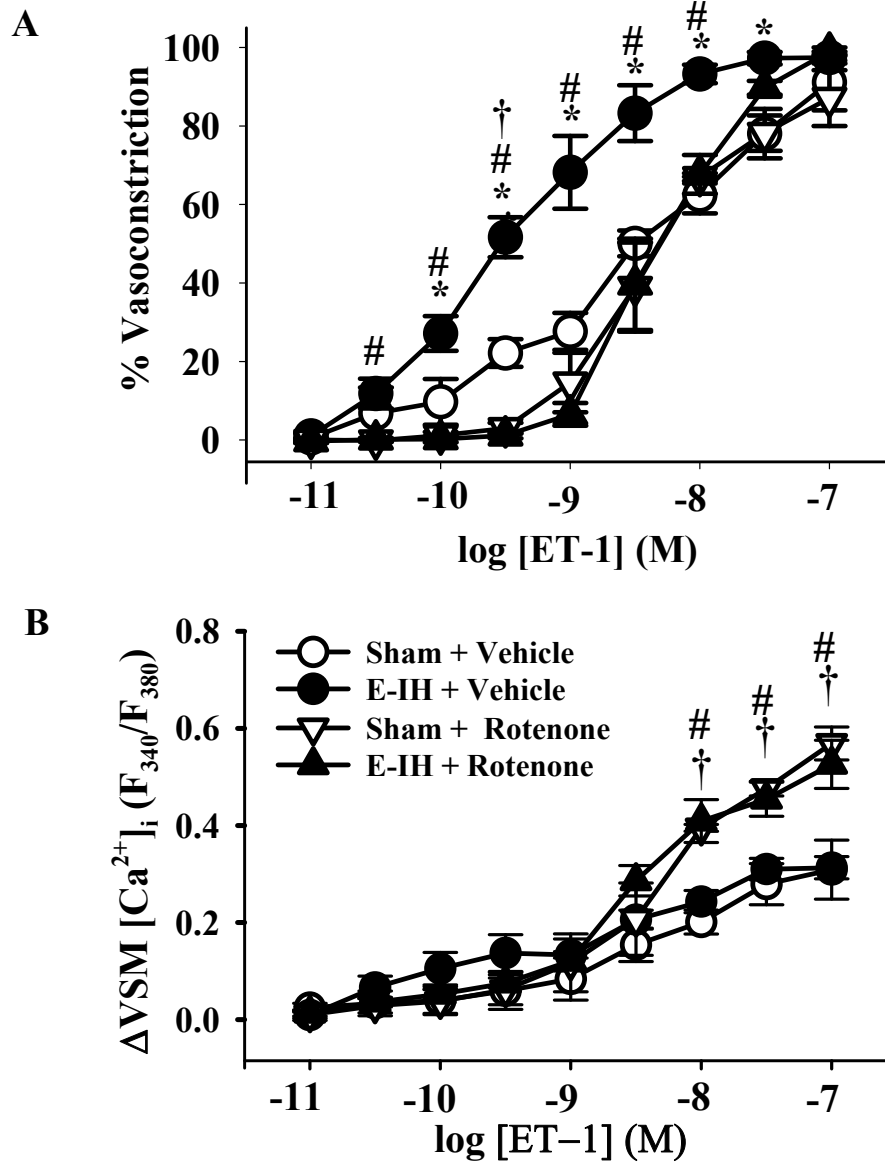


Figure 35. A) Vasoconstrictor and B) VSM $[Ca^{2+}]_i$ responses in the presence and absence of the mitochondrial complex I inhibitor rotenone ($10 \mu M$). (* $P < 0.05$ E-IH vs. Sham; # $P < 0.05$ E-IH vs. E-IH + rotenone; † $P < 0.05$ Sham vs. Sham + rotenone; ‡ $P < 0.05$ Sham + rotenone vs. E-IH + rotenone) Data are means \pm SE of $n = 4-5$ /group.

Specific Aim 4.4 - Determine the effect of E-IH on pulmonary arterial ROS levels under basal and stimulated conditions.

We evaluated effects of E-IH on basal and ET-1-induced DHE fluorescence in isolated, endothelium-disrupted pulmonary arteries. E-IH increased both basal and ET-1-stimulated DHE fluorescence (Figure 36), and this was prevented by pretreatment with tiron. The effect of ET-1 to increase O_2^- levels was unique to E-IH vessels and was not present in Sham arteries. In addition, tiron had no effect on DHE fluorescence in Sham arteries.

Specific Aim 4.5 - Assess the role of ROS-dependent PKC activation in enhanced ET-1-induced vasoconstriction following E-IH.

Effect of Combined ROS Scavenging and PKC Inhibition on Vasoconstrictor Reactivity to ET-1

To address whether ROS and PKC signal through a common pathway, vasoconstrictor and VSM Ca^{2+} responses to ET-1 were assessed in the during combined O_2^- scavenging and PKC inhibition using tiron/Ro 31-8220. Similar to effects of either treatment alone, combined ROS scavenging and PKC inhibition attenuated vasoconstrictor responses to ET-1 in E-IH but not Sham vessels and normalized responses between groups (Figure 37). Furthermore, combined treatment with Ro 31-8220 and tiron did not appear to result in greater inhibition of the vasoconstriction than either treatment alone. However, treatment with Ro 31-8220 and tiron decreased Ca^{2+} responses to ET-1 in E-IH ($10^{-8.5}$ - 10^{-7} M) and Sham ($10^{-7.5}$ M) vessels, similar to effects of Ro 31-8220 alone.

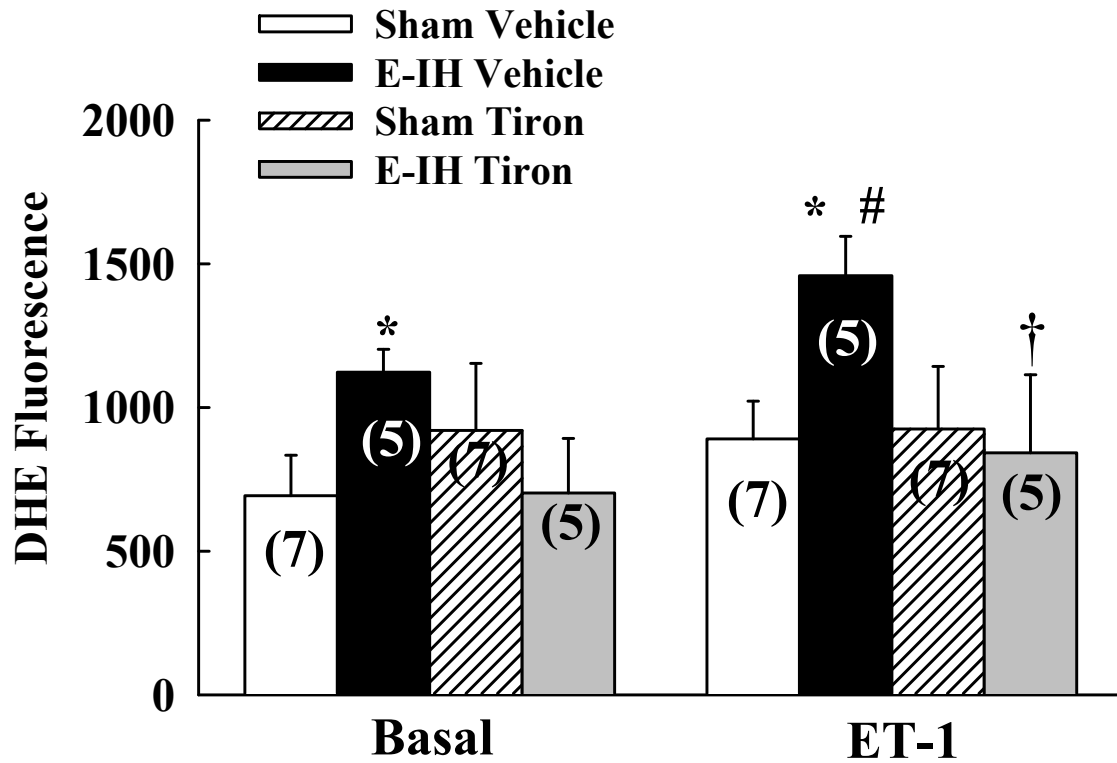


Figure 36. Basal and ET-1-stimulated DHE fluorescence in pulmonary arteries from Sham and E-IH rats in the presence and absence of the superoxide scavenger tiron (10 mM). (* $P < 0.05$ E-IH vs. Sham; † $P < 0.05$ vs. E-IH + vehicle; # $P < 0.05$ vs. basal) Data are means \pm SE of $n = 4-7$ /group.

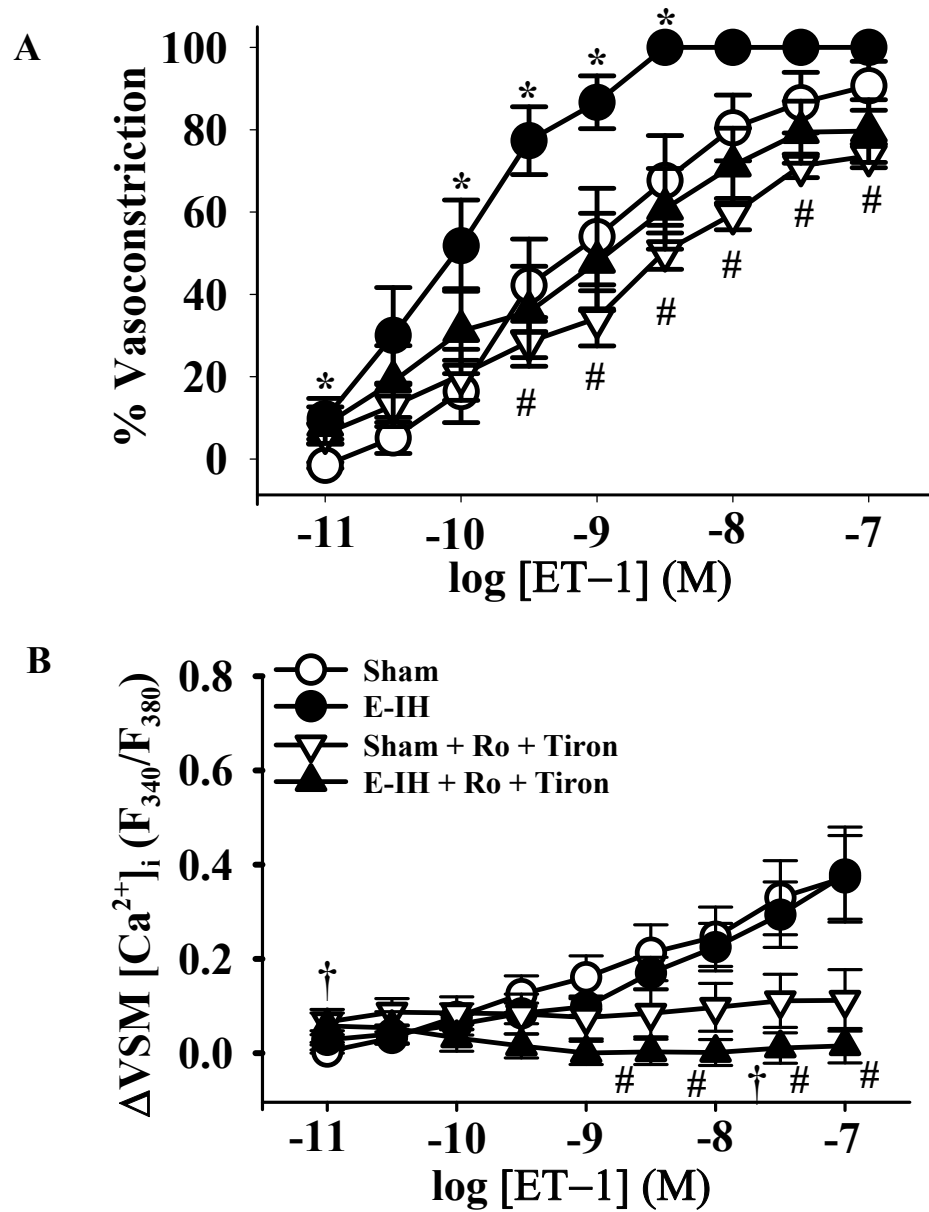


Figure 37. A) Vasoconstrictor and B) VSM $[Ca^{2+}]_i$ responses in the presence and absence of the superoxide scavenger tiron (10 mM) and the PKC inhibitor Ro 31-8220 (Ro, 10 μ M). (* $P < 0.05$ E-IH vs. Sham; # $P < 0.05$ E-IH vs. E-IH + Ro + tiron; † $P < 0.05$ Sham vs. Sham + Ro + tiron) Data are means \pm SE of $n = 4-6$ /group.

In the presence of combined ROS scavenging and PKC α/β inhibition, vasoconstriction to ET-1 was again attenuated in vessels from E-IH rats to the level of Sham vessels (Figure 38A), without altering Ca²⁺ responses to ET-1 (Figure 38B). The effects of combined tiron/myr-PKC treatment were consistent with effects of either drug alone. Therefore, the effect of these two drugs did not appear to be additive suggesting that ROS and PKC α/β signal in series to mediated enhanced ET-1 vasoconstrictor reactivity after E-IH. Sham vessels treated with either the combination of tiron/Ro 31-8220 or tiron/myr-PKC had significantly larger basal inner diameters than the corresponding vehicle-treated Sham arteries. However, neither tiron/Ro 31-8220 nor tiron/myr-PKC altered basal F₃₄₀/F₃₈₀ values (Table 8).

Effect of PKC α/β Inhibition on Basal and ET-1-Stimulated O₂⁻ Levels in Pulmonary Arteries

To determine whether PKC functions at a point proximal or distal to the site of agonist-induced ROS generation in E-IH arteries, we evaluated basal and ET-1-stimulated DHE fluorescence in both the presence and absence of the PKC α/β inhibitor, myr-PKC. Interestingly, myr-PKC prevented both the enhanced basal and ET-1-induced O₂⁻ generation in vessels from E-IH rats (Figure 39), suggesting that PKC α/β mediate both basal and agonist-stimulated ROS production following E-IH.

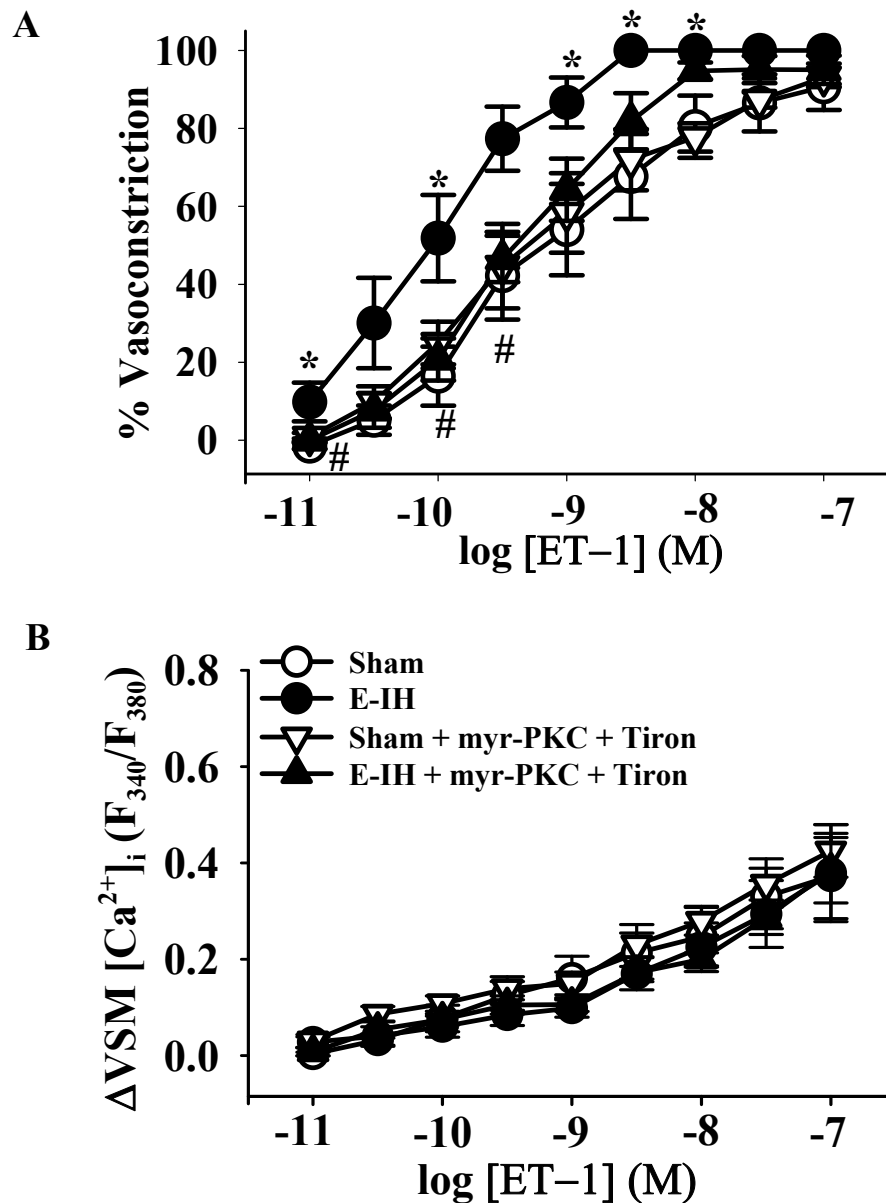


Figure 38. A) Vasoconstrictor and B) VSM $[Ca^{2+}]_i$ responses in the presence and absence of the superoxide scavenger tiron (10mM) and the PKC α/β inhibitor myr-PKC (10 μ M). (* $P < 0.05$ E-IH vs. Sham; # $P < 0.05$ E-IH vs. E-IH + myr-PKC + tiron) Data are means \pm SE of $n = 4-6$ /group.

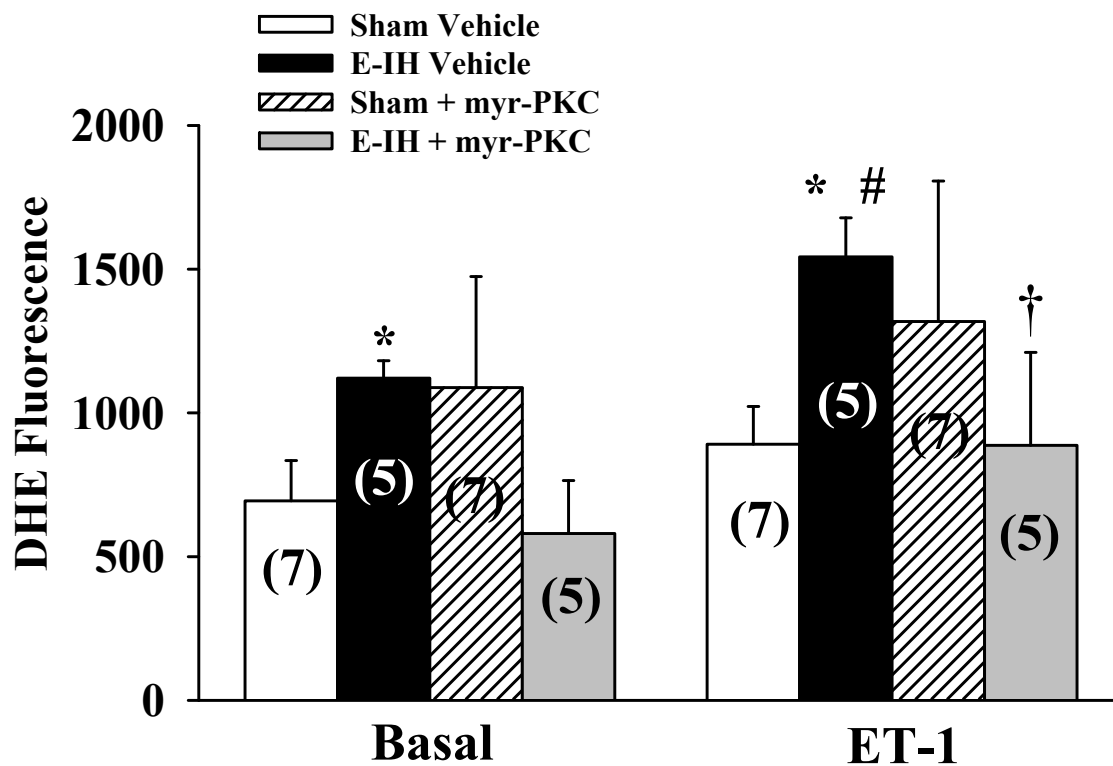


Figure 39. Basal and ET-1-stimulated DHE fluorescence in pulmonary arteries from Sham and E-IH rats in the following treatment with vehicle or the PKC α/β inhibitor myr-PKC (10 μ M). (* P <0.05 E-IH vs. Sham; † P <0.05 vs. E-IH + vehicle; # P <0.05 vs. basal) Data are means \pm SE of n = 5-7/group.

Summary of Results for Specific Aim 4

- *In vivo* treatment with an SOD mimetic prevents E-IH-induced right ventricular hypertrophy.
- Increased ET-1-induced vasoconstriction following E-IH is unaffected by inhibitors of NOX and XO. However, inhibitors of mitochondrial ROS generation prevent elevated ET-1-induced vasoconstrictor reactivity.
- E-IH increases both basal and ET-1-stimulated O_2^- levels in pulmonary arteries.
- Combined PKC α/β inhibition and ROS scavenging decreases augmented vasoconstriction to ET-1 in E-IH vessels, to a similar degree as either treatment alone.
- PKC α/β inhibition prevents ET-1-induced increase in O_2^- in E-IH arteries.

Conclusions

- E-IH induces right ventricular hypertrophy via a superoxide-dependent mechanism. Enhanced pulmonary artery vasoconstrictor reactivity to ET-1 after E-IH is dependent on mitochondrial O_2^- but not NOX, XO or H_2O_2 .
- PKC α/β and ROS signal in series to mediate augmented ET-1-induced vasoconstriction following E-IH. ET-1-induced O_2^- production is dependent on PKC α/β .

CHAPTER IV

DISCUSSION

Pulmonary hypertension during wakefulness has been reported to occur in 17-43% of patients with SA (Arias *et al.*, 2006;Tilkian *et al.*, 1976;Zielinski, 2005) and may be as severe as 70 mmHg (Ogawa *et al.*, 2006). Furthermore, SA coincident with COPD results in a 75% occurrence of PH, suggesting that SA exacerbates PH resulting from COPD (Chaouat *et al.*, 1996;Fletcher *et al.*, 1987;Kessler *et al.*, 1996). Despite growing recognition of the magnitude of this disorder, the cardiovascular sequelae leading to the progression of SA-induced PH in humans remains poorly understood. Therefore, we investigated effects of IH on indices of PH and vasoreactivity using a rat model of SA that has previously been documented to induce systemic hypertension (Allahdadi *et al.*, 2005;Kanagy *et al.*, 2001), a common condition in patients with SA.

The major findings of this study are that IH with supplemental CO₂ (E-IH) elicits RV hypertrophy indicative of PH, which is associated with enhanced vasoconstrictor reactivity but not polycythemia or pulmonary vascular remodeling. In addition, increased vasoconstrictor reactivity following E-IH is mediated by PKC α/β and mitochondrial O₂⁻, but not ROK, and PKC acts proximal to O₂⁻ generation in pulmonary arteries. Consistent with a role for O₂⁻ in enhanced pulmonary vasoconstrictor reactivity, O₂⁻ mediates E-IH-induced RV hypertrophy.

Specific Aim 1: Compare effects of E-IH and H-IH on indices of pulmonary hypertension and vasoconstrictor reactivity.

This aim tested the hypotheses that IH augments pulmonary vasoconstrictor reactivity and indices of pulmonary hypertension and that supplemental CO₂ attenuates IH-induced polycythemia, arterial remodeling, right ventricular hypertrophy, and enhanced vasoconstrictor sensitivity. We found that H-IH induced polycythemia and pulmonary arterial remodeling that was inhibited by supplemental CO₂. However, despite these inhibitory effects of supplemental CO₂, 4 weeks of E-IH exposure produced a degree of RV hypertrophy similar to that of H-IH and increased vasoconstrictor reactivity.

Arterial Blood Gases

The level of IH-induced hypoxemia is similar to that reported in human patients during apneic episodes (Buda *et al.*, 1981). H-IH animals demonstrated a fall in arterial PCO₂ during hypoxia, indicative of hyperventilation in response to hypoxia, but this was prevented by supplemental CO₂. Consistent with these changes in PCO₂, arterial pH remained unchanged in E-IH animals during hypoxia, while H-IH animals became alkalotic during IH. We have previously shown that 4 wk CH results in a greater PO₂ and reduced pH and PCO₂ under both normoxic and hypoxic conditions compared to control animals, reflecting hyperventilation and acid-base adjustments to CH (Resta & Walker, 1994). However, our results in 4 week E-IH animals suggest that similar acclimation does not occur with long term E-IH exposure. This is consistent with previous studies of 35

days of IH exposure in which changes in arterial blood gases are not significantly different at the beginning of IH exposure versus at the end (Kuwahira *et al.*, 1999).

Right Ventricular Hypertrophy

As reported previously, two week exposure to H-IH resulted in increased right ventricular hypertrophy in rats (Snow *et al.*, 2008), suggestive of pulmonary hypertension. While our right ventricular hypertrophy data support the idea that this model of IH elicits PH, we cannot rule out the possibility that there is a dissociation between right ventricular hypertrophy and sustained PH. During hypoxic cycling, there is presumably hypoxic pulmonary vasoconstriction and an associated increase in pulmonary vascular resistance that occurs at each arterial PO₂ nadir. This periodic increase in resistance may provide a sufficient stimulus for a compensatory cardiac hypertrophic response when sustained over a 4 week period, as in the current IH model. Future studies are planned to measure PAP at rest and during cycling conditions to determine effects of E-IH on HPV responses and development of sustained PH.

The mechanism by which CO₂ reduces IH-mediated RV hypertrophy following 2 weeks of IH exposure remains to be established, however, it is possible that CO₂-induced decreases in ROS are involved. CH elicits PH in newborn rats which is associated with an increase in oxidant stress assessed by 8-isoprostane content in the lung (Kantores *et al.*, 2006). Interestingly, exposure of these rats to 10% CO₂ during hypoxia reduced oxidant stress and attenuated CH-induced PH. ROS have additionally been implicated in contributing to PH based on evidence that there is increased oxidant stress in lungs from idiopathic pulmonary hypertension patients (Bowers *et al.*, 2004; Cracowski *et al.*, 2001).

The administration of antioxidants blunts PH (Chen *et al.*, 2001;Hoshikawa *et al.*, 2001) and this response may be mediated by decreased oxidant-produced pulmonary vasoconstrictors, such as 8-isoprostane, peroxynitrite, and ET-1 (Jankov *et al.*, 2008). The effect of CO₂ supplementation to prevent hypoxia-induced increases in lung 8-isoprostane is additionally associated with decreased lung expression of the potent endothelium-derived vasoconstrictor peptide, ET-1 (Kantores *et al.*, 2006), suggesting that multiple mechanisms contribute to the protective effects of CO₂ in the hypertensive pulmonary vasculature.

Polycythemia

CH induces polycythemia via induction of erythropoietin gene expression, and this mechanism compensates for arterial hypoxemia by increasing the O₂ carrying capacity of the blood. Polycythemia increases blood viscosity and may increase pulmonary vascular resistance (Barer *et al.*, 1983) and contribute to PH. However, studies from our laboratory have shown that polycythemia alone, induced by administration of recombinant erythropoietin *in vivo*, is insufficient to cause PH (Walker *et al.*, 2000).

Other models of IH have also been shown to increase hematocrit (Fagan, 2001;Siques *et al.*, 2006). We, therefore, investigated the possibility that IH increases hematocrit in our model of SA. As expected, both rat strains exposed to H-IH developed significant polycythemia. It is likely that IH increases hematocrit via the well known mechanism of hypoxia-induced increases in HIF-1-dependent gene transcription (Fisher, 2003). HIF-1 drives erythropoietin synthesis in the kidney, and the rise in erythropoietin

levels stimulates erythropoiesis in the bone marrow. In contrast to effects of H-IH, E-IH elicited only a modest increase in hematocrit in Sprague Dawley rats and did not increase hematocrit in Wistar rats, suggesting that CO₂ attenuates hypoxia-induced erythropoiesis. Similarly, supplemental CO₂ has been reported to prevent CH-induced polycythemia (Kantores *et al.*, 2006). Although the mechanism by which this occurs is unknown, it is possible that CO₂ attenuates HIF-1-dependent erythropoietin expression. Based on our present findings that CO₂ attenuated both the RV hypertrophy and erythropoietin-dependent polycythemic responses to H-IH, it is possible that CO₂ mediates these responses through a common mechanism of decreased hypoxia-inducible gene expression. In fact, recent studies suggest that IH elicits HIF-1 α accumulation via ROS-dependent mechanisms (Yuan *et al.*, 2008). Therefore, if CO₂ decreases oxidative stress in the lung, this could account for lesser HIF-dependent gene expression.

Pulmonary Arterial Remodeling

Similar to reports of IH causing pulmonary arterial remodeling in mice (Fagan, 2001), the current study indicates that H-IH caused remodeling of small pulmonary arteries. This finding is consistent with a previous study in which H-IH caused pulmonary arterial remodeling, evident by an increase in the number of smooth muscle α -actin positive vessels, a reduction in luminal diameter and increased arterial wall thickness in mice (Nisbet *et al.*, 2008). However, in this study by Nisbet *et al.*, the pulmonary vasculature was not maximally dilated before fixation, which complicates the interpretation of luminal diameter data. Similar to the effect of CO₂ supplementation to prevent H-IH-induced RV hypertrophy (in Sprague Dawley rats) and polycythemia, the

present study shows that CO₂ prevented IH-induced pulmonary arterial remodeling. Again, this may be a function of CO₂ to decrease oxidative stress and/or HIF-dependent (Yuan *et al.*, 2008) ET-1 production as previously reported (Jankov *et al.*, 2008).

Pulmonary Vasoconstrictor Reactivity Following IH

IH elicits RV hypertrophy, indicative of PH, and vasoconstriction may contribute to this response. CH augments pulmonary vasoconstrictor responsiveness to several other agonists, including UTP, sphingosylphosphorylcholine, prostaglandin F_{2α}, angiotensin II, and norepinephrine (Jernigan *et al.*, 2004b;McMurtry *et al.*, 1978;Russell *et al.*, 1990). Therefore, we addressed effects of IH on pulmonary vasoconstrictor reactivity. Given that CH increases pulmonary vasoconstrictor reactivity largely through mechanisms inherent to the VSM (Jernigan *et al.*, 2008), we assessed responses in endothelium-disrupted arteries. We observed that E-IH increased vasoconstrictor reactivity to agonists ET-1, UTP, and 5-HT, indicative of a generalized hyper-reactivity to pulmonary vasoconstrictors. This greater propensity for vasoconstriction was not associated with a greater Ca²⁺ response, suggesting that E-IH increases VSM Ca²⁺ sensitivity. A limitation of studying endothelium-disrupted arteries is the possibility that IH results in compensatory increases in endothelium-dependent dilation, which may offset the observed increase in vasoconstrictor reactivity. However, our previous studies suggest that endothelium-dependent dilation is not altered by IH (Snow *et al.*, 2008). Similar to our present observations of greater agonist-induced vasoconstriction in arteries from E-IH rats, Thomas and Wanstall (Thomas & Wanstall, 2003) found that IH (continuous 10% O₂ for 8 hr/day) enhanced vasoconstriction to various agonists

including U-46619, 5-HT and ET-1 in rat main pulmonary artery rings. Although enhanced vasoconstrictor reactivity could be explained by an increase in receptor expression, the increase in reactivity to multiple agonists argues against this possibility. It is more likely that intracellular signaling mechanisms, which are commonly stimulated by various agonists, are increased by E-IH to contribute to increased pulmonary vasoconstrictor reactivity. Given the observed E-IH-induced RV hypertrophy in the absence of an obvious fixed component due to pulmonary vascular remodeling, increased vasoconstrictor reactivity may provide an important contribution to the pulmonary hypertensive response to IH.

Summary of Aim 1

Findings in Specific Aim 1 suggest that H-IH, but not E-IH, elicits PH in Sprague Dawley rats, suggesting that eucapnia prevents IH-induced PH in these rats. Such an effect of supplemental CO₂ to attenuate PH has previously been reported in the setting of CH (Kantores *et al.*, 2006). However, the current study indicates that 4 weeks of E-IH is a more potent stimulus for the development of PH in Wistar rats. Therefore, we performed all experiments in Specific Aims 2-4 in Wistar rats exposed to 4 weeks of E-IH. Although E-IH elicited substantial RV hypertrophy, polycythemia and pulmonary vascular remodeling were minimal or nonexistent, suggesting that vasoconstriction underlies the development of PH. Consistent with that possibility, E-IH increased vasoconstrictor reactivity to multiple agonists. Studies in Specific Aims 2-4 addressed the VSM signaling mechanisms responsible for this enhanced vasoconstrictor responsiveness following E-IH.

Specific Aim 2: Assess the role of ROK in mediating right ventricular hypertrophy and enhanced agonist-induced pulmonary vasoconstriction following E-IH.

Role of ROK in E-IH-Induced Pulmonary Hypertension

ROK-mediated signaling is increased in pulmonary arteries of patients with idiopathic PH (Guilluy *et al.*, 2009) and ROK contributes to CH- (Nagaoka *et al.*, 2004) and monocrotaline-induced PH (Abe *et al.*, 2004; Homma *et al.*, 2008). Therefore, we investigated the potential role of ROK in mediating IH-induced PH. However, we observed that *in vivo* treatment with fasudil did not significantly inhibit the development of right ventricular hypertrophy. Previous studies have demonstrated that this dose of fasudil prevents CH-induced (Nagaoka *et al.*, 2006) and monocrotaline-induced PH (Abe *et al.*, 2004), suggesting that our dose should be efficacious in the current setting. We conclude that E-IH-induced PH is not mediated by ROK. The reason for the difference between our findings and those in other models of PH is unclear, but it is apparent that CH and E-IH evoke divergent signaling mechanisms responsible for the development of PH.

Role of ROK in Enhanced Vasoconstrictor Reactivity to ET-1 After E-IH

ROK mediates CH-induced pulmonary arterial basal tone (Broughton *et al.*, 2008) and increased vasoconstrictor reactivity (Jernigan *et al.*, 2004b; Jernigan *et al.*, 2008). Furthermore, E-IH enhances vasoconstrictor reactivity via a Ca²⁺ sensitization mechanism. Therefore, we examined the role of ROK in augmented ET-1-induced vasoconstrictor reactivity following E-IH. However, in agreement with our finding that

in vivo fasudil treatment did not prevent RV hypertrophy, we found that inhibition of ROK with fasudil did not affect vasoconstrictor responses to ET-1 in vessels from either E-IH or Sham rats. The reported IC₅₀ of fasudil for ROK (~2 μM) (Davies *et al.*, 2000) and previous studies from our laboratory (Broughton *et al.*, 2008) indicate that 10 μM fasudil inhibits myogenic constriction of pulmonary arteries, lending support to the efficacy of fasudil in the current preparation. These data suggest that ROK is not a mediator of ET-1-induced constriction and that E-IH, in contrast to CH, does not increase ROK-dependent signaling. The lack of a role for ROK in augmented vasoconstrictor reactivity is consistent with our finding that E-IH-induced PH is not mediated by ROK. The differential effect of CH and IH on ROK-dependent vasoconstriction may be related to contrary effects of IH versus CH on RhoA activity or ROK expression, with IH presumably not increasing either.

Summary of Aim 2

ROK does not contribute to E-IH-induced RV hypertrophy or to ET-1-induced pulmonary vasoconstriction in either E-IH or in Sham rats. These findings are surprising given the importance of ROK in ET-1-induced vasoconstriction (Jernigan *et al.*, 2008) and the development of PH in other models of PH (Homma *et al.*, 2008; Nagaoka *et al.*, 2006). Based on these findings, we sought to identify an alternative signaling pathway that could mediate enhanced vasoconstrictor reactivity and E-IH-induced PH. Thus, the next aim is focused on the role of PKC in vasoconstrictor reactivity following E-IH.

Specific Aim 3: Assess the contribution of PKC to increased agonist-mediated vasoconstriction following E-IH.

Role of PKC in ET-1-Induced Vasoconstriction

Based on the finding that ROK is not involved in augmented vasoconstrictor reactivity following E-IH, we investigated a potential role for PKC in mediating ET-1-induced Ca^{2+} sensitization. General PKC inhibition decreased vasoconstrictor reactivity to ET-1 in both Sham and E-IH vessels and normalized responses between groups, while also decreasing the Ca^{2+} response to ET-1. These findings support a role for PKC in increased ET-1-induced vasoconstriction after E-IH and are consistent with a study indicating that ET-1-induced vasoconstriction is mediated in part by PKC in pulmonary arteries of pulmonary hypertensive rats (Barman, 2007). However, the fact that vasoconstriction was reduced in arteries from Sham animals indicates that PKC is not only involved in ET-1-induced vasoconstriction following E-IH, but rather it is active in ET-1-induced vasoconstriction in normotensive animals as well. In addition, the broad-spectrum PKC inhibitor Ro 31-8220 decreased the Ca^{2+} response in both Sham and E-IH arteries, suggesting that a PKC isoform(s) mediates ET-1-induced increases in VSM $[Ca^{2+}]_i$. One potential mechanism by which PKC could mediate increases in Ca^{2+} is via L-type Ca^{2+} channel activation (Shimoda *et al.*, 1998; Snow *et al.*, 2009). Therefore, ET-1-induced activation of PKC may elicit Ca^{2+} influx via L channels in arteries from both Sham and E-IH rats.

Classical PKC isoforms have been shown to contribute to the greater ET-1-induced vasoconstriction in pulmonary arteries from fawn-hooded rats (Barman, 2007).

Consistent with these findings, we saw that PKC α/β inhibition prevented augmented ET-1-induced vasoconstriction in vessels from E-IH rats. Attenuated vasoconstriction in E-IH vessels in the presence of the PKC α/β inhibitor was associated with a Ca²⁺ response that was similar to vehicle-treated E-IH arteries. Furthermore, PKC α/β inhibition had no effect on responses in Sham arteries, indicating that E-IH evokes a signaling mechanism involving PKC α/β -dependent VSM Ca²⁺ sensitization that is not functional in arteries from Sham rats. We conclude that it is this signaling mechanism that accounts for enhanced vasoreactivity to ET-1 following E-IH.

Based on evidence that E-IH increases ET-1-induced vasoconstriction via PKC δ in systemic arteries (Allahdadi *et al.*, 2008b), we hypothesized that PKC δ mediates a portion of the enhanced pulmonary vasoconstriction to ET-1 in following E-IH. However, responses to ET-1 were not attenuated by the PKC δ inhibitor rottlerin, suggesting that PKC δ is either not expressed in PASMCs or is not activated in response to ET-1.

The finding that general PKC inhibition inhibits both ET-1-induced vasoconstriction as well as the associated increase in Ca²⁺ suggests that PKC mediates this vasoconstriction at least in part by causing increases in [Ca²⁺]_i. However, the finding that inhibition of PKC α/β and δ does not inhibit ET-1-induced increases in Ca²⁺ argues against the contribution of these isoforms to this response. Therefore, another isoenzyme must contribute to ET-1-induced increases in VSM [Ca²⁺]_i. A good candidate isoform is PKC ϵ . In pulmonary VSM, it is activated by hypoxia and leads to an increase in [Ca²⁺]_i (Rathore *et al.*, 2008). Therefore, studies designed to address the role of PKC ϵ in

enhanced ET-1-induced increases in Ca^{2+} in Sham and E-IH pulmonary arteries would be useful.

Effect of E-IH on PKC Expression

We hypothesized that E-IH increases PKC α/β expression in PASMCs to increase vasoconstrictor reactivity. We therefore assessed mRNA and protein expression of PKC α/β using real time PCR and western blot analysis, respectively. In contrast to our hypothesis, no increases in pulmonary arterial PKC α/β mRNA or protein were detected following E-IH, suggesting that enhanced ET-1-induced PKC α/β -dependent vasoconstriction is not due to changes in total cellular expression PKC α , β I or β II. A limitation to the current approach is the potential contaminating influence of the endothelium in our samples. The endothelium is a potential source of PKC α/β and could mask changes in SMC PKC levels. An approach which would ameliorate this problem is to isolate PASMCs and perform real time PCR on those cell homogenates. In addition, immunohistochemistry for PKC α/β could address the relative localization of these proteins to the pulmonary artery endothelium and SMC layers.

It is possible, however, that E-IH increases PKC α/β activity, which may correlate with the amount of PKC α/β in membrane fraction. Consistent with this possibility, previous studies in cardiac myocytes (Ding *et al.*, 2004) indicate that IH increases membrane-associated PKC $\alpha/\beta/\epsilon/\delta/\gamma$. Furthermore, ET-1 promotes PKC α membrane translocation in isolated mesenteric artery SMCs (Nelson *et al.*, 2008) and human saphenous vein endothelial cells (Ramzy *et al.*, 2006), but this does not necessarily correlate with increased PKC activity (Ramzy *et al.*, 2006). Future studies are necessary

to evaluate the effect of E-IH on ET-1-induced PKC α/β membrane localization and activation. It is possible that ET-1-induced PKC activation is dependent on increased ROS production following E-IH. The role of ROS in ET-1-induced vasoconstriction will be addressed in the following specific aim.

Summary of Specific Aim 3

In summary, we have investigated the potential contribution of PKC to enhanced pulmonary vasoconstrictor reactivity after E-IH. Our results suggest a role for PKC α/β but not PKC δ in this enhanced vasoconstriction. The increase in PKC-dependent, ET-1-induced vasoconstriction does not appear to be mediated by a simple increase in PKC α or β levels, as pulmonary arterial mRNA and protein expression are unaltered following E-IH. Therefore, it is likely that E-IH increases agonist-induced PKC α/β activity to mediate the observed effects on pulmonary vasoconstriction.

Specific Aim 4: Determine the contribution of ROS to the development of right ventricular hypertrophy and enhanced agonist-induced vasoconstriction after E-IH.

Role of ROS in Mediating E-IH-Induced PH

ROS have been implicated in other forms of PH (Nisbet *et al.*, 2009; Nozick-Grayck *et al.*, 2008) and contribute to enhanced vasoconstrictor sensitivity following CH (Fike *et al.*, 2008; Jernigan *et al.*, 2008). We, therefore, sought to determine the contribution of ROS to E-IH-induced PH. Our finding that *in vivo* treatment with tempol

prevented E-IH-induced RV hypertrophy suggests that ROS mediate E-IH-induced PH. The observed effect of tempol on RV hypertrophy is consistent with a study by Nisbet and coworkers, in which they found that 8 weeks of IH exposure elicits PH, oxidative stress and pulmonary vascular remodeling (Nisbet *et al.*, 2008), suggesting that O_2^- mediates IH-induced PH. The effect of tempol to prevent E-IH-induced PH is also consistent with the idea that E-IH increases pulmonary arterial ROS levels, which could potentially mediate an increase in vascular remodeling as well as vasoconstriction. While it is not clear whether this reflects changes in *in vivo* pulmonary arterial vasoconstriction, it is possible.

Additional mechanisms could mediate the effect of tempol to prevent E-IH-induced PH. For example, it is possible that *in vivo* ROS scavenging down regulates the ET-1 system. In fact, in glomus cells of the carotid body, IH increases ET_A receptor expression, ET-1 release, increased responsiveness to ET-1, all of which are prevented by *in vivo* O_2^- scavenging (Pawar *et al.*, 2009). This is intriguing given that E-IH increases ET_A R expression in whole lung (Allahdadi *et al.*, 2008a). The effect of tempol to prevent an E-IH-induced increase in ET_A receptor expression has not been examined but could potentially mediate the blunted RV hypertrophy by limiting pulmonary vasoconstriction and vascular remodeling following E-IH. Interestingly, HIF-1 α accumulation in response to IH is dependent on ROS generation in PC12 cells (Yuan *et al.*, 2008). Therefore, tempol treatment may impair E-IH-induced HIF activation and subsequent increases in gene expression, including ET-1 expression. Diminished HIF activation could potentially diminish E-IH-induced vasoconstriction. A limitation of our current study is that we only measured RV hypertrophy and not PAP directly. It is possible that

ROS scavenging is interfering with the hypertrophic response of the RV and not PH directly. Future studies will address effects of tempol on E-IH-induced PH. Based on our finding that ROS contribute to E-IH-induced RV hypertrophy, we next assessed the role of ROS in enhanced vasoconstrictor reactivity.

Role of ROS in Mediating an Increase in Pulmonary Artery Vasoconstrictor Reactivity after E-IH

Recent studies from our laboratory have shown that CH increases pulmonary vasoconstrictor reactivity via ROS-dependent Ca^{2+} sensitization (Jernigan *et al.*, 2008). The current study indicates that, similar to CH, E-IH increases O_2^- -dependent vasoconstrictor reactivity potentially via Ca^{2+} sensitization because ROS scavenging prevents the augmented vasoconstrictor reactivity following E-IH without decreasing the VSM Ca^{2+} response. The effect of tiron to reduce vasoconstrictor reactivity in E-IH arteries is consistent with the observed effect of tempol to prevent E-IH-induced RV hypertrophy. These findings are, further, consistent with studies demonstrating that O_2^- mediates pulmonary VSM Ca^{2+} sensitization (Jernigan *et al.*, 2008;Knock *et al.*, 2008). However, whereas O_2^- activates ROK-dependent Ca^{2+} sensitization (Jernigan *et al.*, 2008;Knock *et al.*, 2008), in these studies, our current study suggests that ROS mediate their vasoconstrictor effect via ROK-independent mechanisms.

Some evidence suggests that H_2O_2 is a pulmonary vasodilator (Burke & Wolin, 1987). Specifically, exogenous H_2O_2 dilates isolated, precontracted calf pulmonary arteries (Mohazzab *et al.*, 1996). However, others have shown that endogenous H_2O_2 constricts pulmonary arteries via increases in VSM $[Ca^{2+}]_i$ (Lin *et al.*, 2007). In addition

to increasing VSM Ca^{2+} , exogenous H_2O_2 was recently shown to increase RhoA activity in PASMC (Chi *et al.*, 2009). Another study found that exogenous H_2O_2 acts as either a constrictor or dilator and this is dependent upon concentration, with lower concentrations causing vasorelaxation and higher concentrations potentiating contraction in hypoxia-contracted guinea pig pulmonary arteries (Abdalla & Will, 1995). Despite the evidence that H_2O_2 controls the pulmonary arterial contractile state, the lack of an inhibitory effect of PEG-catalase on constrictions to ET-1 in the current study further supports the finding that increased vasoconstriction to ET-1 in E-IH vessels is attributable to O_2^- and not H_2O_2 production. The lack of a role for H_2O_2 is additionally consistent with a recent study (Knock *et al.*, 2008) showing that exogenous O_2^- constricts small pulmonary arteries independent of H_2O_2 .

Effect of E-IH on Basal and ET-1-Stimulated ROS Levels

The detection of increased basal and ET-1-stimulated pulmonary artery O_2^- production following E-IH is consistent with our current vasoconstrictor studies in isolated vessels. Both basal and ET-1-stimulated ROS could contribute to signaling which promotes PASMC contraction after E-IH.

Although DHE fluorescence is often used as a measure of cellular O_2^- production, there are limitations to this approach. First, it is possible that the observed increase in fluorescence is due to an artifact of arterial constriction as the SMC layers in the plane of acquisition increase in thickness. However, the lack of effect of ET-1 to increase DHE fluorescence in Sham arteries, despite a significant constriction provides evidence against this possibility. Another limitation of this approach is related to the fluorescent products

detected. In the presence of O_2^- , DHE is converted to 2-hydroxyethidium and ethidium. It was initially thought that the primary fluorescent product detected was ethidium (Bucana *et al.*, 1986). However, more recent studies suggest that 2-hydroxyethidium is the primary product of the reaction of DHE with O_2^- but is not optimally detected when using the standard excitation/emission spectra (F_{550} ; F_{600}) (Zhao *et al.*, 2003). In addition, it has been suggested that exciting DHE at 396 nm and collecting 579 nm emissions results in more selective detection of 2-hydroxyethidium and may serve as a better index of O_2^- generation (Robinson *et al.*, 2006). Nevertheless, our data provide direct evidence that our method of detection is sensitive to O_2^- production because tiron abolished the effect of ET-1 to increase DHE fluorescence.

O_2^- levels are a function of not only O_2^- production but also of the rate of scavenging by endogenous antioxidant enzymes. It is, therefore, possible that a decrease in expression or activity of antioxidant enzymes such as SOD occurs following E-IH. Moreover, IH decreases SOD activity in total lung tissue (Altan *et al.*, 2009). It would be interesting to address effects of E-IH on expression and activity of cellular SODs.

Potential origins of O_2^- in the vasculature include NOX, XO and mitochondrial sources. We, therefore, addressed the potential contribution of these sources to the augmented vasoconstrictor reactivity following E-IH.

Role of NOX and XO in Agonist-Induced Constriction after E-IH

A major source of O_2^- in the vasculature is NOX (Griendling *et al.*, 2000), and NOX2 contributes to IH-induced RV hypertrophy (Nisbet *et al.*, 2008). Based on these studies, we thought it was likely that E-IH would increase NOX-dependent constriction,

given the role of ROS in ET-1-induced vasoconstriction after E-IH. However, inhibition of NOX with apocynin did not alter constrictions to ET-1 in either group, arguing against a potential role of NOX1/2. However, a limitation of using apocynin is its lack of specificity for NOX. A recent study raised concerns about using apocynin as a NOX inhibitor, indicating that it is a general antioxidant, rather than a NOX inhibitor (Heumuller *et al.*, 2008). This would be a concern in our study if we had observed an effect of apocynin on vasoconstrictor or VSM Ca^{2+} responses to ET-1, however regardless of potential antioxidant properties, the lack of effect of apocynin suggests that NOX1/2 are not involved. Apocynin would not be expected to inhibit NOX4, and thus we cannot rule out a possible contribution of NOX4 to ET-1-dependent constrictions after E-IH. Consistent with this possibility, chronic sustained hypoxia leads to an increase in mouse pulmonary artery NOX4 mRNA and protein expression (Mittal *et al.*, 2007). In addition, lungs from IPAH patients have greater NOX4 expression than healthy donor lungs and isolated human PASMCs exposed to hypoxia demonstrate an increase in NOX4 mRNA expression. Furthermore, Nesbit *et al.* found that IH increases lung and pulmonary artery NOX4 levels. The role of NOX4 in E-IH-induced increases in vasoconstrictor reactivity warrants future studies.

XO activity is elevated in patients with idiopathic PH (Spiekermann *et al.*, 2009) raising the possibility that XO contributes to the development of PH. Consistent with this possibility, CH increases lung XO activity and vascular XO-derived O_2^- production in rat pups (Jankov *et al.*, 2008). Furthermore, XO inhibition *in vivo* with allopurinol attenuates CH-induced vascular remodeling and RV hypertrophy (Jankov *et al.*, 2008). In addition, hypoxia can acutely increase lung XO activity (Hoshikawa *et al.*, 2001).

However, in the present study, XO inhibition did not alter vasoconstrictor reactivity to ET-1 in pulmonary arteries from either Sham or E-IH vessels, indicating that XO does not contribute to the augmented O_2^- -dependent vasoconstriction induced by ET-1 following E-IH. Although we did not see an effect of allopurinol, this concentration of allopurinol is effective in isolated artery preparations (Erdei *et al.*, 2006). We, therefore, investigated the potential role of mitochondrial ROS generation in this response.

Role of Mitochondrial ROS in Agonist-Induced Constriction after E-IH

Mitochondria produce low levels of ROS under physiological conditions but under pathological conditions can generate high levels of ROS. ROS production by the mitochondria occurs predominantly at complexes I and III of the electron transport chain (Bell *et al.*, 2007; Fato *et al.*, 2008). Acute hypoxia increases mitochondrial ROS to mediate pulmonary artery vasoconstriction (Desireddi *et al.*, 2009; Waypa *et al.*, 2006). Therefore, we examined the potential role of mitochondrial ROS generation in ET-1-induced vasoconstriction following E-IH by scavenging mitochondrial ROS with the mitochondrial-targeted nitroxyl compound MITO-CP. Nitroxyl compounds such as MITO-CP act as general antioxidants, exhibiting both SOD activity as well as limiting H_2O_2 -induced damage (Dhanasekaran *et al.*, 2005). MITO-CP permeates the mitochondria because of its large lipophilic cation group (Dhanasekaran *et al.*, 2005). MITO-CP prevented the increased vasoconstrictor reactivity to ET-1 in E-IH vessels, suggesting an important role for mitochondrial ROS generation in the augmented ET-1-induced constriction following E-IH. Because nitroxyl compounds can impair fluorescence (Dhanasekaran *et al.*, 2005), one limitation of using MITO-CP when

measuring fura-2 fluorescence is that it might impair the signal and interfere with measurement of VSM Ca^{2+} . However, our *in situ* calibration data indicate that MITO-CP did not quench fura-2 fluorescence, as measured by F_{340}/F_{380} . In order to strengthen our conclusion that mitochondrial ROS mediate enhanced vasoconstrictor reactivity, we additionally assessed responses to ET-1 in the presence of the complex I inhibitor rotenone. Consistent with a role for mitochondrial ROS to mediate increased vasoconstrictor reactivity following E-IH, rotenone also attenuated vasoconstrictor reactivity to ET-1 in E-IH arteries and normalized responses between groups.

Mitochondria produce both O_2^- and H_2O_2 . Although acute hypoxia mediates PASMC contraction via mitochondrial H_2O_2 -dependent increases in VSM Ca^{2+} (Desireddi *et al.*, 2009), our findings suggest that E-IH increases vasoconstrictor reactivity via mitochondrial O_2^- , independent of H_2O_2 , because catalase had no effect on vasoconstriction or changes in Ca^{2+} . It is generally thought that O_2^- is fairly membrane impermeable, whereas H_2O_2 is more membrane permeable (Michelakis *et al.*, 2004; Muller *et al.*, 2004). Therefore, the mechanism by which O_2^- leaves the mitochondria to exert its effects on cytosolic components to elicit cell contraction is unclear, however it has been suggested that mitochondrial anion channels may conduct O_2^- (Aon *et al.*, 2004; O'Rourke *et al.*, 2007).

The question of how mitochondrial O_2^- could mediate increased vasoconstriction remains unanswered. Complex I produces ROS in the mitochondrial matrix, whereas complex III generates O_2^- at the Q_0 site, which results in the release of O_2^- into either the intermembrane space or the mitochondrial matrix (Muller *et al.*, 2004). Both mechanisms of O_2^- generation would require movement of O_2^- across one or both

mitochondrial membranes. The exact site of ROS generation in the mitochondria is unclear, however it is likely that either complex I or III or both generate the enhanced O_2^- following E-IH, because complex I inhibition in the current study prevented the increased vasoconstrictor reactivity to ET-1. In fact, hypoxia-induced increases in ROS are abolished by genetic or pharmacologic disruption of complex III (Guzy *et al.*, 2005), lending further support to the idea that complex III may be the main O_2^- generator in pulmonary arteries from E-IH animals.

Interestingly, the decrease in vasoconstrictor reactivity in the presence of MITO-CP was associated with a diminished Ca^{2+} response to ET-1 in both groups, indicating that mitochondrial ROS may contribute to ET-1-induced increases in VSM $[Ca^{2+}]_i$ in both Sham and E-IH vessels. Consistent with this idea, mitochondrial ROS have been shown to mediate an increase in PASMC $[Ca^{2+}]_i$ (Desireddi *et al.*, 2009; Guzy *et al.*, 2005). However, these findings are at odds with reports that hypoxia, via a decrease in mitochondrial ROS, increases pulmonary VSM $[Ca^{2+}]_i$ (Archer & Michelakis, 2002; Michelakis *et al.*, 2004). On the other hand, the O_2^- scavenger tiron did not alter Ca^{2+} responses to ET-1 in the present study, and the reasons for contrasting effects of tiron and MITO-CP on VSM Ca^{2+} are unclear. One possible explanation is that O_2^- signals in cellular microdomains so that scavenging cytosolic ROS may not be sufficient to inhibit rapid mitochondrial O_2^- -dependent signaling, which could presumably mediate an increase in VSM Ca^{2+} . Consistent with ROS production in cellular microdomains, Zhang *et al.* showed that the sarcoplasmic reticulum (SR) produce local increases in O_2^- in coronary arterial myocytes (Zhang *et al.*, 2008). In contrast to the effect of MITO-CP on ET-1-induced increases in Ca^{2+} , the mitochondrial complex I inhibitor rotenone

exhibited an opposite effect on Ca^{2+} responses to ET-1. Such an effect of rotenone to facilitate an increase in VSM Ca^{2+} is consistent with studies showing that rotenone mimics acute hypoxia, decreasing mitochondrial ROS, causing a reduction in the cellular redox potential with inactivates plasmalemmal K^+ channels in PASMCs (Archer *et al.*, 1993). The resultant membrane depolarization activates L-type VGCCs to mediate increased PASMC $[\text{Ca}^{2+}]_i$ (Archer & Michelakis, 2002). If, in the presence of rotenone, the end effect is enhanced Ca^{2+} influx through L-type VGCCs, it is difficult to explain the diminished vasoconstriction associated with this response. Two possible explanations are that 1) eliminating complex I-dependent ROS decreases a Ca^{2+} sensitization mechanism, accounting for attenuated constriction despite augmented Ca^{2+} ; 2) rotenone is attenuating ATP synthesis by inhibiting electron transport. A decrease in ATP levels would be expected to inhibit Ca^{2+} extrusion and uptake into the SR via ATP-dependent proteins (e.g. Na/K ATPase, SERCA), and result in cytosolic Ca^{2+} accumulation. However, the achievement of near maximal vasoconstriction in response to ET-1 in the presence of rotenone argues against an effect of rotenone to inhibit ATP synthesis to a degree sufficient to limit VSM contractility.

In summary, the effects of both MITO-CP and rotenone to attenuate vasoconstrictor reactivity to ET-1 following E-IH and normalize responses between Sham and E-IH arteries lend support to the idea that mitochondrial ROS mediate vasoconstriction following E-IH. Future studies will be designed to measure mitochondrial ROS production and to address the mechanism by which mitochondrial ROS mediate vasoconstriction.

Interaction Between PKC and ROS

Our current findings support a primary role for both PKC α/β and ROS in enhanced pulmonary vasoreactivity to ET-1 following E-IH, although whether these second messengers signal in parallel pathways or in series to mediate this response is not apparent from experiments involving PKC α/β inhibition or ROS scavenging alone. Supporting a series mechanism is evidence that ROS activate PKC signaling in cultured PC12 cells exposed to IH (Yuan *et al.*, 2008) and in PASMCs exposed to acute hypoxia (Rathore *et al.*, 2008). We therefore hypothesized that ROS activate PKC to elicit Ca²⁺ sensitization following agonist stimulation of E-IH vessels. We initially addressed this hypothesis by evaluating vasoconstrictor responses to ET-1 in the presence of combined ROS scavenging and PKC α/β inhibition. Our results are consistent with ROS and PKC signaling through a common pathway, since the combination of tiron and myr-PKC did not appear to decrease vasoconstriction to ET-1 further in comparison to tiron or myr-PKC alone. To further define whether ROS signal proximally or distally to PKC activation, we determined effects of selective PKC α/β inhibition on ET-1-induced O₂⁻ generation in isolated pulmonary arteries from Sham and E-IH rats. However, in contrast to our hypothesis, we found that PKC α/β inhibition prevented ET-1-mediated increases in DHE fluorescence in E-IH arteries, indicating that PKC α/β mediate ROS generation rather than the converse. These findings are consistent with evidence that PKC can increase ROS (Rathore *et al.*, 2008). In fact, ET-1 stimulates O₂⁻ production via PKC α/β activation in retinal microvessels, however this may be dependent on NOX (Matsuo *et al.*, 2009). Whereas PKC-dependent activation of NOX represents a major mechanism of

O_2^- generation (El Benna *et al.*, 1996; Wolfson *et al.*, 1985), our studies suggest that NOX does not mediate the augmented ET-1-induced vasoconstriction after E-IH.

Although our results suggest roles for both mitochondrial ROS generation and PKC to mediate elevated ET-1-induced constriction after E-IH, it is not clear whether PKC activates mitochondrial ROS generation. However, the role of PKC in modulating mitochondria in the setting of ischemia reperfusion injury is well established (Budas & Mochly-Rosen, 2007). Ischemia reperfusion represents a similar disease state to SA because of the cyclical fall in arterial PO_2 . Specifically PKC ϵ mediates cardioprotective effects incurred by ischemic preconditioning (Budas & Mochly-Rosen, 2007), potentially through its effects on mitochondrial electron transport chain components (Ogbi & Johnson, 2006), the mitochondrial permeability transition pore (Baines *et al.*, 2002) or mitochondrial ATP-sensitive K^+ channels (Jaburek *et al.*, 2006). Therefore, it is possible that E-IH promotes a similar interaction between PKC and mitochondrial components which control ROS production in PSMCs.

Summary of Specific Aim 4

The goal of this Specific Aim was to investigate the role of ROS in E-IH-induced changes in pulmonary vasoconstrictor reactivity and indices of pulmonary hypertension. ROS generation contributes to the E-IH-induced PH, therefore we determined the role of ROS in vasoconstrictor reactivity. We have identified a novel effect of E-IH to increase O_2^- -dependent, H_2O_2 -independent pulmonary vasoconstrictor reactivity. This increase in O_2^- is mediated by mitochondrial ROS generation and not by NOX or XO. Furthermore, ET-1-induced ROS generation following E-IH is mediated by PKC α/β . Mitochondrial

ROS generation contributes to augmented vasoconstriction following E-IH, which may represent a critical component of E-IH-induced PH.

Conclusions

The aim of this dissertation was to examine the mechanism of IH-induced changes in vasoconstrictor reactivity which may underlie the possible development of PH. We found that following E-IH, there is evidence for PH that is associated with modest polycythemia and vascular remodeling, but with a general increase in agonist-induced pulmonary vasoconstrictor reactivity. Elevated vasoconstrictor reactivity to ET-1 is mediated by PKC α/β and mitochondrial ROS. Although ROS-dependent PKC activation following E-IH could elicit VSM Ca²⁺ sensitization via decreased MLCP activity, we found that ET-1-induced O₂⁻ production is conversely mediated by PKC. Therefore, the mechanism by which ROS contribute to enhanced ET-1-dependent vasoconstriction remains to be established. We propose a mechanism (Figure 40) in which E-IH enhances ET-1-induced PKC α/β activation, which generates mitochondrial O₂⁻. The increased O₂⁻ production contributes to increased pulmonary VSM cell contraction and vasoconstriction. The resultant increase in pulmonary vascular resistance may then contribute to E-IH-induced PH.

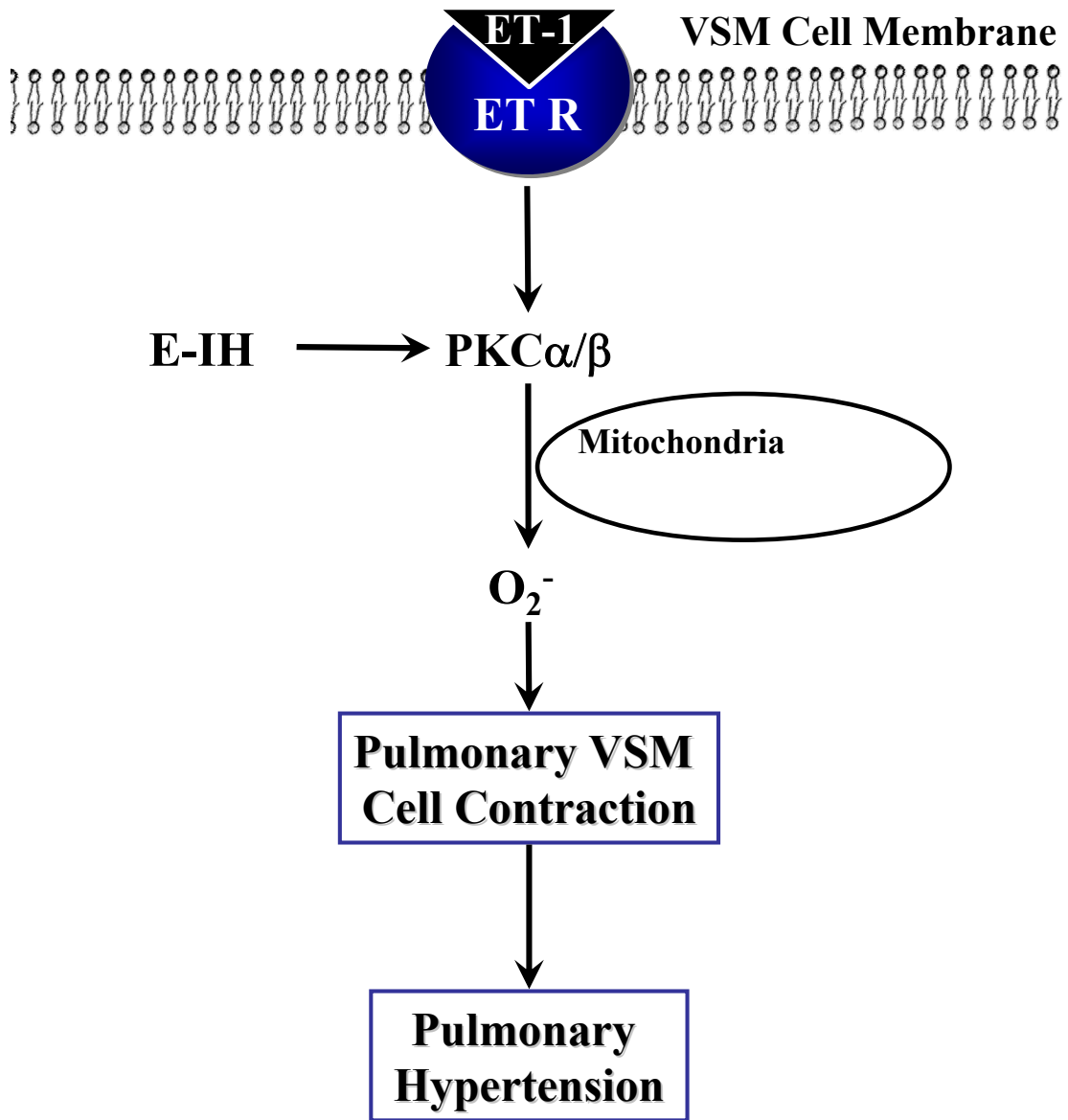


Figure 40. Proposed mechanism for E-IH-induced pulmonary hypertension. E-IH increases agonist-induced PKC α/β activation which increases mitochondrial O₂⁻ generation to mediate pulmonary VSM cell contraction. This augmented pulmonary vasoconstriction may contribute to E-IH-induced PH.

Clinical Significance

SA causes IH and results in PH, which may lead to right heart failure. Over 18 million adult Americans suffer from SA and 20-40% of those are additionally pulmonary hypertensive (Sajkov & McEvoy, 2009). Pulmonary vasoconstriction increases pulmonary vascular resistance, and thus inhibiting vasoconstriction represents an important target in the prevention and treatment of SA-induced PH. We have shown that E-IH augments pulmonary artery vasoconstriction to a variety of agonists, and this appears to be largely dependent on Ca^{2+} sensitization mechanisms. Given that E-IH did not elicit detectable pulmonary arterial remodeling or polycythemia, it seems likely that the observed increase in vasoconstrictor reactivity may provide an important contribution to the development of E-IH-induced PH. Furthermore, this increase in vasoconstrictor reactivity is mediated by ROS and PKC, and ROS contribute to the development of E-IH-induced PH. Consequently, both antioxidants and PKC inhibitors represent potential targets in the treatment of PH in patients with SA.

Future Directions

Although the results of the current study demonstrate roles for both mitochondrial O_2^- and $PKC\alpha/\beta$ in enhanced ET-1-induced pulmonary vasoconstriction following E-IH, several questions remain unanswered by the current study. Future studies are necessary to establish whether our model of E-IH elicits sustained PH and whether inhibitory effects of ROS scavenging on E-IH-induced RV hypertrophy occur secondary to reduced PH. In addition, it is important to determine the effect of E-IH on pulmonary arterial PKC activity. The lack of increase in pulmonary arterial $PKC\alpha/\beta$

expression suggests a possible increase in ET-1-induced PKC activity following E-IH. Consistent with this possibility, Ding and colleagues found that IH increases basal PKC α/ϵ and δ in cardiac myocytes only in the membrane fraction (Ding *et al.*, 2004), suggesting that IH increases basal PKC activity. Therefore, future studies will address the effect of E-IH on basal and ET-1 stimulated PKC α/β in the membrane and cytosolic fractions, using western blotting and immunofluorescence approaches. Another possibility is that ET receptors and PKC/ROS signaling are more tightly coupled following E-IH. Caveolin-dependent membrane localization of PKC may be responsible for such a coupling. In smooth muscle lacking functional caveolin-1, ET-1-induced force generation is attenuated (Shakirova *et al.*, 2006), suggesting that caveolin-1 mediates ET-1-induced contraction. Furthermore, PKC activation is dependent on caveolin in VSM (Je *et al.*, 2004). Studies could be designed to determine the effect of disrupting caveolin-dependent interactions on ET-1-induced vasoconstrictor reactivity following E-IH.

In addition, it is unclear what the role of PKC is in mediating agonist-induced increases in mitochondrial ROS. Studies using the mitochondrial-targeted DHE molecule MITO-SOX will help us address whether the increase in total cellular ROS is due to mitochondrial ROS generation and whether PKC inhibition prevents ET-1-induced ROS generation in E-IH arteries. Perhaps the most difficult question to address is how ET-1-induced O₂⁻ generation following E-IH mediates PASMC contraction. While greater ET-1-induced vasoconstriction in E-IH arteries is not associated with a greater Ca²⁺ response and mitochondrial ROS generation attenuates the vasoconstriction, inhibitors of mitochondrial ROS generation had opposite effects on VSM Ca²⁺. This result makes the

role of Ca^{2+} in this response difficult to address. If, in fact, mitochondrial ROS contribute to ET-1-induced VSM Ca^{2+} sensitization in E-IH vessels, the mechanism by which this occurs is unclear, given that PKC appears to act upstream of ROS generation, and ROK is not involved in the response. Actin polymerization can mediate an increase in SMC tension, which may contribute to the observed contractile response (Mehta & Gunst, 1999). Inhibiting actin polymerization with an agent such as cytochalasin D (Mehta & Gunst, 1999) would allow us to address its role in enhanced ET-1-induced vasoconstriction following E-IH. Other potential mediators of Ca^{2+} sensitization are integrin-linked kinase and zipper interacting protein kinase (Ihara *et al.*, 2007), however pharmacological inhibitors of these kinases are not readily available. The potential interaction between ROS and these kinases remains to be determined.

Future studies should also address the role of PKC and ROS-dependent vasoconstriction in E-IH-induced PH. By acutely administering PKC α/β inhibitors and O_2^- scavengers to isolated lungs or whole animals following E-IH and measuring PAP, the role of these respective components in the development of PH could be addressed.

It is also unclear whether pulmonary arterial ET_{A/B} receptor expression is altered by E-IH, which might explain the increased vasoconstrictor reactivity to ET-1. However, our results suggest that an ET-1-stimulated signaling pathway that is mediated by O_2^- and PKC α/β is present only following E-IH, and this argues against a simple increase in ET receptor expression mediating the augmented constriction. Also, the increase in vasoconstrictor reactivity to 5-HT and UTP supports a role for a generalized increase in agonist-induced vasoconstriction, which is unlikely to be due to increases in the expression of receptors for each of these agonists. Nevertheless, ET receptor expression

should be addressed by performing real time PCR and western blotting for pulmonary arterial ET_{A/B} receptor mRNA and protein levels, respectively. However, a more precise approach would involve isolating PSMCs and evaluating ET receptor expression because the endothelium would be expected to express ET_B receptors and provide a contaminating influence. Furthermore, the identity of the ET receptor that mediates ET-1-induced pulmonary vasoconstriction and whether this is altered by E-IH is unclear and could be addressed using selective ET_{A/B} receptor antagonists. It is additionally important to investigate whether endogenous vasoconstrictor compounds, such as ET-1, contribute to E-IH-induced PH. The role of ET-1 in mediating E-IH-induced PH via vasoconstriction could be addressed by acutely administering ET receptor antagonists such as Bosentan following E-IH exposure and measuring PAP. If ET-1-induced vasoconstriction underlies the greater presumed increase in PAP following E-IH, then acute inhibition of ET receptors would be expected to lower PAP in E-IH animals.

Appendix A- Abbreviations and Acronyms

Chronic hypoxia- CH

Chronic obstructive pulmonary disease- COPD

Diacylglycerol- DAG

Dihydroethidium- DHE

Endoplasmic reticulum- ER

Endothelial nitric oxide synthase- eNOS

Endothelin-1- ET-1

Eucapnic intermittent hypoxia- E-IH

Hypocapnic intermittent hypoxia- H-IH

Intermittent hypoxia- IH

Myosin light chain- MLC

Myosin light chain kinase- MLCK

Myosin light chain phosphatase- MLCP

NADPH oxidase- NOX

Nitric oxide- NO

Peroxynitrite- ONOO⁻

Pulmonary artery- PA

Pulmonary artery pressure- PAP

Pulmonary artery smooth muscle cell- PASMC

Pulmonary hypertension- PH

Reactive oxygen species- ROS

Receptor-operated Ca^{2+} entry- ROCE

Receptor-operated non-selective cation channels – ROC

Rho kinase- ROK

Right Ventricle- RV

Sarcoplasmic endoplasmic reticulum Ca^{2+} ATPase- SERCA

Sarcoplasmic reticulum- SR

Sleep apnea- SA

Store- operated Ca^{2+} entry- SOCE

Superoxide dismutase- SOD

Transient receptor potential cation- TRPC

Vascular smooth muscle- VSM

Voltage-gated Ca^{2+} channels- VGCC

Xanthine oxidase- XO

Reference List

- Abdalla, S. & Will, J. A. (1995). Potentiation of the hypoxic contraction of guinea-pig isolated pulmonary arteries by two inhibitors of superoxide dismutase. *Gen.Pharmacol.* **26**, 785-792.
- Abe, K., Shimokawa, H., Morikawa, K., Uwatoku, T., Oi, K., Matsumoto, Y., Hattori, T., Nakashima, Y., Kaibuchi, K., Sueishi, K., & Takeshit, A. (2004). Long-term treatment with a Rho-kinase inhibitor improves monocrotaline-induced fatal pulmonary hypertension in rats. *Circ.Res.* **94**, 385-393.
- Alchanatis, M., Tourkohoriti, G., Kakouros, S., Kosmas, E., Podaras, S., & Jordanoglou, J. B. (2001). Daytime pulmonary hypertension in patients with obstructive sleep apnea: the effect of continuous positive airway pressure on pulmonary hemodynamics. *Respiration* **68**, 566-572.
- Alford, N. J., Fletcher, E. C., & Nickeson, D. (1986). Acute oxygen in patients with sleep apnea and COPD. *Chest* **89**, 30-38.
- Allahdadi, K. J., Cherng, T. W., Pai, H., Silva, A. Q., Walker, B. R., Nelin, L. D., & Kanagy, N. L. (2008a). Endothelin type A receptor antagonist normalizes blood pressure

in rats exposed to eucapnic intermittent hypoxia. *Am.J Physiol Heart Circ.Physiol* **295**, H434-H440.

Allahdadi, K. J., Duling, L. C., Walker, B. R., & Kanagy, N. L. (2008b). Eucapnic intermittent hypoxia augments endothelin-1 vasoconstriction in rats: role of PKCdelta. *Am.J.Physiol Heart Circ.Physiol* **294**, H920-H927.

Allahdadi, K. J., Walker, B. R., & Kanagy, N. L. (2005). Augmented endothelin vasoconstriction in intermittent hypoxia-induced hypertension. *Hypertension* **45**, 705-709.

Altan, M., Atukeren, P., Mengi, M., Metin, G., Cakar, L., & Gumustas, K. (2009). Influence of intermittent hypobaric exposure on SOD and TBARS levels in trained rats. *Chin J Physiol* **52**, 106-112.

Ambalavanan, N., Li, P., Bulger, A., Murphy-Ullrich, J., Oparil, S., & Chen, Y. F. (2007). Endothelin-1 mediates hypoxia-induced increases in vascular collagen in the newborn mouse lung. *Pediatr.Res.* **61**, 559-564.

Aon, M. A., Cortassa, S., & O'Rourke, B. (2004). Percolation and criticality in a mitochondrial network. *Proc.Natl.Acad.Sci.U.S.A* **101**, 4447-4452.

Archer, S. & Michelakis, E. (2002). The mechanism(s) of hypoxic pulmonary vasoconstriction: potassium channels, redox O(2) sensors, and controversies. *News Physiol Sci.* **17**, 131-137.

Archer, S. L., Gomberg-Maitland, M., Maitland, M. L., Rich, S., Garcia, J. G., & Weir, E. K. (2008). Mitochondrial metabolism, redox signaling, and fusion: a mitochondria-ROS-HIF-1 α -Kv1.5 O₂-sensing pathway at the intersection of pulmonary hypertension and cancer. *Am.J Physiol Heart Circ.Physiol* **294**, H570-H578.

Archer, S. L., Huang, J., Henry, T., Peterson, D., & Weir, E. K. (1993). A redox-based O₂ sensor in rat pulmonary vasculature. *Circ.Res.* **73**, 1100-1112.

Archer, S. L., Nelson, D. P., & Weir, E. K. (1989). Simultaneous measurement of O₂ radicals and pulmonary vascular reactivity in rat lung. *J Appl.Physiol* **67**, 1903-1911.

Ardanaz, N., Beierwaltes, W. H., & Pagano, P. J. (2008). Distinct hydrogen peroxide-induced constriction in multiple mouse arteries: potential influence of vascular polarization. *Pharmacol.Rep.* **60**, 61-67.

Arias, M. A., Garcia-Rio, F., Alonso-Fernandez, A., Martinez, I., & Villamor, J. (2006). Pulmonary hypertension in obstructive sleep apnoea: effects of continuous positive airway pressure: a randomized, controlled cross-over study. *Eur.Heart J* **27**, 1106-1113.

Bady, E., Achkar, A., Pascal, S., Orvoen-Frija, E., & Laaban, J. P. (2000). Pulmonary arterial hypertension in patients with sleep apnoea syndrome. *Thorax* **55**, 934-939.

Baines, C. P., Zhang, J., Wang, G. W., Zheng, Y. T., Xiu, J. X., Cardwell, E. M., Bolli, R., & Ping, P. (2002). Mitochondrial PKCepsilon and MAPK form signaling modules in the murine heart: enhanced mitochondrial PKCepsilon-MAPK interactions and differential MAPK activation in PKCepsilon-induced cardioprotection. *Circ.Res.* **90**, 390-397.

Barer, G. R., Bee, D., & Wach, R. A. (1983). Contribution of polycythaemia to pulmonary hypertension in simulated high altitude in rats. *J Physiol* **336**, 27-38.

Barman, S. A. (2007). Vasoconstrictor effect of endothelin-1 on hypertensive pulmonary arterial smooth muscle involves Rho-kinase and protein kinase C. *Am.J Physiol Lung Cell Mol.Physiol* **293**, L472-L479.

Bell, E. L., Klimova, T. A., Eisenbart, J., Moraes, C. T., Murphy, M. P., Budinger, G. R., & Chandel, N. S. (2007). The Qo site of the mitochondrial complex III is required for the transduction of hypoxic signaling via reactive oxygen species production. *J Cell Biol.* **177**, 1029-1036.

Benumof, J. L. (1983). Intermittent hypoxia increases lobar hypoxic pulmonary vasoconstriction. *Anesthesiology* **58**, 399-404.

Bertuglia, S. & Reiter, R. J. (2009). Melatonin reduces microvascular damage and insulin resistance in hamsters due to chronic intermittent hypoxia. *J Pineal Res.* **46**, 307-313.

Bobik, A., Grooms, A., Millar, J. A., Mitchell, A., & Grinpukel, S. (1990). Growth factor activity of endothelin on vascular smooth muscle. *Am.J Physiol* **258**, C408-C415.

Bonnet, S., Michelakis, E. D., Porter, C. J., Andrade-Navarro, M. A., Thebaud, B., Bonnet, S., Haromy, A., Harry, G., Moudgil, R., McMurtry, M. S., Weir, E. K., & Archer, S. L. (2006). An abnormal mitochondrial-hypoxia inducible factor-1alpha-Kv channel pathway disrupts oxygen sensing and triggers pulmonary arterial hypertension in fawn hooded rats: similarities to human pulmonary arterial hypertension. *Circulation* **113**, 2630-2641.

Bonsignore, M. R., Marrone, O., Insalaco, G., & Bonsignore, G. (1994). The cardiovascular effects of obstructive sleep apnoeas: analysis of pathogenic mechanisms. *Eur.Respir.J* **7**, 786-805.

Borges, F., Fernandes, E., & Roleira, F. (2002). Progress towards the discovery of xanthine oxidase inhibitors. *Curr.Med.Chem.* **9**, 195-217.

Bowers, R., Cool, C., Murphy, R. C., Tuder, R. M., Hopken, M. W., Flores, S. C., & Voelkel, N. F. (2004). Oxidative stress in severe pulmonary hypertension. *Am.J Respir.Crit Care Med.* **169**, 764-769.

Bradford, A. (2004). Effects of chronic intermittent asphyxia on haematocrit, pulmonary arterial pressure and skeletal muscle structure in rats. *Exp.Physiol* **89**, 44-52.

Bradley, T. D., Rutherford, R., Grossman, R. F., Lue, F., Zamel, N., Moldofsky, H., & Phillipson, E. A. (1985). Role of daytime hypoxemia in the pathogenesis of right heart failure in the obstructive sleep apnea syndrome. *Am.Rev.Respir.Dis.* **131**, 835-839.

Broughton, B. R., Walker, B. R., & Resta, T. C. (2008). Chronic hypoxia induces Rho kinase-dependent myogenic tone in small pulmonary arteries. *Am.J Physiol Lung Cell Mol.Physiol* **294**, L797-L806.

Bucana, C., Saiki, I., & Nayar, R. (1986). Uptake and accumulation of the vital dye hydroethidine in neoplastic cells. *J Histochem.Cytochem.* **34**, 1109-1115.

Buda, A. J., Schroeder, J. S., & Guilleminault, C. (1981). Abnormalities of pulmonary artery wedge pressures in sleep-induced apnea. *Int.J Cardiol.* **1**, 67-74.

Budas, G. R. & Mochly-Rosen, D. (2007). Mitochondrial protein kinase Cepsilon (PKCepsilon): emerging role in cardiac protection from ischaemic damage. *Biochem.Soc.Trans.* **35**, 1052-1054.

Budzyn, K., Ravi, R. M., Miller, A. A., & Sobey, C. G. (2008). Mechanisms of augmented vasoconstriction induced by 5-hydroxytryptamine in aortic rings from spontaneously hypertensive rats. *Br.J Pharmacol.* **155**, 210-216.

Burke, T. M. & Wolin, M. S. (1987). Hydrogen peroxide elicits pulmonary arterial relaxation and guanylate cyclase activation. *Am.J Physiol* **252**, H721-H732.

Campen, M. J., Shimoda, L. A., & O'Donnell, C. P. (2005). Acute and chronic cardiovascular effects of intermittent hypoxia in C57BL/6J mice. *J Appl.Physiol* **99**, 2028-2035.

Carlson, J. T., Hedner, J., Elam, M., Ejnell, H., Sellgren, J., & Wallin, B. G. (1993). Augmented resting sympathetic activity in awake patients with obstructive sleep apnea. *Chest* **103**, 1763-1768.

Cave, A. (2009). Selective targeting of NADPH oxidase for cardiovascular protection. *Curr.Opin.Pharmacol.* **9**, 208-213.

Chaouat, A., Weitzenblum, E., Krieger, J., Oswald, M., & Kessler, R. (1996). Pulmonary hemodynamics in the obstructive sleep apnea syndrome. Results in 220 consecutive patients. *Chest* **109**, 380-386.

Chen, M. J., Chiang, L. Y., & Lai, Y. L. (2001). Reactive oxygen species and substance P in monocrotaline-induced pulmonary hypertension. *Toxicol.Appl.Pharmacol.* **171**, 165-173.

Chi, A. Y., Waypa, G. B., Mungai, P. T., & Schumacker, P. T. (2009). Prolonged Hypoxia Increases ROS Signaling and RhoA Activation in Pulmonary Artery Smooth Muscle and Endothelial Cells. *Antioxid.Redox.Signal*.

Choi, J. B., Lored, J. S., Norman, D., Mills, P. J., Ancoli-Israel, S., Ziegler, M. G., & Dimsdale, J. E. (2006). Does obstructive sleep apnea increase hematocrit? *Sleep Breath*. **10**, 155-160.

Cipolla, M. J., Gokina, N. I., & Osol, G. (2002). Pressure-induced actin polymerization in vascular smooth muscle as a mechanism underlying myogenic behavior. *FASEB J* **16**, 72-76.

Cracowski, J. L., Cracowski, C., Bessard, G., Pepin, J. L., Bessard, J., Schwebel, C., Stanke-Labesque, F., & Pison, C. (2001). Increased lipid peroxidation in patients with pulmonary hypertension. *Am.J Respir.Crit Care Med*. **164**, 1038-1042.

Damron, D. S., Kanaya, N., Homma, Y., Kim, S. O., & Murray, P. A. (2002). Role of PKC, tyrosine kinases, and Rho kinase in alpha-adrenoreceptor-mediated PASM contraction. *Am.J Physiol Lung Cell Mol.Physiol* **283**, L1051-L1064.

Davie, N., Haleen, S. J., Upton, P. D., Polak, J. M., Yacoub, M. H., Morrell, N. W., & Wharton, J. (2002). ET(A) and ET(B) receptors modulate the proliferation of human pulmonary artery smooth muscle cells. *Am.J Respir.Crit Care Med*. **165**, 398-405.

Davies, S. P., Reddy, H., Caivano, M., & Cohen, P. (2000). Specificity and mechanism of action of some commonly used protein kinase inhibitors. *Biochem.J* **351**, 95-105.

DeMarco, V. G., Habibi, J., Whaley-Connell, A. T., Schneider, R. I., Heller, R. L., Bosanquet, J. P., Hayden, M. R., Delcour, K., Cooper, S. A., Andresen, B. T., Sowers, J. R., & Dellspenger, K. C. (2008). Oxidative stress contributes to pulmonary hypertension in the transgenic (mRen2)27 rat. *Am.J Physiol Heart Circ.Physiol* **294**, H2659-H2668.

Desireddi, J. R., Farrow, K. N., Marks, J. D., Waypa, G. B., & Schumacker, P. T. (2009). Hypoxia Increases ROS Signaling and Cytosolic Ca²⁺ in Pulmonary Artery Smooth Muscle Cells of Mouse Lungs Slices. *Antioxid.Redox.Signal*.

Dhanasekaran, A., Kotamraju, S., Karunakaran, C., Kalivendi, S. V., Thomas, S., Joseph, J., & Kalyanaraman, B. (2005). Mitochondria superoxide dismutase mimetic inhibits peroxide-induced oxidative damage and apoptosis: role of mitochondrial superoxide. *Free Radic.Biol.Med.* **39**, 567-583.

DiCarlo, V. S., Chen, S. J., Meng, Q. C., Durand, J., Yano, M., Chen, Y. F., & Oparil, S. (1995). ETA-receptor antagonist prevents and reverses chronic hypoxia-induced pulmonary hypertension in rat. *Am.J Physiol* **269**, L690-L697.

Dikalov, S., Griendling, K. K., & Harrison, D. G. (2007). Measurement of reactive oxygen species in cardiovascular studies. *Hypertension* **49**, 717-727.

Dikalov, S. I., Dikalova, A. E., Bikineyeva, A. T., Schmidt, H. H., Harrison, D. G., & Griendling, K. K. (2008). Distinct roles of Nox1 and Nox4 in basal and angiotensin II-stimulated superoxide and hydrogen peroxide production. *Free Radic.Biol.Med.* **45**, 1340-1351.

Dimsdale, J. E., Loreda, J. S., & Profant, J. (2000). Effect of continuous positive airway pressure on blood pressure : a placebo trial. *Hypertension* **35**, 144-147.

Ding, H. L., Zhu, H. F., Dong, J. W., Zhu, W. Z., & Zhou, Z. N. (2004). Intermittent hypoxia protects the rat heart against ischemia/reperfusion injury by activating protein kinase C. *Life Sci.* **75**, 2587-2603.

Dziadek, M. A. & Johnstone, L. S. (2007). Biochemical properties and cellular localisation of STIM proteins. *Cell Calcium* **42**, 123-132.

Ebert, B. L. & Bunn, H. F. (1999). Regulation of the erythropoietin gene. *Blood* **94**, 1864-1877.

Eckert, D. J., Jordan, A. S., Merchia, P., & Malhotra, A. (2007). Central sleep apnea: Pathophysiology and treatment. *Chest* **131**, 595-607.

Eichinger, M. R. & Walker, B. R. (1994). Enhanced pulmonary arterial dilation to arginine vasopressin in chronically hypoxic rats. *Am.J Physiol* **267**, H2413-H2419.

Eichinger, M. R. & Walker, B. R. (1996). Nitric oxide and cGMP do not affect fluid flux in isolated rat lungs. *J Appl.Physiol* **80**, 69-76.

El Benna, J., Faust, R. P., Johnson, J. L., & Babior, B. M. (1996). Phosphorylation of the respiratory burst oxidase subunit p47phox as determined by two-dimensional phosphopeptide mapping. Phosphorylation by protein kinase C, protein kinase A, and a mitogen-activated protein kinase. *J Biol.Chem.* **271**, 6374-6378.

Elmedal, B., de Dam, M. Y., Mulvany, M. J., & Simonsen, U. (2004). The superoxide dismutase mimetic, tempol, blunts right ventricular hypertrophy in chronic hypoxic rats. *Br.J Pharmacol.* **141**, 105-113.

Erdei, N., Toth, A., Pasztor, E. T., Papp, Z., Edes, I., Koller, A., & Bagi, Z. (2006). High-fat diet-induced reduction in nitric oxide-dependent arteriolar dilation in rats: role of xanthine oxidase-derived superoxide anion. *Am.J Physiol Heart Circ.Physiol* **291**, H2107-H2115.

Esteve, J. M., Launay, J. M., Kellermann, O., & Maroteaux, L. (2007). Functions of serotonin in hypoxic pulmonary vascular remodeling. *Cell Biochem.Biophys.* **47**, 33-44.

Fagan, K. A. (2001). Selected Contribution: Pulmonary hypertension in mice following intermittent hypoxia. *J Appl.Physiol* **90**, 2502-2507.

Fanburg, B. L. & Lee, S. L. (1997). A new role for an old molecule: serotonin as a mitogen. *Am.J Physiol* **272**, L795-L806.

Faraci, F. M. & Didion, S. P. (2004). Vascular protection: superoxide dismutase isoforms in the vessel wall. *Arterioscler.Thromb.Vasc.Biol.* **24**, 1367-1373.

Fato, R., Bergamini, C., Leoni, S., & Lenaz, G. (2008). Mitochondrial production of reactive oxygen species: role of complex I and quinone analogues. *Biofactors* **32**, 31-39.

Feng, J., Ito, M., Ichikawa, K., Isaka, N., Nishikawa, M., Hartshorne, D. J., & Nakano, T. (1999). Inhibitory phosphorylation site for Rho-associated kinase on smooth muscle myosin phosphatase. *J Biol.Chem.* **274**, 37385-37390.

Fike, C. D., Slaughter, J. C., Kaplowitz, M. R., Zhang, Y., & Aschner, J. L. (2008). Reactive oxygen species from NADPH oxidase contribute to altered pulmonary vascular responses in piglets with chronic hypoxia-induced pulmonary hypertension. *Am.J Physiol Lung Cell Mol.Physiol* **295**, L881-L888.

Fisher, J. W. (2003). Erythropoietin: physiology and pharmacology update. *Exp.Biol.Med.(Maywood.)* **228**, 1-14.

Flavahan, N. A., Bailey, S. R., Flavahan, W. A., Mitra, S., & Flavahan, S. (2005). Imaging remodeling of the actin cytoskeleton in vascular smooth muscle cells after

mechanosensitive arteriolar constriction. *Am.J Physiol Heart Circ.Physiol* **288**, H660-H669.

Fletcher, E. C. (1990). Chronic lung disease in the sleep apnea syndrome. *Lung* **168 Suppl**, 751-761.

Fletcher, E. C., Bao, G., & Miller, C. C., III (1995). Effect of recurrent episodic hypocapnic, eucapnic, and hypercapnic hypoxia on systemic blood pressure. *J Appl.Physiol* **78**, 1516-1521.

Fletcher, E. C., Schaaf, J. W., Miller, J., & Fletcher, J. G. (1987). Long-term cardiopulmonary sequelae in patients with sleep apnea and chronic lung disease. *Am.Rev.Respir.Dis.* **135**, 525-533.

Forstermann, U. (2008). Oxidative stress in vascular disease: causes, defense mechanisms and potential therapies. *Nat.Clin.Pract.Cardiovasc.Med.* **5**, 338-349.

Fried, R., Meyrick, B., Rabinovitch, M., & Reid, L. (1983). Polycythemia and the acute hypoxic response in awake rats following chronic hypoxia. *J Appl.Physiol* **55**, 1167-1172.

Fujio, H., Nakamura, K., Matsubara, H., Kusano, K. F., Miyaji, K., Nagase, S., Ikeda, T., Ogawa, A., Ohta-Ogo, K., Miura, D., Miura, A., Miyazaki, M., Date, H., & Ohe, T. (2006). Carvedilol inhibits proliferation of cultured pulmonary artery smooth muscle

cells of patients with idiopathic pulmonary arterial hypertension. *J Cardiovasc.Pharmacol.* **47**, 250-255.

Golovina, V. A., Platoshyn, O., Bailey, C. L., Wang, J., Limsuwan, A., Sweeney, M., Rubin, L. J., & Yuan, J. X. (2001). Upregulated TRP and enhanced capacitative Ca(2+) entry in human pulmonary artery myocytes during proliferation. *Am.J.Physiol Heart Circ.Physiol* **280**, H746-H755.

Greenberg, B. & Kishiyama, S. (1993). Endothelium-dependent and -independent responses to severe hypoxia in rat pulmonary artery. *Am.J Physiol* **265**, H1712-H1720.

Griendling, K. K., Sorescu, D., & Ushio-Fukai, M. (2000). NAD(P)H oxidase: role in cardiovascular biology and disease. *Circ.Res.* **86**, 494-501.

Griendling, K. K. & Ushio-Fukai, M. (1998). Redox control of vascular smooth muscle proliferation. *J Lab Clin.Med.* **132**, 9-15.

Grill, H. P., Zweier, J. L., Kuppusamy, P., Weisfeldt, M. L., & Flaherty, J. T. (1992). Direct measurement of myocardial free radical generation in an in vivo model: effects of postischemic reperfusion and treatment with human recombinant superoxide dismutase. *J Am.Coll.Cardiol.* **20**, 1604-1611.

Grishko, V., Solomon, M., Breit, J. F., Killilea, D. W., Ledoux, S. P., Wilson, G. L., & Gillespie, M. N. (2001). Hypoxia promotes oxidative base modifications in the pulmonary artery endothelial cell VEGF gene. *FASEB J* **15**, 1267-1269.

Grobe, A. C., Wells, S. M., Benavidez, E., Oishi, P., Azakie, A., Fineman, J. R., & Black, S. M. (2006). Increased oxidative stress in lambs with increased pulmonary blood flow and pulmonary hypertension: role of NADPH oxidase and endothelial NO synthase. *Am.J Physiol Lung Cell Mol.Physiol* **290**, L1069-L1077.

Guidry, U. C., Mendes, L. A., Evans, J. C., Levy, D., O'Connor, G. T., Larson, M. G., Gottlieb, D. J., & Benjamin, E. J. (2001). Echocardiographic features of the right heart in sleep-disordered breathing: the Framingham Heart Study. *Am.J Respir.Crit Care Med.* **164**, 933-938.

Guilluy, C., Eddahibi, S., Agard, C., Guignabert, C., Izikki, M., Tu, L., Savale, L., Humbert, M., Fadel, E., Adnot, S., Loirand, G., & Pacaud, P. (2009). RhoA and Rho Kinase Activation in Human Pulmonary Hypertension - Role of 5-HT Signaling. *Am.J Respir.Crit Care Med.*

Gupte, S. A., Kaminski, P. M., George, S., Kouznestova, L., Olson, S. C., Mathew, R., Hintze, T. H., & Wolin, M. S. (2009). Peroxide generation by p47phox-Src activation of Nox2 has a key role in protein kinase C-induced arterial smooth muscle contraction. *Am.J Physiol Heart Circ.Physiol* **296**, H1048-H1057.

Guzy, R. D., Hoyos, B., Robin, E., Chen, H., Liu, L., Mansfield, K. D., Simon, M. C., Hammerling, U., & Schumacker, P. T. (2005). Mitochondrial complex III is required for hypoxia-induced ROS production and cellular oxygen sensing. *Cell Metab* **1**, 401-408.

Haller, H., Lindschau, C., Quass, P., Distler, A., & Luft, F. C. (1995). Differentiation of vascular smooth muscle cells and the regulation of protein kinase C-alpha. *Circ.Res.* **76**, 21-29.

Hassoun, P. M., Yu, F. S., Shedd, A. L., Zulueta, J. J., Thannickal, V. J., Lanzillo, J. J., & Fanburg, B. L. (1994). Regulation of endothelial cell xanthine dehydrogenase xanthine oxidase gene expression by oxygen tension. *Am.J Physiol* **266**, L163-L171.

Heumuller, S., Wind, S., Barbosa-Sicard, E., Schmidt, H. H., Busse, R., Schroder, K., & Brandes, R. P. (2008). Apocynin is not an inhibitor of vascular NADPH oxidases but an antioxidant. *Hypertension* **51**, 211-217.

Hislop, A. & Reid, L. (1976). New findings in pulmonary arteries of rats with hypoxia-induced pulmonary hypertension. *Br.J Exp.Pathol.* **57**, 542-554.

Hofmann, T., Schaefer, M., Schultz, G., & Gudermann, T. (2000). Transient receptor potential channels as molecular substrates of receptor-mediated cation entry. *J Mol.Med.* **78**, 14-25.

Homma, N., Nagaoka, T., Karoor, V., Imamura, M., Taraseviciene-Stewart, L., Walker, L. A., Fagan, K. A., McMurtry, I. F., & Oka, M. (2008). Involvement of RhoA/Rho kinase signaling in protection against monocrotaline-induced pulmonary hypertension in pneumonectomized rats by dehydroepiandrosterone. *Am.J Physiol Lung Cell Mol.Physiol* **295**, L71-L78.

Hopkins, N. & McLoughlin, P. (2002). The structural basis of pulmonary hypertension in chronic lung disease: remodelling, rarefaction or angiogenesis? *J Anat.* **201**, 335-348.

Hoshikawa, Y., Ono, S., Suzuki, S., Tanita, T., Chida, M., Song, C., Noda, M., Tabata, T., Voelkel, N. F., & Fujimura, S. (2001). Generation of oxidative stress contributes to the development of pulmonary hypertension induced by hypoxia. *J Appl.Physiol* **90**, 1299-1306.

Howell, K., Ooi, H., Preston, R., & McLoughlin, P. (2004). Structural basis of hypoxic pulmonary hypertension: the modifying effect of chronic hypercapnia. *Exp.Physiol* **89**, 66-72.

Howell, K., Preston, R. J., & McLoughlin, P. (2003). Chronic hypoxia causes angiogenesis in addition to remodelling in the adult rat pulmonary circulation. *J Physiol* **547**, 133-145.

Huang, H. Q., Zhang, P., Jiang, Z., & Chen, H. Z. (2009). [Overexpression of endothelin-1 induces hypertrophy of rat pulmonary arterial microvascular smooth muscle cells via Akt/mTOR pathway]. *Zhonghua Jie.He.He.Hu Xi.Za Zhi.* **32**, 287-291.

Hyvelin, J. M., Howell, K., Nichol, A., Costello, C. M., Preston, R. J., & McLoughlin, P. (2005). Inhibition of Rho-kinase attenuates hypoxia-induced angiogenesis in the pulmonary circulation. *Circ.Res.* **97**, 185-191.

Ihara, E., Edwards, E., Borman, M. A., Wilson, D. P., Walsh, M. P., & MacDonald, J. A. (2007). Inhibition of zipper-interacting protein kinase function in smooth muscle by a myosin light chain kinase pseudosubstrate peptide. *Am.J Physiol Cell Physiol* **292**, C1951-C1959.

Inoguchi, T., Sonta, T., Tsubouchi, H., Etoh, T., Kakimoto, M., Sonoda, N., Sato, N., Sekiguchi, N., Kobayashi, K., Sumimoto, H., Utsumi, H., & Nawata, H. (2003). Protein kinase C-dependent increase in reactive oxygen species (ROS) production in vascular tissues of diabetes: role of vascular NAD(P)H oxidase. *J Am.Soc.Nephrol.* **14**, S227-S232.

Iqbal, M., Cawthon, D., Wideman, R. F., Jr., & Bottje, W. G. (2001). Lung mitochondrial dysfunction in pulmonary hypertension syndrome. II. Oxidative stress and inability to improve function with repeated additions of adenosine diphosphate. *Poult.Sci.* **80**, 656-665.

Jaburek, M., Costa, A. D., Burton, J. R., Costa, C. L., & Garlid, K. D. (2006). Mitochondrial PKC epsilon and mitochondrial ATP-sensitive K⁺ channel copurify and coreconstitute to form a functioning signaling module in proteoliposomes. *Circ.Res.* **99**, 878-883.

Jankov, R. P., Kantores, C., Pan, J., & Belik, J. (2008). Contribution of xanthine oxidase-derived superoxide to chronic hypoxic pulmonary hypertension in neonatal rats. *Am.J Physiol Lung Cell Mol.Physiol* **294**, L233-L245.

Je, H. D., Gallant, C., Leavis, P. C., & Morgan, K. G. (2004). Caveolin-1 regulates contractility in differentiated vascular smooth muscle. *Am.J Physiol Heart Circ.Physiol* **286**, H91-H98.

Jernigan, N. L., Broughton, B. R., Walker, B. R., & Resta, T. C. (2006). Impaired NO-dependent inhibition of store- and receptor-operated calcium entry in pulmonary vascular smooth muscle after chronic hypoxia. *Am.J Physiol Lung Cell Mol.Physiol* **290**, L517-L525.

Jernigan, N. L., Paffett, M. L., Walker, B. R., & Resta, T. C. (2009). ASIC1 contributes to pulmonary vascular smooth muscle store-operated Ca²⁺ entry. *Am.J Physiol Lung Cell Mol.Physiol* **297**, L271-L285.

Jernigan, N. L., Resta, T. C., & Walker, B. R. (2004a). Contribution of oxygen radicals to altered NO-dependent pulmonary vasodilation in acute and chronic hypoxia. *Am.J Physiol Lung Cell Mol.Physiol* **286**, L947-L955.

Jernigan, N. L., Walker, B. R., & Resta, T. C. (2004b). Chronic hypoxia augments protein kinase G-mediated Ca²⁺ desensitization in pulmonary vascular smooth muscle through inhibition of RhoA/Rho kinase signaling. *Am.J Physiol Lung Cell Mol.Physiol* **287**, L1220-L1229.

Jernigan, N. L., Walker, B. R., & Resta, T. C. (2004c). Endothelium-derived reactive oxygen species and endothelin-1 attenuate NO-dependent pulmonary vasodilation following chronic hypoxia. *Am.J Physiol Lung Cell Mol.Physiol* **287**, L801-L808.

Jernigan, N. L., Walker, B. R., & Resta, T. C. (2008). Reactive oxygen species mediate RhoA/Rho kinase-induced Ca²⁺ sensitization in pulmonary vascular smooth muscle following chronic hypoxia. *Am.J Physiol Lung Cell Mol.Physiol* **295**, L515-L529.

Jin, L., Ying, Z., & Webb, R. C. (2004). Activation of Rho/Rho kinase signaling pathway by reactive oxygen species in rat aorta. *Am.J Physiol Heart Circ.Physiol* **287**, H1495-H1500.

Jousset, H., Frieden, M., & Demaurex, N. (2007). STIM1 knockdown reveals that store-operated Ca²⁺ channels located close to sarco/endoplasmic Ca²⁺ ATPases (SERCA) pumps silently refill the endoplasmic reticulum. *J Biol.Chem.* **282**, 11456-11464.

Kanagy, N. L., Walker, B. R., & Nelin, L. D. (2001). Role of endothelin in intermittent hypoxia-induced hypertension. *Hypertension* **37**, 511-515.

Kantores, C., McNamara, P. J., Teixeira, L., Engelberts, D., Murthy, P., Kavanagh, B. P., & Jankov, R. P. (2006). Therapeutic hypercapnia prevents chronic hypoxia-induced pulmonary hypertension in the newborn rat. *Am.J Physiol Lung Cell Mol.Physiol* **291**, L912-L922.

Kawano, Y., Yoshimura, T., & Kaibuchi, K. (2002). Smooth muscle contraction by small GTPase Rho. *Nagoya J Med.Sci.* **65**, 1-8.

Kessler, R., Chaouat, A., Weitzenblum, E., Oswald, M., Ehrhart, M., Apprill, M., & Krieger, J. (1996). Pulmonary hypertension in the obstructive sleep apnoea syndrome: prevalence, causes and therapeutic consequences. *Eur.Respir.J* **9**, 787-794.

Khalil, R. A., Lajoie, C., Resnick, M. S., & Morgan, K. G. (1992a). Ca(2+)-independent isoforms of protein kinase C differentially translocate in smooth muscle. *Am.J Physiol* **263**, C714-C719.

Khalil, R. A., Lajoie, C., Resnick, M. S., & Morgan, K. G. (1992b). Ca(2+)-independent isoforms of protein kinase C differentially translocate in smooth muscle. *Am.J Physiol* **263**, C714-C719.

Killilea, D. W., Hester, R., Balczon, R., Babal, P., & Gillespie, M. N. (2000). Free radical production in hypoxic pulmonary artery smooth muscle cells. *Am.J Physiol Lung Cell Mol.Physiol* **279**, L408-L412.

Kitazawa, T., Takizawa, N., Ikebe, M., & Eto, M. (1999). Reconstitution of protein kinase C-induced contractile Ca²⁺ sensitization in triton X-100-demembrated rabbit arterial smooth muscle. *J Physiol* **520 Pt 1**, 139-152.

Knock, G. A., Snetkov, V. A., Shaifta, Y., Connolly, M., Drndarski, S., Noah, A., Pourmahram, G. E., Becker, S., Aaronson, P. I., & Ward, J. P. (2008). Superoxide constricts rat pulmonary arteries via Rho-kinase-mediated Ca²⁺ sensitization. *Free Radic.Biol.Med.*

Knot, H. J. & Nelson, M. T. (1998). Regulation of arterial diameter and wall [Ca²⁺] in cerebral arteries of rat by membrane potential and intravascular pressure. *J Physiol* **508 (Pt 1)**, 199-209.

Ko, F. N. (1997). Low-affinity thromboxane receptor mediates proliferation in cultured vascular smooth muscle cells of rats. *Arterioscler.Thromb.Vasc.Biol.* **17**, 1274-1282.

Kumar, G. K., Rai, V., Sharma, S. D., Ramakrishnan, D. P., Peng, Y. J., Souvannakitti, D., & Prabhakar, N. R. (2006). Chronic intermittent hypoxia induces hypoxia-evoked catecholamine efflux in adult rat adrenal medulla via oxidative stress. *J Physiol* **575**, 229-239.

Kuri, B. A., Khan, S. A., Chan, S. A., Prabhakar, N. R., & Smith, C. B. (2007). Increased secretory capacity of mouse adrenal chromaffin cells by chronic intermittent hypoxia: involvement of protein kinase C. *J Physiol* **584**, 313-319.

Kuwahira, I., Kamiya, U., Iwamoto, T., Moue, Y., Urano, T., Ohta, Y., & Gonzalez, N. C. (1999). Splenic contraction-induced reversible increase in hemoglobin concentration in intermittent hypoxia. *J Appl. Physiol* **86**, 181-187.

Lamanna, J. C., Vendel, L. M., & Farrell, R. M. (1992). Brain adaptation to chronic hypobaric hypoxia in rats. *J Appl. Physiol* **72**, 2238-2243.

Leach, R. M., Robertson, T. P., Twort, C. H., & Ward, J. P. (1994). Hypoxic vasoconstriction in rat pulmonary and mesenteric arteries. *Am. J Physiol* **266**, L223-L231.

Lee, S. L., Wang, W. W., Lanzillo, J. J., & Fanburg, B. L. (1994). Regulation of serotonin-induced DNA synthesis of bovine pulmonary artery smooth muscle cells. *Am. J Physiol* **266**, L53-L60.

Li, H., Elton, T. S., Chen, Y. F., & Oparil, S. (1994). Increased endothelin receptor gene expression in hypoxic rat lung. *Am. J Physiol* **266**, L553-L560.

Li, H., Witte, K., August, M., Brausch, I., Godtel-Armbrust, U., Habermeier, A., Closs, E. I., Oelze, M., Munzel, T., & Forstermann, U. (2006). Reversal of endothelial nitric

oxide synthase uncoupling and up-regulation of endothelial nitric oxide synthase expression lowers blood pressure in hypertensive rats. *J Am.Coll.Cardiol.* **47**, 2536-2544.

Lin, M. J., Leung, G. P., Zhang, W. M., Yang, X. R., Yip, K. P., Tse, C. M., & Sham, J. S. (2004). Chronic hypoxia-induced upregulation of store-operated and receptor-operated Ca²⁺ channels in pulmonary arterial smooth muscle cells: a novel mechanism of hypoxic pulmonary hypertension. *Circ.Res.* **95**, 496-505.

Lin, M. J., Yang, X. R., Cao, Y. N., & Sham, J. S. (2007). Hydrogen peroxide-induced Ca²⁺ mobilization in pulmonary arterial smooth muscle cells. *Am.J Physiol Lung Cell Mol.Physiol* **292**, L1598-L1608.

Liu, J. Q., Zelko, I. N., Erbynn, E. M., Sham, J. S., & Folz, R. J. (2006). Hypoxic pulmonary hypertension: role of superoxide and NADPH oxidase (gp91phox). *Am.J Physiol Lung Cell Mol.Physiol* **290**, L2-10.

Liu, Q., Sham, J. S., Shimoda, L. A., & Sylvester, J. T. (2001). Hypoxic constriction of porcine distal pulmonary arteries: endothelium and endothelin dependence. *Am.J Physiol Lung Cell Mol.Physiol* **280**, L856-L865.

Lu, W., Wang, J., Peng, G., Shimoda, L. A., & Sylvester, J. T. (2009). Knockdown of stromal interaction molecule 1 attenuates store-operated Ca²⁺ entry and Ca²⁺ responses to acute hypoxia in pulmonary arterial smooth muscle. *Am.J Physiol Lung Cell Mol.Physiol* **297**, L17-L25.

Ma, H. T., Peng, Z., Hiragun, T., Iwaki, S., Gilfillan, A. M., & Beaven, M. A. (2008). Canonical transient receptor potential 5 channel in conjunction with Orai1 and STIM1 allows Sr²⁺ entry, optimal influx of Ca²⁺, and degranulation in a rat mast cell line. *J Immunol.* **180**, 2233-2239.

MacNee, W., Wathen, C. G., Hannan, W. J., Flenley, D. C., & Muir, A. L. (1983). Effects of pirbuterol and sodium nitroprusside on pulmonary haemodynamics in hypoxic cor pulmonale. *Br.Med.J (Clin.Res.Ed)* **287**, 1169-1172.

Madden, J. A., Vadula, M. S., & Kurup, V. P. (1992). Effects of hypoxia and other vasoactive agents on pulmonary and cerebral artery smooth muscle cells. *Am.J Physiol* **263**, L384-L393.

Maekawa, M., Ishizaki, T., Boku, S., Watanabe, N., Fujita, A., Iwamatsu, A., Obinata, T., Ohashi, K., Mizuno, K., & Narumiya, S. (1999). Signaling from Rho to the actin cytoskeleton through protein kinases ROCK and LIM-kinase. *Science* **285**, 895-898.

Marrone, O., Bellia, V., Ferrara, G., Milone, F., Romano, L., Salvaggio, A., Stallone, A., & Bonsignore, G. (1989). Transmural pressure measurements. Importance in the assessment of pulmonary hypertension in obstructive sleep apneas. *Chest* **95**, 338-342.

Massey, V., Komai, H., Palmer, G., & Elion, G. B. (1970). On the mechanism of inactivation of xanthine oxidase by allopurinol and other pyrazolo[3,4-d]pyrimidines. *J Biol.Chem.* **245**, 2837-2844.

Matsubara, T. & Ziff, M. (1986). Superoxide anion release by human endothelial cells: synergism between a phorbol ester and a calcium ionophore. *J Cell Physiol* **127**, 207-210.

Matsuno, K., Yamada, H., Iwata, K., Jin, D., Katsuyama, M., Matsuki, M., Takai, S., Yamanishi, K., Miyazaki, M., Matsubara, H., & Yabe-Nishimura, C. (2005). Nox1 is involved in angiotensin II-mediated hypertension: a study in Nox1-deficient mice. *Circulation* **112**, 2677-2685.

Matsuo, J., Oku, H., Kanbara, Y., Kobayashi, T., Sugiyama, T., & Ikeda, T. (2009). Involvement of NADPH oxidase and protein kinase C in endothelin-1-induced superoxide production in retinal microvessels. *Exp. Eye Res.* **89**, 693-699.

Mayo Clinic. Sleep Apnea. <http://www.mayoclinic.com/health/sleep-apnea/DS00148> . 2009.

Ref Type: Internet Communication

McGown, A. D., Makker, H., Elwell, C., Al Rawi, P. G., Valipour, A., & Spiro, S. G. (2003). Measurement of changes in cytochrome oxidase redox state during obstructive sleep apnea using near-infrared spectroscopy. *Sleep* **26**, 710-716.

McGuire, M. & Bradford, A. (1999). Chronic intermittent hypoxia increases haematocrit and causes right ventricular hypertrophy in the rat. *Respir. Physiol* **117**, 53-58.

McMurtry, I. F., Bauer, N. R., Fagan, K. A., Nagaoka, T., Gebb, S. A., & Oka, M. (2003). Hypoxia and Rho/Rho-kinase signaling. Lung development versus hypoxic pulmonary hypertension. *Adv.Exp.Med.Biol.* **543**, 127-137.

McMurtry, I. F., Morris, K. G., & Petrun, M. D. (1980). Blunted hypoxic vasoconstriction in lungs from short-term high-altitude rats. *Am.J Physiol* **238**, H849-H857.

McMurtry, I. F., Petrun, M. D., & Reeves, J. T. (1978). Lungs from chronically hypoxic rats have decreased pressor response to acute hypoxia. *Am.J Physiol* **235**, H104-H109.

McNamara, P. J., Murthy, P., Kantores, C., Teixeira, L., Engelberts, D., van Vliet, T., Kavanagh, B. P., & Jankov, R. P. (2008). Acute vasodilator effects of Rho-kinase inhibitors in neonatal rats with pulmonary hypertension unresponsive to nitric oxide. *Am.J Physiol Lung Cell Mol.Physiol* **294**, L205-L213.

Mehta, D. & Gunst, S. J. (1999). Actin polymerization stimulated by contractile activation regulates force development in canine tracheal smooth muscle. *J Physiol* **519 Pt 3**, 829-840.

Meyrick, B. & Reid, L. (1978). The effect of continued hypoxia on rat pulmonary arterial circulation. An ultrastructural study. *Lab Invest* **38**, 188-200.

Meyrick, B. & Reid, L. (1980). Endothelial and subintimal changes in rat hilar pulmonary artery during recovery from hypoxia. A quantitative ultrastructural study. *Lab Invest* **42**, 603-615.

Michelakis, E. D., Hampl, V., Nsair, A., Wu, X., Harry, G., Haromy, A., Gurtu, R., & Archer, S. L. (2002). Diversity in mitochondrial function explains differences in vascular oxygen sensing. *Circ.Res.* **90**, 1307-1315.

Michelakis, E. D., Thebaud, B., Weir, E. K., & Archer, S. L. (2004). Hypoxic pulmonary vasoconstriction: redox regulation of O₂-sensitive K⁺ channels by a mitochondrial O₂-sensor in resistance artery smooth muscle cells. *J Mol.Cell Cardiol.* **37**, 1119-1136.

Mittal, M., Roth, M., Konig, P., Hofmann, S., Dony, E., Goyal, P., Selbitz, A. C., Schermuly, R. T., Ghofrani, H. A., Kwapiszewska, G., Kummer, W., Klepetko, W., Hoda, M. A., Fink, L., Hanze, J., Seeger, W., Grimminger, F., Schmidt, H. H., & Weissmann, N. (2007). Hypoxia-dependent regulation of nonphagocytic NADPH oxidase subunit NOX4 in the pulmonary vasculature. *Circ.Res.* **101**, 258-267.

Mohazzab, H., Fayngersh, R. P., & Wolin, M. S. (1996). Nitric oxide inhibits pulmonary artery catalase and H₂O₂-associated relaxation. *Am.J Physiol* **271**, H1900-H1906.

Mohazzab, K. M., Kaminski, P. M., & Wolin, M. S. (1994). NADH oxidoreductase is a major source of superoxide anion in bovine coronary artery endothelium. *Am.J Physiol* **266**, H2568-H2572.

Mohsenin, V. (2001). Sleep-related breathing disorders and risk of stroke. *Stroke* **32**, 1271-1278.

Moinard, J., Manier, G., Pillet, O., & Castaing, Y. (1994). Effect of inhaled nitric oxide on hemodynamics and VA/Q inequalities in patients with chronic obstructive pulmonary disease. *Am.J Respir.Crit Care Med.* **149**, 1482-1487.

Muller, F. L., Liu, Y., & Van Remmen, H. (2004). Complex III releases superoxide to both sides of the inner mitochondrial membrane. *J Biol.Chem.* **279**, 49064-49073.

Nagaoka, T., Fagan, K. A., Gebb, S. A., Morris, K. G., Suzuki, T., Shimokawa, H., McMurtry, I. F., & Oka, M. (2005). Inhaled Rho kinase inhibitors are potent and selective vasodilators in rat pulmonary hypertension. *Am.J Respir.Crit Care Med.* **171**, 494-499.

Nagaoka, T., Gebb, S. A., Karoor, V., Homma, N., Morris, K. G., McMurtry, I. F., & Oka, M. (2006). Involvement of RhoA/Rho kinase signaling in pulmonary hypertension of the fawn-hooded rat. *J Appl.Physiol* **100**, 996-1002.

Nagaoka, T., Morio, Y., Casanova, N., Bauer, N., Gebb, S., McMurtry, I., & Oka, M. (2004). Rho/Rho kinase signaling mediates increased basal pulmonary vascular tone in chronically hypoxic rats. *Am.J Physiol Lung Cell Mol.Physiol* **287**, L665-L672.

Naik, J. S., Earley, S., Resta, T. C., & Walker, B. R. (2005). Pressure-induced smooth muscle cell depolarization in pulmonary arteries from control and chronically hypoxic rats does not cause myogenic vasoconstriction. *J Appl. Physiol* **98**, 1119-1124.

Neckar, J., Szarszoi, O., Herget, J., Ostadal, B., & Kolar, F. (2003). Cardioprotective effect of chronic hypoxia is blunted by concomitant hypercapnia. *Physiol Res*. **52**, 171-175.

Nelson, C. P., Willets, J. M., Davies, N. W., Challiss, R. A., & Standen, N. B. (2008). Visualizing the temporal effects of vasoconstrictors on PKC translocation and Ca²⁺ signaling in single resistance arterial smooth muscle cells. *Am.J Physiol Cell Physiol* **295**, C1590-C1601.

Nisbet, R. E., Bland, J. M., Kleinhenz, D. J., Mitchell, P. O., Walp, E. R., Sutliff, R. L., & Hart, C. M. (2009). Rosiglitazone Attenuates Chronic Hypoxia-induced Pulmonary Hypertension in a Mouse Model. *Am.J Respir. Cell Mol. Biol.*

Nisbet, R. E., Graves, A. S., Kleinhenz, D. J., Rupnow, H. L., Reed, A. L., Fan, T. H., Mitchell, P. O., Sutliff, R. L., & Hart, C. M. (2008). The Role of NADPH Oxidase in Chronic Intermittent Hypoxia-induced Pulmonary Hypertension in Mice. *Am.J Respir. Cell Mol. Biol.*

Nobili, L., Schiavi, G., Bozano, E., De Carli, F., Ferrillo, F., & Nobili, F. (2000). Morning increase of whole blood viscosity in obstructive sleep apnea syndrome. *Clin.Hemorheol.Microcirc.* **22**, 21-27.

Nozik-Grayck, E., Suliman, H. B., Majka, S., Albietz, J., Van Rheen, Z., Roush, K., & Stenmark, K. R. (2008). Lung EC-SOD overexpression attenuates hypoxic induction of Egr-1 and chronic hypoxic pulmonary vascular remodeling. *Am.J Physiol Lung Cell Mol.Physiol* **295**, L422-L430.

O'Rourke, B., Cortassa, S., Akar, F., & Aon, M. (2007). Mitochondrial ion channels in cardiac function and dysfunction. *Novartis.Found.Symp.* **287**, 140-151.

Ogawa, A., Emori, T., Sumita, W., Watanabe, A., Fujio, H., Miyaji, K., & Ohe, T. (2006). Continuous positive airway pressure ameliorated severe pulmonary hypertension associated with obstructive sleep apnea. *Acta Med.Okayama* **60**, 191-195.

Ogbi, M. & Johnson, J. A. (2006). Protein kinase Cepsilon interacts with cytochrome c oxidase subunit IV and enhances cytochrome c oxidase activity in neonatal cardiac myocyte preconditioning. *Biochem.J* **393**, 191-199.

Oka, M., Fagan, K. A., Jones, P. L., & McMurtry, I. F. (2008). Therapeutic potential of RhoA/Rho kinase inhibitors in pulmonary hypertension. *Br.J Pharmacol.* **155**, 444-454.

Oka, M., Morris, K. G., & McMurtry, I. F. (1993). NIP-121 is more effective than nifedipine in acutely reversing chronic pulmonary hypertension. *J Appl. Physiol* **75**, 1075-1080.

Okabe, S., Hida, W., Kikuchi, Y., Taguchi, O., Ogawa, H., Mizusawa, A., Miki, H., & Shirato, K. (1995). Role of hypoxia on increased blood pressure in patients with obstructive sleep apnoea. *Thorax* **50**, 28-34.

Ooi, H., Cadogan, E., Sweeney, M., Howell, K., O'Regan, R. G., & McLoughlin, P. (2000). Chronic hypercapnia inhibits hypoxic pulmonary vascular remodeling. *Am.J Physiol Heart Circ. Physiol* **278**, H331-H338.

Oparil, S., Chen, S. J., Meng, Q. C., Elton, T. S., Yano, M., & Chen, Y. F. (1995). Endothelin-A receptor antagonist prevents acute hypoxia-induced pulmonary hypertension in the rat. *Am.J Physiol* **268**, L95-100.

Orton, E. C., Raffestin, B., & McMurtry, I. F. (1990). Protein kinase C influences rat pulmonary vascular reactivity. *Am.Rev.Respir.Dis.* **141**, 654-658.

Packer L. (2002). *Educational Methods in Enzymology* Academic Press, San Diego, CA.

Pagano, P. J., Tornheim, K., & Cohen, R. A. (1993). Superoxide anion production by rabbit thoracic aorta: effect of endothelium-derived nitric oxide. *Am.J Physiol* **265**, H707-H712.

Parekh, A. B. & Putney, J. W., Jr. (2005). Store-operated calcium channels. *Physiol Rev.* **85**, 757-810.

Park, J. W. & Babior, B. M. (1997). Activation of the leukocyte NADPH oxidase subunit p47phox by protein kinase C. A phosphorylation-dependent change in the conformation of the C-terminal end of p47phox. *Biochemistry* **36**, 7474-7480.

Partinen, M. & Guilleminault, C. (1990). Daytime sleepiness and vascular morbidity at seven-year follow-up in obstructive sleep apnea patients. *Chest* **97**, 27-32.

Pawar, A., Nanduri, J., Yuan, G., Khan, S. A., Wang, N., Kumar, G. K., & Prabhakar, N. R. (2009). Reactive oxygen species-dependent endothelin signaling is required for augmented hypoxic sensory response of the neonatal carotid body by intermittent hypoxia. *Am.J Physiol Regul.Integr.Comp Physiol* **296**, R735-R742.

Peng, Y. J., Overholt, J. L., Kline, D., Kumar, G. K., & Prabhakar, N. R. (2003). Induction of sensory long-term facilitation in the carotid body by intermittent hypoxia: implications for recurrent apneas. *Proc.Natl.Acad.Sci.U.S.A* **100**, 10073-10078.

Peng, Y. J., Yuan, G., Jacono, F. J., Kumar, G. K., & Prabhakar, N. R. (2006). 5-HT evokes sensory long-term facilitation of rodent carotid body via activation of NADPH oxidase. *J Physiol* **576**, 289-295.

Pitt, B. R., Weng, W., Steve, A. R., Blakely, R. D., Reynolds, I., & Davies, P. (1994).

Serotonin increases DNA synthesis in rat proximal and distal pulmonary vascular smooth muscle cells in culture. *Am.J Physiol* **266**, L178-L186.

Porcelli, R. J. & Bergman, M. J. (1983). Effects of chronic hypoxia on pulmonary vascular responses to biogenic amines. *J Appl.Physiol* **55**, 534-540.

Potier, M., Gonzalez, J. C., Motiani, R. K., Abdullaev, I. F., Bisailon, J. M., Singer, H. A., & Trebak, M. (2009). Evidence for S. *FASEB J*.

Putney, J. W., Jr. (1986). A model for receptor-regulated calcium entry. *Cell Calcium* **7**, 1-12.

Raffestin, B., Adnot, S., Eddahibi, S., Macquin-Mavier, I., Braquet, P., & Chabrier, P. E. (1991). Pulmonary vascular response to endothelin in rats. *J Appl.Physiol* **70**, 567-574.

Ramzy, D., Rao, V., Tumati, L. C., Xu, N., Sheshgiri, R., Miriuka, S., Delgado, D. H., & Ross, H. J. (2006). Elevated endothelin-1 levels impair nitric oxide homeostasis through a PKC-dependent pathway. *Circulation* **114**, I319-I326.

Rathore, R., Zheng, Y. M., Li, X. Q., Wang, Q. S., Liu, Q. H., Ginnan, R., Singer, H. A., Ho, Y. S., & Wang, Y. X. (2006). Mitochondrial ROS-PKCepsilon signaling axis is uniquely involved in hypoxic increase in $[Ca^{2+}]_i$ in pulmonary artery smooth muscle cells. *Biochem.Biophys.Res.Commun.* **351**, 784-790.

Rathore, R., Zheng, Y. M., Niu, C. F., Liu, Q. H., Korde, A., Ho, Y. S., & Wang, Y. X. (2008). Hypoxia activates NADPH oxidase to increase [ROS](i) and [Ca(2+)](i) through the mitochondrial ROS-PKCvarepsilon signaling axis in pulmonary artery smooth muscle cells. *Free Radic.Biol.Med.*

Reeve, H. L., Michelakis, E., Nelson, D. P., Weir, E. K., & Archer, S. L. (2001). Alterations in a redox oxygen sensing mechanism in chronic hypoxia. *J Appl.Physiol* **90**, 2249-2256.

Resta, T. C., Chicoine, L. G., Omdahl, J. L., & Walker, B. R. (1999a). Maintained upregulation of pulmonary eNOS gene and protein expression during recovery from chronic hypoxia. *Am.J Physiol* **276**, H699-H708.

Resta, T. C., Chicoine, L. G., Omdahl, J. L., & Walker, B. R. (1999b). Maintained upregulation of pulmonary eNOS gene and protein expression during recovery from chronic hypoxia. *Am.J.Physiol* **276**, H699-H708.

Resta, T. C., Gonzales, R. J., Dail, W. G., Sanders, T. C., & Walker, B. R. (1997). Selective upregulation of arterial endothelial nitric oxide synthase in pulmonary hypertension. *Am.J Physiol* **272**, H806-H813.

Resta, T. C., Kanagy, N. L., & Walker, B. R. (2001). Estradiol-induced attenuation of pulmonary hypertension is not associated with altered eNOS expression. *Am.J Physiol Lung Cell Mol.Physiol* **280**, L88-L97.

Resta, T. C. & Walker, B. R. (1994). Orally administered L-arginine does not alter right ventricular hypertrophy in chronically hypoxic rats. *Am.J.Physiol* **266**, R559-R563.

Resta, T. C. & Walker, B. R. (1996). Chronic hypoxia selectively augments endothelium-dependent pulmonary arterial vasodilation. *Am.J Physiol* **270**, H888-H896.

Rhee, S. G., Kang, S. W., Netto, L. E., Seo, M. S., & Stadtman, E. R. (1999). A family of novel peroxidases, peroxiredoxins. *Biofactors* **10**, 207-209.

Robertson, T. P., Aaronson, P. I., & Ward, J. P. (2003). Ca²⁺ sensitization during sustained hypoxic pulmonary vasoconstriction is endothelium dependent. *Am.J Physiol Lung Cell Mol.Physiol* **284**, L1121-L1126.

Robertson, T. P., Hague, D., Aaronson, P. I., & Ward, J. P. (2000). Voltage-independent calcium entry in hypoxic pulmonary vasoconstriction of intrapulmonary arteries of the rat. *J Physiol* **525 Pt 3**, 669-680.

Robinson, K. M., Janes, M. S., Pehar, M., Monette, J. S., Ross, M. F., Hagen, T. M., Murphy, M. P., & Beckman, J. S. (2006). Selective fluorescent imaging of superoxide in vivo using ethidium-based probes. *Proc.Natl.Acad.Sci.U.S.A* **103**, 15038-15043.

Rodat, L., Savineau, J. P., Marthan, R., & Guibert, C. (2007). Effect of chronic hypoxia on voltage-independent calcium influx activated by 5-HT in rat intrapulmonary arteries. *Pflugers Arch.* **454**, 41-51.

Rose, F., Grimminger, F., Appel, J., Heller, M., Pies, V., Weissmann, N., Fink, L., Schmidt, S., Krick, S., Camenisch, G., Gassmann, M., Seeger, W., & Hanze, J. (2002). Hypoxic pulmonary artery fibroblasts trigger proliferation of vascular smooth muscle cells: role of hypoxia-inducible transcription factors. *FASEB J* **16**, 1660-1661.

Rubanyi, G. M. & Vanhoutte, P. M. (1986). Superoxide anions and hyperoxia inactivate endothelium-derived relaxing factor. *Am.J Physiol* **250**, H822-H827.

Russell, P. C., Emery, C. J., Cai, Y. N., Barer, G. R., & Howard, P. (1990). Enhanced reactivity to bradykinin, angiotensin I and the effect of captopril in the pulmonary vasculature of chronically hypoxic rats. *Eur.Respir.J* **3**, 779-785.

Ryland, D. & Reid, L. (1975). The pulmonary circulation in cystic fibrosis. *Thorax* **30**, 285-292.

Sajkov, D. & McEvoy, R. D. (2009). Obstructive sleep apnea and pulmonary hypertension. *Prog.Cardiovasc.Dis.* **51**, 363-370.

Salamanca, D. A. & Khalil, R. A. (2005). Protein kinase C isoforms as specific targets for modulation of vascular smooth muscle function in hypertension. *Biochem.Pharmacol* **70**, 1537-1547.

- Sato, K., Morio, Y., Morris, K. G., Rodman, D. M., & McMurtry, I. F. (2000). Mechanism of hypoxic pulmonary vasoconstriction involves ET(A) receptor-mediated inhibition of K(ATP) channel. *Am.J Physiol Lung Cell Mol.Physiol* **278**, L434-L442.
- Schafer, H., Hasper, E., Ewig, S., Koehler, U., Latzelsberger, J., Tasci, S., & Luderitz, B. (1998). Pulmonary haemodynamics in obstructive sleep apnoea: time course and associated factors. *Eur.Respir.J* **12**, 679-684.
- Semenza, G. L. & Wang, G. L. (1992). A nuclear factor induced by hypoxia via de novo protein synthesis binds to the human erythropoietin gene enhancer at a site required for transcriptional activation. *Mol.Cell Biol.* **12**, 5447-5454.
- Shahar, E., Whitney, C. W., Redline, S., Lee, E. T., Newman, A. B., Javier, N. F., O'Connor, G. T., Boland, L. L., Schwartz, J. E., & Samet, J. M. (2001). Sleep-disordered breathing and cardiovascular disease: cross-sectional results of the Sleep Heart Health Study. *Am.J Respir.Crit Care Med.* **163**, 19-25.
- Shakirova, Y., Bonnevier, J., Albinsson, S., Adner, M., Rippe, B., Broman, J., Arner, A., & Sward, K. (2006). Increased Rho activation and PKC-mediated smooth muscle contractility in the absence of caveolin-1. *Am.J Physiol Cell Physiol* **291**, C1326-C1335.
- Shimoda, L. A., Sham, J. S., Shimoda, T. H., & Sylvester, J. T. (2000). L-type Ca(2+) channels, resting [Ca(2+)](i), and ET-1-induced responses in chronically hypoxic pulmonary myocytes. *Am.J.Physiol Lung Cell Mol.Physiol* **279**, L884-L894.

Shimoda, L. A., Sylvester, J. T., Booth, G. M., Shimoda, T. H., Meeker, S., Undem, B. J., & Sham, J. S. (2001). Inhibition of voltage-gated K(+) currents by endothelin-1 in human pulmonary arterial myocytes. *Am.J Physiol Lung Cell Mol.Physiol* **281**, L1115-L1122.

Shimoda, L. A., Sylvester, J. T., & Sham, J. S. (1998). Inhibition of voltage-gated K⁺ current in rat intrapulmonary arterial myocytes by endothelin-1. *Am.J.Physiol* **274**, L842-L853.

Short, M., Nemenoff, R. A., Zawada, W. M., Stenmark, K. R., & Das, M. (2004). Hypoxia induces differentiation of pulmonary artery adventitial fibroblasts into myofibroblasts. *Am.J Physiol Cell Physiol* **286**, C416-C425.

Sime, F., Penaloza, D., & Ruiz, L. (1971). Bradycardia, increased cardiac output, and reversal of pulmonary hypertension in altitude natives living at sea level. *Br.Heart J* **33**, 647-657.

Siques, P., Brito, J., Leon-Velarde, F., Barrios, L., Cruz, J. J., Lopez, V., & Herruzo, R. (2006). Time course of cardiovascular and hematological responses in rats exposed to chronic intermittent hypobaric hypoxia (4600 m). *High Alt.Med.Biol.* **7**, 72-80.

Snow, J. B., Kanagy, N. L., Walker, B. R., & Resta, T. C. (2009). Rat Strain Differences in Pulmonary Artery Smooth Muscle Ca(2⁺) Entry Following Chronic Hypoxia. *Microcirculation.* 1-12.

Snow, J. B., Kitzis, V., Norton, C. E., Torres, S. N., Johnson, K. D., Kanagy, N. L., Walker, B. R., & Resta, T. C. (2008). Differential effects of chronic hypoxia and intermittent hypocapnic and eucapnic hypoxia on pulmonary vasoreactivity. *J Appl. Physiol* **104**, 110-118.

Somlyo, A. P. & Somlyo, A. V. (2003). Ca²⁺ sensitivity of smooth muscle and nonmuscle myosin II: modulated by G proteins, kinases, and myosin phosphatase. *Physiol Rev.* **83**, 1325-1358.

Spiekermann, S., Schenk, K., & Hoeper, M. M. (2009). Increased xanthine oxidase activity in idiopathic pulmonary arterial hypertension. *Eur. Respir. J* **34**, 276.

Stenmark, K. R., Fagan, K. A., & Frid, M. G. (2006). Hypoxia-induced pulmonary vascular remodeling: cellular and molecular mechanisms. *Circ. Res.* **99**, 675-691.

Suzuki, Y. J. & Ford, G. D. (1999). Redox regulation of signal transduction in cardiac and smooth muscle. *J Mol. Cell Cardiol.* **31**, 345-353.

Sweeney, M., McDaniel, S. S., Platoshyn, O., Zhang, S., Yu, Y., Lapp, B. R., Zhao, Y., Thistlethwaite, P. A., & Yuan, J. X. (2002a). Role of capacitative Ca²⁺ entry in bronchial contraction and remodeling. *J. Appl. Physiol* **92**, 1594-1602.

Sweeney, M., Yu, Y., Platoshyn, O., Zhang, S., McDaniel, S. S., & Yuan, J. X. (2002b). Inhibition of endogenous TRP1 decreases capacitative Ca²⁺ entry and attenuates

pulmonary artery smooth muscle cell proliferation. *Am.J.Physiol Lung Cell Mol.Physiol* **283**, L144-L155.

Takashima, S. (2009). Phosphorylation of myosin regulatory light chain by myosin light chain kinase, and muscle contraction. *Circ.J* **73**, 208-213.

Teng, J. C., Kay, H., Chen, Q., Adams, J. S., Grilli, C., Guglielmo, G., Zambrano, C., Krass, S., Bell, A., & Young, L. H. (2008). Mechanisms related to the cardioprotective effects of protein kinase C epsilon (PKC epsilon) peptide activator or inhibitor in rat ischemia/reperfusion injury. *Naunyn Schmiedebergs Arch.Pharmacol.* **378**, 1-15.

Thamilselvan, V., Menon, M., & Thamilselvan, S. (2009). OXALATE-INDUCED ACTIVATION OF PKC ALPHA AND DELTA REGULATES NADPH OXIDASE-MEDIATED OXIDATIVE INJURY IN RENAL TUBULAR EPITHELIAL CELLS. *Am.J Physiol Renal Physiol.*

Thomas, B. J. & Wanstall, J. C. (2003). Alterations in pulmonary vascular function in rats exposed to intermittent hypoxia. *Eur.J Pharmacol.* **477**, 153-161.

Tilkian, A. G., Guilleminault, C., Schroeder, J. S., Lehrman, K. L., Simmons, F. B., & Dement, W. C. (1976). Hemodynamics in sleep-induced apnea. Studies during wakefulness and sleep. *Ann.Intern.Med.* **85**, 714-719.

- Trebak, M., St, J. B., McKay, R. R., Birnbaumer, L., & Putney, J. W., Jr. (2003). Signaling mechanism for receptor-activated canonical transient receptor potential 3 (TRPC3) channels. *J Biol.Chem.* **278**, 16244-16252.
- Troncoso Brindeiro, C. M., da Silva, A. Q., Allahdadi, K. J., Youngblood, V., & Kanagy, N. L. (2007). Reactive oxygen species contribute to sleep apnea-induced hypertension in rats. *Am.J Physiol Heart Circ.Physiol* **293**, H2971-H2976.
- Venkatachalam, K., Zheng, F., & Gill, D. L. (2003). Regulation of canonical transient receptor potential (TRPC) channel function by diacylglycerol and protein kinase C. *J Biol.Chem.* **278**, 29031-29040.
- Violin, J. D. & Newton, A. C. (2003). Pathway illuminated: visualizing protein kinase C signaling. *IUBMB.Life* **55**, 653-660.
- Walker, B. R., Resta, T. C., & Nelin, L. D. (2000). Nitric oxide-dependent pulmonary vasodilation in polycythemic rats. *Am.J Physiol Heart Circ.Physiol* **279**, H2382-H2389.
- Wang, J., Weigand, L., Foxson, J., Shimoda, L. A., & Sylvester, J. T. (2007). Ca²⁺ signaling in hypoxic pulmonary vasoconstriction: effects of myosin light chain and Rho kinase antagonists. *Am.J.Physiol Lung Cell Mol.Physiol* **293**, L674-L685.
- Wang, J., Weigand, L., Lu, W., Sylvester, J. T., Semenza, G. L., & Shimoda, L. A. (2006a). Hypoxia inducible factor 1 mediates hypoxia-induced TRPC expression and

elevated intracellular Ca²⁺ in pulmonary arterial smooth muscle cells. *Circ.Res.* **98**, 1528-1537.

Wang, X., Tong, M., Chinta, S., Raj, J. U., & Gao, Y. (2006b). Hypoxia-induced reactive oxygen species downregulate ETB receptor-mediated contraction of rat pulmonary arteries. *Am.J Physiol Lung Cell Mol.Physiol* **290**, L570-L578.

Wanstall, J. C. & O'Donnell, S. R. (1990). Endothelin and 5-hydroxytryptamine on rat pulmonary artery in pulmonary hypertension. *Eur.J Pharmacol.* **176**, 159-168.

Warnecke, C., Zaborowska, Z., Kurreck, J., Erdmann, V. A., Frei, U., Wiesener, M., & Eckardt, K. U. (2004). Differentiating the functional role of hypoxia-inducible factor (HIF)-1alpha and HIF-2alpha (EPAS-1) by the use of RNA interference: erythropoietin is a HIF-2alpha target gene in Hep3B and Kelly cells. *FASEB J* **18**, 1462-1464.

Waypa, G. B., Chandel, N. S., & Schumacker, P. T. (2001). Model for hypoxic pulmonary vasoconstriction involving mitochondrial oxygen sensing. *Circ.Res.* **88**, 1259-1266.

Waypa, G. B., Guzy, R., Mungai, P. T., Mack, M. M., Marks, J. D., Roe, M. W., & Schumacker, P. T. (2006). Increases in mitochondrial reactive oxygen species trigger hypoxia-induced calcium responses in pulmonary artery smooth muscle cells. *Circ.Res.* **99**, 970-978.

Weigand, L., Sylvester, J. T., & Shimoda, L. A. (2006). Mechanisms of endothelin-1-induced contraction in pulmonary arteries from chronically hypoxic rats. *Am.J Physiol Lung Cell Mol.Physiol* **290**, L284-L290.

Weir, E. K. & Archer, S. L. (1995). The mechanism of acute hypoxic pulmonary vasoconstriction: the tale of two channels. *FASEB J* **9**, 183-189.

Weissmann, N., Nollen, M., Gerigk, B., Ardeschir, G. H., Schermuly, R. T., Gunther, A., Quanz, K., Fink, L., Hanze, J., Rose, F., Seeger, W., & Grimminger, F. (2003). Downregulation of hypoxic vasoconstriction by chronic hypoxia in rabbits: effects of nitric oxide. *Am.J Physiol Heart Circ.Physiol* **284**, H931-H938.

Weitzenblum, E., Chaouat, A., Kessler, R., & Canuet, M. (2008). Overlap syndrome: obstructive sleep apnea in patients with chronic obstructive pulmonary disease. *Proc.Am.Thorac.Soc.* **5**, 237-241.

Weitzenblum, E., Krieger, J., Apprill, M., Vallee, E., Ehrhart, M., Ratomaharo, J., Oswald, M., & Kurtz, D. (1988). Daytime pulmonary hypertension in patients with obstructive sleep apnea syndrome. *Am.Rev.Respir.Dis.* **138**, 345-349.

Welsh, D. J., Harnett, M., MacLean, M., & Peacock, A. J. (2004). Proliferation and signaling in fibroblasts: role of 5-hydroxytryptamine_{2A} receptor and transporter. *Am.J Respir.Crit Care Med.* **170**, 252-259.

Wolfson, M., McPhail, L. C., Nasrallah, V. N., & Snyderman, R. (1985). Phorbol myristate acetate mediates redistribution of protein kinase C in human neutrophils: potential role in the activation of the respiratory burst enzyme. *J Immunol.* **135**, 2057-2062.

Wolin, M. S. (2009). Reactive oxygen species and the control of vascular function. *Am.J Physiol Heart Circ.Physiol* **296**, H539-H549.

Young, T., Palta, M., Dempsey, J., Skatrud, J., Weber, S., & Badr, S. (1993). The occurrence of sleep-disordered breathing among middle-aged adults. *N.Engl.J Med.* **328**, 1230-1235.

Young, T., Peppard, P. E., & Gottlieb, D. J. (2002). Epidemiology of obstructive sleep apnea: a population health perspective. *Am.J Respir. Crit Care Med.* **165**, 1217-1239.

Yu, Y., Fantozzi, I., Remillard, C. V., Landsberg, J. W., Kunichika, N., Platoshyn, O., Tigno, D. D., Thistlethwaite, P. A., Rubin, L. J., & Yuan, J. X. (2004). Enhanced expression of transient receptor potential channels in idiopathic pulmonary arterial hypertension. *Proc.Natl.Acad.Sci.U.S.A* **101**, 13861-13866.

Yuan, G., Nanduri, J., Khan, S., Semenza, G. L., & Prabhakar, N. R. (2008). Induction of HIF-1alpha expression by intermittent hypoxia: involvement of NADPH oxidase, Ca²⁺ signaling, prolyl hydroxylases, and mTOR. *J Cell Physiol* **217**, 674-685.

Yuan, J. X., Aldinger, A. M., Juhaszova, M., Wang, J., Conte, J. V., Jr., Gaine, S. P., Orens, J. B., & Rubin, L. J. (1998). Dysfunctional voltage-gated K⁺ channels in pulmonary artery smooth muscle cells of patients with primary pulmonary hypertension. *Circulation* **98**, 1400-1406.

Zhang, F., Jin, S., Yi, F., Xia, M., Dewey, W. L., & Li, P. L. (2008). Local production of O₂⁻ by NAD(P)H oxidase in the sarcoplasmic reticulum of coronary arterial myocytes: cADPR-mediated Ca²⁺ regulation. *Cell Signal*. **20**, 637-644.

Zhang, S., Dong, H., Rubin, L. J., & Yuan, J. X. (2007). Upregulation of Na⁺/Ca²⁺ exchanger contributes to the enhanced Ca²⁺ entry in pulmonary artery smooth muscle cells from patients with idiopathic pulmonary arterial hypertension. *Am.J Physiol Cell Physiol* **292**, C2297-C2305.

Zhao, H., Joseph, J., Fales, H. M., Sokoloski, E. A., Levine, R. L., Vasquez-Vivar, J., & Kalyanaraman, B. (2005). Detection and characterization of the product of hydroethidine and intracellular superoxide by HPLC and limitations of fluorescence. *Proc.Natl.Acad.Sci.U.S.A* **102**, 5727-5732.

Zhao, H., Kalivendi, S., Zhang, H., Joseph, J., Nithipatikom, K., Vasquez-Vivar, J., & Kalyanaraman, B. (2003). Superoxide reacts with hydroethidine but forms a fluorescent product that is distinctly different from ethidium: potential implications in intracellular fluorescence detection of superoxide. *Free Radic.Biol.Med.* **34**, 1359-1368.

Zielinski, J. (2005). [Effects of intermittent hypoxia on pulmonary haemodynamics].
Pneumonol.Alergol.Pol. **73**, 86-93.